

Ministry of Education and Science of Ukraine
Sumy State University



I. B. Karintsev, I. V. Pavlenko

HYDROAEROELASTICITY

Textbook

Recommended by the Academic Council of Sumy State University



Sumy
Sumy State University
2017

УДК [534.1+532.591]:533.69.01
K23

Reviewers:

Jozef Zajac – Dr. h. c., prof. Ing., C. Sc., Technical University of Košice, Prešov, Slovakia;

Czesław Kundera – Prof. dr hab. inż., Kielce University of Technology, Kielce, Poland;

Vitalii I. Simonovskiy – Prof., D. Sc., Sumy State University, Ukraine

*Recommended for publication
by the Academic Council of Sumy State University
as textbook
(minutes No. 11 of 15.06.2017)*

Karintsev I. B.

K23 Hydroaeroelasticity : textbook /
I. B. Karintsev, I. V. Pavlenko. – Sumy : Sumy State
University, 2017. – 235 p.
ISBN 978-966-657-692-0

The textbook is devoted to investigate the stability problems for deformable systems streamlined by fluid or gas flow. Special attention is paid to the study of hydrodynamic forces acting on deformable surfaces. The textbook will be intended for engineering students and postgraduate students of higher educational institutions.

УДК [534.1+532.591]:533.69.01

© Karintsev I. B., Pavlenko I. V., 2017
ISBN 978-966-657-692-0 © Sumy State University, 2017

Contents

	P.
Preface	5
List of symbols	7
1 Introduction to hydroaeroelasticity	13
1.1 A brief historical overview	14
1.2 The subject of hydroaeroelasticity	21
1.3 Static problems	23
1.4 Dynamic problems	24
2 Determination of the dynamic forces acting on deformable surfaces	27
2.1 Potential flow equations	28
2.2 Using small perturbation method for linearization of equations	35
2.3 Aircraft wing oscillations in two- dimensional incompressible fluid flow	40
2.4 Determination of aerodynamic forces in case of high supersonic speed	68
3 Static aeroelasticity	81
3.1 Characteristics of the aircraft wing profiles ..	82
3.2 Divergence of an elastically fixed wing element	88
3.3 Critical velocity of aileron's reverse	92
3.4 Divergence of a full-cantilever wing	98
3.5 Using the influence functions for solving the problems of aeroelasticity	101
4 Flexural-torsional flutter of beams and plates	104
4.1 Equations of small flexural-torsional oscillations of a wing in the gas flow	105
4.2 Using Galerkin method for determination of the critical flutter velocity	111

4.3	Flutter of a single-mass system with two degrees of freedom	116
4.4	Using Routh–Hurwitz criterion for determination of the critical flutter velocity ..	121
4.5	Flexural-torsional flutter of a plate	126
5	Oscillations of poorly streamlined beams in the gas flow	135
5.1	Oscillations of a cylinder in the gas flow	136
5.2	The Tacoma Narrows Bridge failure	145
5.3	Other examples of instability	151
6	Panel flutter	155
6.1	Problem shaping	156
6.2	Flutter of a rectangular plate with two opposite freely supported edges	158
6.3	Divergence of a cylindrical panel	164
6.4	Flutter of a cylindrical panel	168
6.5	Euler–Lagrange variational method	174
6.6	Nonlinear problems of a panel flutter	179
7	Other problems of hydroaeroelasticity	185
7.1	Aeroelastic phenomena in turbomachines	186
7.2	Stability of the automatic balancing devices of centrifugal pumps	188
7.3	Analysis of the operation of seals with deformable floating rings	194
7.4	Aeroelasticity phenomena in the processes of gas separation	198
	Author Index	202
	Subject Index	203
	References	214

Preface

Hydroaeroelasticity as the branch of mechanics, which studies the interactions between the inertial, elastic and aerodynamic forces that occur when an elastic body is exposed to a fluid flow, is the highly important discipline for the process of formation of modern engineers. Its problems for many years were focused on applications in the field of aircraft and aeronautical industry.

However, up-to-date subject of hydroaeroelasticity supplements the theory of hydraulic machines and turbochargers, particularly within the problems designing the impellers and seals. The problems of hydroaeroelasticity also important in the field of chemical engineering, gas and oil industry, particularly for investigating the process of inertia-filtering separation of gas-liquid mixtures. Generally, hydroaeroelasticity draws on the study of solid and fluid mechanics, structural dynamics and dynamical systems. The synthesis of aeroelasticity with thermodynamics is known as aerothermoelasticity, and its synthesis with control theory is known as aeroservoelasticity.

The theory of hydroaeroelasticity may be broadly classified into two fields:

1. Static aeroelasticity, which deals with the static or steady response of an elastic body to a fluid flow.
2. Dynamic hydroaeroelasticity, which deals with the body dynamics as typically vibrational response.

General approaches used for studying the hydroaeroelasticity phenomena, are closely intersected with the issues of strength of materials and the theory of elasticity, as well as the theory of linear and nonlinear oscillation of mechanical systems. The most nonlinear boundary problems of hydroaeroelasticity can be solved in 2D and 3D formulation by using modern computer programmes that are studied by students of engineering specialties. Therefore the reader should

have basic skills in the field of numerical solution of problems of applied mechanics.

This textbook will be intended for students of engineering specialties and post-graduate students from higher educational institutions. It is devoted to investigate the stability problems for deformable systems streamlined by fluid or gas flow. Special attention is paid to the study of hydrodynamic forces acting on deformable surfaces.

The textbook consists of seven chapters, arranged in the order of presentation of the educational material on the didactic principle “from simple to complex”. Each chapter concludes material for self-examination and knowledge control of students. List of symbols, as well as subject and author indexes located at the end of the textbook, help students to accelerate the search for the necessary educational material.

The entire material of the textbook is based on the authors’ teaching experience at Sumy State University within the disciplines “Strength of materials”, “Hydroaeroelasticity” and “Theory of plates and shells” for students of specialty “Dynamics and strength”, “Computational mechanics” and “Computational engineering in mechanics”, as well as on the research experience in close cooperation between the Department of Materials Strength and Mechanical Engineering and the Department of General Mechanics and Machine Dynamics of the Faculty of Technical Systems and Energy Efficient Technologies at Sumy State University.

The authors are grateful to the dean of the Faculty of Technical Systems and Energy Efficient Technologies O. G. Gusak for the opportunity to publish this textbook.

The authors sincerely hope that material presented in the textbook will be quite clear for understanding, and all readers can gain new ideas for themselves for future scientific growth.

Authors:

*I. B. Karintsev,
I. V. Pavlenko.*

List of symbols

A – oscillation amplitude; arbitrary constant; total work of external forces;
 $A_0, A_1, A_2, \dots; A, B, C, \dots$ – coefficients of complex potential;
 A_{12}, A_{22} – stiffness coefficients;
 A, B – constants determined from the boundary conditions;
 A, B, ω_a – parameters of the Harmonic function;
 A_i – coefficients of the characteristic polynomial;
 A_i, B_j – coefficients of minimizing forms;
 a – acceleration; complex acceleration vector; plate width;
 a, b, c – coefficients of the biquadratic polynomial;
 a^2 – sound velocity; velocity of small perturbations extension;
 a_i, b_i, c_i – coefficients of the characteristic polynomial;
 coefficients of the Fourier transform; unknown parameters;
 a_{ij} – coefficients of the system of linear homogeneous differential equations;
 a_{ij}, b_{ij}, c_{ij} – parameters of the matrix determinant for the frequency equation;
 a_{ij}, k_{ij} – compliance and stiffness coefficients;
 a_x, a_y – components of the acceleration;
 $B_{11}, B_{12}, B_{21}, B_{22}$ – damping coefficients;
 b – half-chord;
 C – constant of the Barotropic law;
 C, D – arbitrary constants;
 C_k – Carman's coefficient;
 C_m – dimensionless moment ratio;
 C_x, C_y – lift and drag coefficients;
 $C(k)$ – Theodorsen function;
 $C(x), D(x), \dots$ – linearly independent functions;
 c – stiffness coefficient;
 c, d – additional parameters in equations of flexural-torsional oscillations;

c_i – coefficients of the plate deflection function;
 D – cylindrical stiffness;
 d – total differential sign; diameter of a streamlined cylinder;
hydraulic diameter;
 $d, g, R, \lambda, \sigma, \omega_0, \Omega$ – additional parameters of equation of plate
small oscillations;
 div – divergence sign;
 E – Young's modulus;
 e – eccentricity;
 F – unloading force; cross-sectional area;
 \vec{F} – vector specific mass force;
 $F(k), G(k)$ – real and imagine components of the Theodorsen
function;
 $F(x, y, z, t)$ – equation of the streamlined surface;
 f – vortex shedding frequency; oscillation frequency;
 f, \bar{f} – maximum bending and its dimensionless value;
frequency of vortex shedding;
 $f(\dots)$ – function sign;
 G – shear modulus;
 $G(z, \zeta)$ – influence functions;
 $grad$ – gradient sign;
 H_1, H_2 – complex Bessel functions;
 h – plate thickness;
 I – axial moment of inertia;
 I_n, J_n – n -order Bessel functions of the first kind;
 I_p, I_a – polar moment of inertia;
 i – serial number;
 i, j – imaginary unit;
 $\vec{i}, \vec{j}, \vec{k}$ – unit vectors of axes x, y, z ;
 K – aerodynamic ratio;
 K_0, K_2 – definite integral with infinite boundary;

k – adiabatic index; dimensionless oscillation frequency; specific frequency;
 k, k_i – characteristic index; roots of the characteristic polynomial;
 k_y – linear stiffness coefficient;
 k_α – spring stiffness; angular (torsional) stiffness coefficient;
 $L(t), M(t)$ – aerodynamic force and moment (torque);
 L, X – specific lift and drag (per unit of span);
 l – plate length;
 M – Mach number; specific aerodynamic moment;
 $M_{1/2}$ – aerodynamic moment about the chord's midpoint;
 M_B – aerodynamic moment relative to the rotation axis;
 M_{spr} – elastic (spring) recovery moment;
 M_t – torque;
 M_z – experimentally measured moment;
 m – mass; specific mass;
 N_x, N_y – specific tensile forces;
 \bar{N}_x, \bar{N}_y – dimensionless tensile forces;
 n – damping coefficient; number of half-waves;
 P – pressure function;
 P_1 – inlet pressure;
 P_2 – pressure in the pump chamber;
 P_3 – outlet pressure;
 \tilde{P} – modified pressure function;
 p – pressure;
 p_0 – initial pressure;
 $p(x, y, t)$ – component of aerodynamic pressure due to deviation of the plate from its unperturbed position;
 p, p_i – real parts of characteristic indexes;
 Q – specific share force;
 Q_j – load;

- q – kinetic head; specific hydrodynamic load; intensity of external forces;
- q_0 – amplitude of the specific harmonic hydrodynamic force;
- $q(x, y, t)$ – external distributed load;
- q_{div} – critical value of the kinetic head and velocity in case of divergence;
- R – universal gas constant;
- Re – Reynolds number;
- R_i – reaction forces;
- r – radius of inertia;
- r, s – Riemann invariants;
- $r, r_1; \theta, \theta_1$ – linear and angular dimensions for a circle;
- rot – rotor sign;
- S – surface area;
- S, T – parameters determined from differential equations;
- St – Strouhal number;
- $S(z), T(z)$ – form functions;
- $S_i(z), T_i(z)$ – linearly independent functions;
- T – oscillation period; axial force acting to the pump rotor;
- T_0 – normal temperature on the Kelvin scale;
- t – time;
- U, V, W – unperturbed components of velocity;
- U – potential energy of deformation;
- U_{cr} – critical flow velocity; critical velocity of the aileron's reverse; critical flutter velocity;
- U_{div} – critical divergence velocity;
- u – dimensionless face gap value;
- u, v, w – components of velocity;
- V – velocity module; plate volume; volume of the pump chamber;
- \vec{V} – vector of velocity;
- v_l, v_u – boundary velocities for the lower and upper surfaces;

W – complex velocity or acceleration potential;
 W_i – displacement;
 $w(x, y, t)$, $w_1(x, t)$, $w_n(x)$ – plate displacement functions;
 X, Y, Z – components of specific mass force;
 x, y, z – coordinates;
 x_m, e – coordinate of the point of force application;
 $Y(x, t)$ – profile function;
 $Y_l, Y_u; y_l, y_u$ – equations of the lower and upper surfaces;
 y_0 – dimensionless amplitude;
 y_C – coordinate of the centre of mass;
 $\dot{y}, \ddot{\alpha}; \ddot{y}, \ddot{\alpha}$ – first and second time derivatives;
 $\bar{y}_l, \bar{y}_u; \bar{y}_m$ – dimensionless coordinates of lower and upper surfaces and its average value;
 z – face gap value;
 α – attack angle;
 α_m – average attack angle;
 α, α_0 – parameters for describing the rotational motion;
 α, β – real and image parts of roots;
 β – pressure difference ratio;
 γ_{xy} – shear deformation;
 Δ – delta sign; determinant;
 ΔP – total pressure difference;
 $\Delta P_1, \Delta P_2$ – pressure difference through the radial and axial gap;
 δ – variation sign; damping coefficient; logarithmic decrement of damping;
 δA – elementary work;
 ε – linear parameter ($0 \leq \varepsilon \leq 2$); dimensionless eccentricity;
 $\varepsilon_x, \varepsilon_y$ – normal deformations;
 ζ, z – complex variables (vectors);
 θ – argument of the complex vector; rotation angle;
 Θ – total rotation angle;
 κ – polytropic index;

λ – characteristic index; parameter of the deflection function;
 λ, λ_i – roots of the characteristic polynomial;
 λ_{cr} – critical value of the coefficient for determining the critical flutter velocity;
 μ – specific mass; Poisson's ratio;
 ν – kinematic viscosity;
 ξ – dimensionless coordinate;
 ξ, η – axes of the complex plane;
 ξ_1, ξ_2 – axes of fixed coordinate systems;
 Π – potential energy;
 ρ – density;
 σ_x, σ_y – normal stress;
 τ – time delay; phase shift;
 τ_{xy} – shear stress;
 v – parameter of the Joukowski transformation;
 Φ – generalized external impact;
 Φ, Ψ – real and imaginary parts of the complex acceleration potential;
 φ – velocity potential;
 φ, ψ – real and imaginary parts of the complex velocity potential;
 $\varphi_i(x, y)$ – linearly independent coordinate functions;
 Ψ_1, Ψ_2 – components of an imaginary part of the complex acceleration potential;
 ω – oscillation frequency; eigenfrequency;
 ω, ω_i – imaginary parts of characteristic indexes;
 $\omega_a, \omega_x, \omega_y$ – partial frequencies;
 \dots_0 – unperturbed parameter sign;
 \dots_n – normal component sign;
 \dots_w – wing sign;
 \dots^{\prime} – perturbed parameter sign; modified parameter sign;
 ∂ – partial differential sign;
 ∇ – differential operator (nabla sign);
 ∇^2 – Laplace operator.

CHAPTER 1.

Introduction to hydroaeroelasticity

§ 1.1. A brief historical overview

Until the middle of the twentieth century the problems of hydroaeroelasticity were not such important as today. This is due to the fact that the aircrafts had a low flight velocity, as well as the structures were quite rigid, that prevented the appearance of the most of the aeroelasticity phenomena. However, increasing velocities with almost invariable design loads and absence of the rational rigidity criterion led constructors to solve wide varieties of the hydroelasticity problems.

Perhaps for the first time the problems of aeroelasticity became actual in 1903, when a monoplane, designed by the professor S. P. Langley (Figure 1.1), suffered an accident on the river Potomac [1]. The phenomenon that had caused the failure was called torsional divergence of the wing. The accident of the Langley's plane occurred shortly before the brothers Wright flew their biplane. It can be assumed that the success of the Wright brothers and the failure of the Langley's monoplane are the initial causes of adherence to biplanes at the dawn of aircraft industry. But only in the middle of 1930th designers ventured to build a military monoplane [2, 3].

It should be noted, that biplanes were also characterized by mistakes that led to the aeroelasticity phenomenon, such as



*S. P. Langley
(1834–1906)*

Samuel Pierpont Langley – an American astronomer, physicist, inventor and pioneer of aviation. Professor of mathematics at the United States Naval Academy. In 1867 – director of the Allegheny Observatory, professor of astronomy at the Western University of Pennsylvania, secretary of the Smithsonian Institution. Founder of the Smithsonian Astrophysical Observatory.



Figure 1.1 – S. P. Langley's monoplane

flutter of tail plane feathers. This phenomenon was invented on the American bomber “Handley Page” (Figure 1.2). Several lives had been lost before the means of eliminating this phenomenon were found by a rigid torsion connection of the elevators [4].



O. Wright
(1871–1948)



W. Wright
(1867–1912)

Brothers Wright – inventors, and aviation pioneers, who are generally credited with inventing, building, and flying the world's first successful airplane. They made the first controlled, sustained flight of a powered, heavier-than-air aircraft on December 17, 1903, four miles south of Kitty Hawk (North Carolina).

In 1904 the brothers developed their flying machine into the first practical fixed-wing aircraft. Although not the first to build and fly experimental aircraft, the Wright brothers were the first to invent aircraft controls that made fixed-wing powered flight possible.

The problem of aeroelasticity was especially acute for the transition from biplanes to monoplanes, which can be clearly seen on the example of the German plane “Fokker D.VIII” (Figure 1.3). The first version of this aircraft was a free-carrying monoplane with a high wing. It had excellent characteristics and was quickly introduced into production [5]. However, during its exploitation, especially with air



Figure 1.2 – American bomber “Handley Page”

maneuvers, wings began to tear off. Since these planes were provided for the best pilots and aviation units, there was a danger of total destruction of the German Air Forces. This led to a confrontation between the military engineers and the company “Fokker”. Six planes were subjected to static strength tests, which showed a six-time factor of safety. This fact gave rise to a serious dilemma. It became clear that it was necessary either to find the cause of the damages, or to stop the production of the “Fokker D.VIII”. Repeated static tests were carried out and wear deformations were carefully measured. After the test, A. Fokker thought, that increasing the attack angle of wing ends is a result of increasing the load, which is

the cause of broken wings. Obviously, the pressure load of a dive increases faster at the ends of the wing than in its middle. As a result, the cause of damage is the twisting of the wing during maneuvers. It was the first documented incident, when due to the influence of static aeroelasticity the air loading was redistributed, which led to the damage of the wing.



Figure 1.3 – German airplane “Fokker D.VIII”

In the thirties of the twentieth century, with the advent of high-speed aircrafts, a wave of catastrophes rushed through almost all countries in the world. Casual eyewitnesses, who watched the plane crashes, saw an almost identical picture: the plane was flying perfectly normal, and nothing foretold



A. Fokker
(1890–1939)

Anton Herman Gerard (Anthony) Fokker – a Dutch aviation pioneer and aircraft manufacturer. He was the most famous in the field of the fighter aircraft during the First World War. His company was responsible for a variety of successful aircraft including the Fokker trimotor, a successful passenger aircraft of the inter-war years.

troubles. But suddenly an unknown force destroyed the airplane in an instant. All the eyewitnesses used one expression: “It was an explosion”. However, inspection of the fallen fragments did not confirm this version, because there were no any traces of soot and burns. The surviving pilots as the most reliable source of information could not say anything significant due to unexpected and rapidly evolving events. According to them, a few seconds before the fall “nothing foreshadowed the trouble, but suddenly – shock, crackling, din, and the plane breaks into pieces”.

The new formidable phenomenon was given the name – “flutter”. However, as Moliere once said, “The patient does not get any easier from the fact that he knows the name of his disease”. One by one, alarming news came about the mysterious death of French, British, American and Russian high-speed aircrafts [6].

Thus, in the beginning, engineers and pilots had not yet recognized the special form of oscillatory instability in the abovementioned threatening phenomenon. Only later it was found that flutter is instability of flexural-torsional oscillations of the wing. Now the flutter theory is widely investigated, and the determination of the flutter critical velocity is not the particularly difficult problem.

To the problems of aeroelasticity it is also necessary to include the well-known destruction of the Tacoma Narrows Bridge [7]. For a centuries-old history of bridging techniques, calculation methods have been developed for building reliable bridges. However, there are many historical cases of bridge destructions. There will not be mentioned about incidents associated with resonance, but only about the destructions that occurred in the storm. There are known about ten such facts. The eleventh one is the Tacoma Narrows Bridge (Figure 1.4). About this incident, unlike all the previous ones, not only

testimonies of eyewitnesses and non-specialists were preserved, but also documentary materials, which confirmed the cause of the collapse.



Figure 1.4 – The Tacoma Narrows Bridge collapse

The Tacoma Narrows Bridge was built in 1940 through the Tacoma Canyon. This bridge was always in sight of the researchers, because it had a higher sensitivity to the wind impact. In six months after commissioning it had collapsed due to the relative low wind, the speed of which was equal to 18.7 m/s. It is considered that in a strong storm the wind speed does not exceed 45 m/s, and the Tacoma Narrows Bridge was designed to withstand this extreme load.

The collapse of the bridge had attracted great attention of researchers. Immediately, T. Karman published a technique for calculating the critical speed of divergence [8]. However, the existing documentary video film proved that the destruction occurred due to flexural-torsional oscillations. Later, some attempts were made to correlate the destruction of the bridge with the classical flutter phenomenon. However, the last general accepted explanation is associated with the vortex

breakdown. This aeroelasticity phenomenon was named as a stall flutter [9]. Moreover, stall flutter occurs in case of aircraft wing streamlining if the attack angle exceeds 15° . In addition, propellers of turbines and compressors are increasingly exposed to stall flutter in case of large attack angles.

§ 1.2. The subject of hydroaeroelasticity

Hydroaeroelasticity is a science that investigates the interaction of bodies of finite rigidity with a fluid or gas flow. Hydroelasticity problems are aimed at the research of an interaction between hydroaerodynamic, elastic and inertia forces, as well as its impact on deformable body. It can be explained by the following example. Up-to-date aircraft designs are highly flexible, which is the main cause of various phenomena of aeroelasticity. When flying an airplane, the aerodynamic forces cause deformations of the structure. At the same time, the deformation of the structure of the aircraft leads to additional aerodynamic forces, which can cause even greater forces. Eventually, the design either collapses or is in a stable equilibrium.

Thus, the intrinsic elasticity of the structure is a significant factor for hydroaeroelasticity problems in contrast to the approaches of the classical hydro- and aerodynamics [10, 11], where it is assumed that the design is absolutely rigid. Furthermore, an important factor is taking into account the reverse effect of design deformation to the motion of gas or liquid. Therefore, main equations of hydroaeroelasticity must include the system of all forces acting on the deformable body placed into fluid or gas flow. These are elastic, hydroaerodynamic and inertia forces.

The main problems shaped and solved by the theory of hydroaeroelasticity, can be graphically presented by the Collar's triangle of forces (Figure 1.5) [12].

Consequently, the theory of hydroaeroelasticity is the complex area of mechanics, that combines techniques of the theory of elasticity, structural mechanics and hydroaerodynamics. Since the predominant part of the aeroelastic phenomena has a dynamic nature, therefore,

methods of the theory of oscillations [13–20] are widely used for solving the hydroaeroelasticity problems.

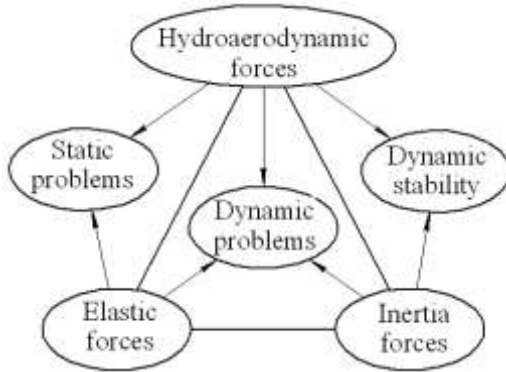


Figure 1.5 – Collar's triangle of forces

The temperature factor is highly significant for up-to-date designs. These problems are the subjects of the theory of aerothermoelasticity [21–22]. Finally, in case of sufficiently flexible structures, elastic deformations have a noticeable impact on the steady motion and control processes, and vice versa. Hence, in the most general case it is necessary to take into account the complicated interaction of elastic, hydroaerodynamic and inertia forces, thermal loads and processes of the control system [23].



A. R. Collar
(1908–1986)

Arthur Roderick Collar – a scientist and engineer, who made significant contributions in the areas of aeroelasticity matrix theory and its applications in engineering dynamics. From 1963 to 1964 – the president of Royal Aeronautical Society.

§ 1.3. Static problems

The simplest static problem of hydroaeroelasticity is the determination of quasi-static loads of the flow acting on the structure taking into account elastic deformations. For solving this problem joint consideration of static equations of the theory of elasticity [24–28] or structural mechanics [29–38] and equations of stationary fluid or gas flow [10, 11] is required.

If the design is sufficiently flexible, a static instability of the original shape occurs due to the critical velocity of the flow. The most famous example of static instability is the divergence of the aircraft wings. Another one is the static buckling of plates and shells, streamlined by a gas stream. Along with aerodynamic forces an important role is played by initial forces in the middle surface and temperature loads.

Other static phenomena include the impact of static elastic deformations on the stability of the control system, for example, the reverse of rudders and ailerons. When the aileron is deflected downwards, the lift force on the wing increases, and the heeling moment is being created. However, the aileron deflection also creates an aerodynamic diving moment, which twists the wing in the direction of reducing the lift force and, consequently, leads to the decrease of the heeling moment. Because the stiffness of the wing does not depend on the flight velocity, but the aerodynamic force depends on the square of the velocity U^2 , then there is a critical velocity U_{cr} at which the aileron is completely ineffective. This velocity is called “the critical velocity of aileron’s reverse”. A similar effect also occurs with the reverse of lift rudders and steering wheels.

§ 1.4. Dynamic problems

The most important example of the dynamic problems of hydroaeroelasticity is the flutter of the aircraft wings as a phenomenon of self-oscillations [39, 40] supported by the energy of motion or flow energy. Another example is panel flutter as self-oscillations of plates and shells [41–45] streamlined by the flow. An important role for this interaction is the relationship between different forms of oscillations. It is enough to use the linearized theory of potential flow [46, 47] for describing the classical flutter.

There are self-oscillating aeroelastic phenomena, the origin of which has a different nature. For example, a stall flutter [9, 48, 49] of blades and screws, that occurs in case of high values of attack angles. Another one is self-oscillations of the wires of chimneys, beams of rigidity for suspension bridges [50] and other poorly streamlined bodies. The abovementioned phenomena are accompanied by flow disruptions on the streamlined surface and by the formation of the Karman vortex street (Figure 1.6) [51–61], as well as other non-classical features.

In addition, one of the problem of aeroelasticity is buffeting as a phenomenon, in which the deformation of the



T. Karman
(1881–1963)

Theodore von Karman – a Hungarian-American mathematician, aerospace engineer and physicist, who was active primarily in the fields of aeronautics and astronautics. He was responsible for many key advances in aerodynamics, notably his work on supersonic and hypersonic airflow characterization. He is regarded as the outstanding aerodynamic theoretician of the twentieth century.

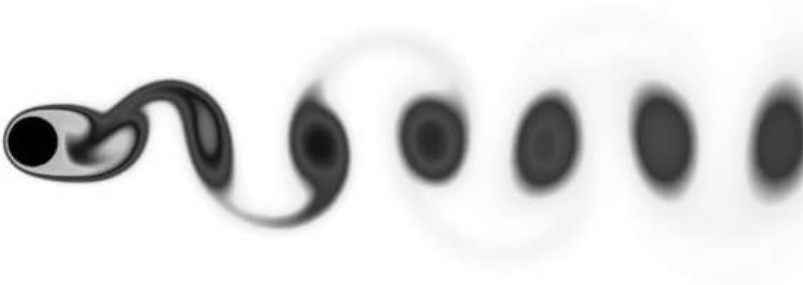


Figure 1.6 – Karman vortex street

supporting surface (e. g., the aircraft wing) is caused by the action of powerful vortex flows formed in front of the supporting surface. This phenomenon is mainly affects on aircraft tails and blades of turbomachines. Unfortunately, theoretically this problem is quite complicated, because the nature of the jet motion behind the wing is not completely investigated [62–67].

Questions for self-control

1. What problems had predetermined the emergence of the subject “hydroaeroelasticity”?
2. What mistakes of aircraft industry led to the aeroelasticity phenomenon?
3. Describe the first documented incident which led to damage of the aircraft wing.
4. Describe the life example of manifestation of the phenomenon of aeroelasticity.
5. What phenomena of aeroelasticity can be described by the Karman’s theory?
6. Set the subject of hydroaeroelasticity. Explain, what disciplines, in your opinion, should precede the study of hydroaeroelasticity.
7. Describe in detail the Collar’s triangle of forces. What is its physical meaning?
8. In which disciplines the interdisciplinary connections are shown with the contribution of hydroaeroelasticity?
9. What techniques does the theory of hydroaeroelasticity combine?
10. What scientists made the first contribution to the development of elasticity? Describe their participation.

CHAPTER 2.
Determination of the dynamic
forces acting on deformable
surfaces

§ 2.1. Potential flow equations

For the determination of the hydroaeroelastic forces [68] equations of fluid or gas motion and deformable shapes are used. In the general case this problem is extremely complicated. Therefore, it is necessary to take a number of simplifying assumptions, such as gas, which streamlines the body (e. g. wing, blade, part of the aircraft skin), and it is ideal. Therefore its motion is described by Euler's equations [69]:

$$\left\{ \begin{array}{l} \frac{du}{dt} = \frac{\partial u}{\partial t} + u \frac{\partial u}{\partial x} + v \frac{\partial u}{\partial y} + w \frac{\partial u}{\partial z} = X - \frac{1}{\rho} \frac{\partial p}{\partial x}; \\ \frac{dv}{dt} = \frac{\partial v}{\partial t} + u \frac{\partial v}{\partial x} + v \frac{\partial v}{\partial y} + w \frac{\partial v}{\partial z} = Y - \frac{1}{\rho} \frac{\partial p}{\partial y}; \\ \frac{dw}{dt} = \frac{\partial w}{\partial t} + u \frac{\partial w}{\partial x} + v \frac{\partial w}{\partial y} + w \frac{\partial w}{\partial z} = Z - \frac{1}{\rho} \frac{\partial p}{\partial z}, \end{array} \right. \quad (2.1)$$

or in vector form:

$$\frac{d\vec{V}}{dt} = \vec{F} - \frac{1}{\rho} \text{grad } p, \quad (2.2)$$



L. Euler
(1707–1783)

Leonhard Euler – a Swiss mathematician, physicist, astronomer, logician and engineer, who made important and influential discoveries in infinitesimal calculus and graph theory, topology and analytic theory. He also introduced much of the modern mathematical terminology and notation, particularly for mathematical analysis, such as the notion of a mathematical function. He is known for his works in mechanics and fluid dynamics.

where u, v, w are the components of the velocity:

$$\vec{V} = u\vec{i} + v\vec{j} + w\vec{k}; \quad (2.3)$$

X, Y, Z – the components of specific mass force, N/m^3 ;
 p – pressure; ρ – density; $\vec{i}, \vec{j}, \vec{k}$ – unit vectors of axes x, y, z ;
 $grad$ – gradient operator:

$$grad\ p = \frac{\partial p}{\partial x}\vec{i} + \frac{\partial p}{\partial y}\vec{j} + \frac{\partial p}{\partial z}\vec{k}. \quad (2.4)$$

Euler's equation can be rewritten as Gromeka–Lamb equation:

$$\frac{\partial \vec{V}}{\partial t} - grad\left(\frac{\vec{V}^2}{2}\right) + (rot\ \vec{V} \times \vec{V}) = \vec{F} - \frac{1}{\rho} grad\ p, \quad (2.5)$$

where the vortex part is explicitly shown:

$$rot\ \vec{V} \times \vec{V} = \begin{vmatrix} \vec{i} & \vec{j} & \vec{k} \\ (rot\ \vec{V})_x & (rot\ \vec{V})_y & (rot\ \vec{V})_z \\ u & v & w \end{vmatrix}; \quad (2.6)$$



Ippolit Stepanovich Gromeka – a Russian mechanical scientist, professor at Kazan University. He gave an original explanation of the theory of capillary phenomena. The flow of an ideal fluids is described by the Gromeka–Lamb equation.

*I. S. Gromeka
(1851–1889)*

$rot\vec{V}$, $(rot\vec{V})_{x,y,z}$ – rotor operator and its projections:

$$rot\vec{V} = \begin{vmatrix} \vec{i} & \vec{j} & \vec{k} \\ \frac{\partial}{\partial x} & \frac{\partial}{\partial y} & \frac{\partial}{\partial z} \\ u & v & w \end{vmatrix} = (rot\vec{V})_x \vec{i} + (rot\vec{V})_y \vec{j} + (rot\vec{V})_z \vec{k} \quad (2.7)$$

$$(rot\vec{V})_x = \frac{\partial w}{\partial y} - \frac{\partial v}{\partial z}; (rot\vec{V})_y = \frac{\partial u}{\partial z} - \frac{\partial w}{\partial x}; (rot\vec{V})_z = \frac{\partial v}{\partial x} - \frac{\partial u}{\partial y}. \quad (2.8)$$

For closing the system of equations (2.1) it must be supplemented by a continuity equation and its vector form:

$$\frac{\partial \rho}{\partial t} + \frac{\partial}{\partial x}(\rho u) + \frac{\partial}{\partial y}(\rho v) + \frac{\partial}{\partial z}(\rho w) = 0, \quad (2.9)$$

$$\frac{\partial \rho}{\partial t} + div(\rho \vec{V}) = 0, \quad (2.10)$$

where div is divergence operator:

$$div(\rho \vec{V}) = \frac{\partial}{\partial x}(\rho u) + \frac{\partial}{\partial y}(\rho v) + \frac{\partial}{\partial z}(\rho w). \quad (2.11)$$



H. Lamb
(1849–1934)

Horace Lamb – an English applied mathematician, author of several influential texts on classical physics, among them “Hydrodynamics” (1895) and “Dynamical theory of sound” (1910).

Let's take the following assumptions:

1. The flow is potential:

$$u = \frac{\partial \varphi}{\partial x}; v = \frac{\partial \varphi}{\partial y}; w = \frac{\partial \varphi}{\partial z}, \quad (2.12)$$

where φ is the velocity potential, m²/s. Due to the equation (2.8) it can be assumed, that

$$\text{rot} \vec{V} = 0. \quad (2.13)$$

2. Mass forces are negligibly small: $X = Y = Z = 0$.

3. Fluid motion is barotropic. This means that the gas density is a function of only the pressure: $\rho = \rho(p)$, which occurs, for example, in such cases:

a) incompressible fluid: $\rho = \text{const}$;

b) isothermal flow: $p = \rho \cdot RT_0$, where R – universal gas constant; T_0 – normal temperature on the Kelvin scale;

c) adiabatic flow: $p = C \cdot \rho^k$, where $C = \text{const}$; k – adiabatic index (e.g., for air $k = 1,45$).

Due to the abovementioned assumptions equations of fluid motion (2.5) will take the following form:

$$\begin{aligned} \frac{\partial}{\partial x} \left(\frac{\partial \varphi}{\partial t} + \frac{\vec{V}^2}{2} + P \right) = 0; \quad \frac{\partial}{\partial y} \left(\frac{\partial \varphi}{\partial t} + \frac{\vec{V}^2}{2} + P \right) = 0; \\ \frac{\partial}{\partial z} \left(\frac{\partial \varphi}{\partial t} + \frac{\vec{V}^2}{2} + P \right) = 0, \end{aligned} \quad (2.14)$$



W. T. Kelvin
(1824–1907)

William Thomson Kelvin – a Scots-Irish mathematical physicist, the creator of “absolute zero” temperature, the low limit temperature units of which are now presented in units of Kelvin scale in his honour. He is popularly known and remembered for his outstanding achievements in the field of physics and mechanics. Kelvin also propounded the first and second laws of thermodynamics.

or

$$\text{grad}\left(\frac{\partial\varphi}{\partial t} + \frac{\vec{V}^2}{2} + P\right) = 0, \quad (2.15)$$

where P – pressure function:

$$P = \int_{p_0}^p \frac{dp}{\rho(p)}; \quad (2.16)$$

$$\frac{\partial P}{\partial x} = \frac{1}{\rho} \frac{\partial p}{\partial x}; \quad \frac{\partial P}{\partial y} = \frac{1}{\rho} \frac{\partial p}{\partial y}; \quad \frac{\partial P}{\partial z} = \frac{1}{\rho} \frac{\partial p}{\partial z};$$

p_0 – initial pressure.

As a result the Bernoulli integral can be obtained:

$$\frac{\partial\varphi}{\partial t} + \frac{\vec{V}^2}{2} + P = f(t). \quad (2.17)$$

With an appropriate choice of the boundary conditions, an unknown time function $f(t) = 0$ can be always obtained. Thus,

$$\frac{\partial\varphi}{\partial t} + \frac{\vec{V}^2}{2} + \int \frac{dp}{\rho} = 0. \quad (2.18)$$



D. Bernoulli
(1700–1782)

Daniel Bernoulli – a Swiss mathematician and physicist, one of the many prominent mathematicians in the Bernoulli family. He is particularly remembered for his applications of mathematics to mechanics, especially fluid mechanics, and for his pioneering work in probability and statistics. His name is commemorated in the Bernoulli's principle, a particular example of the conservation of energy.

A continuity equation (2.10) can be rewritten in the following form:

$$\frac{\partial \rho}{\partial t} + \rho \operatorname{div} \vec{V} + \vec{V} \operatorname{grad} \rho = 0, \quad (2.19)$$

or

$$\frac{a^2}{\rho} \frac{\partial \rho}{\partial t} + a^2 \operatorname{div} \vec{V} + a^2 \vec{V} \frac{\operatorname{grad} \rho}{\rho} = 0, \quad (2.20)$$

where a^2 – sound velocity or velocity of small perturbations extension:

$$a^2 = \frac{\partial p}{\partial \rho}. \quad (2.21)$$

The pressure function (2.16) takes the form

$$P = \int \frac{dp}{\rho} = \int \frac{dp}{\rho} \frac{d\rho}{d\rho} = a^2 \int \frac{d\rho}{\rho} = a^2 \ln \rho, \quad (2.22)$$

and the equation (2.15) can be rewritten:

$$\operatorname{grad} \left(\frac{\partial \varphi}{\partial t} + \frac{\vec{V}^2}{2} + a^2 \ln \rho \right) = 0, \quad (2.23)$$

or taking into account

$$\operatorname{grad} (a^2 \ln \rho) = a^2 \frac{\operatorname{grad} \rho}{\rho}, \quad (2.24)$$

it can be obtained:

$$\begin{aligned} \text{grad}\left(\frac{\partial\varphi}{\partial t} + \frac{\vec{V}^2}{2}\right) + a^2 \frac{\text{grad}\rho}{\rho} &= 0; \\ \frac{\partial}{\partial t}\left(\frac{\partial\varphi}{\partial t} + \frac{\vec{V}^2}{2}\right) + \frac{a^2}{\rho} \frac{\partial\rho}{\partial t} &= 0, \end{aligned} \quad (2.25)$$

that after substitution in equation (2.20) gives

$$\nabla^2\varphi - \frac{1}{a^2} \left[\frac{\partial^2\varphi}{\partial t^2} + \frac{\partial}{\partial t}(\vec{V}^2) + \vec{V} \text{grad} \frac{\vec{V}^2}{2} \right] = 0. \quad (2.26)$$

Thus, the problem consists in solving the equation (2.26) and the Bernoulli integral (2.18) within the boundary conditions. Equation of the streamlined surface $F(x, y, z, t) = 0$ can be written separately for the upper and lower surfaces:

$$\begin{aligned} y_u &= Y_u(x, y, z, t); \\ y_l &= Y_l(x, y, z, t), \end{aligned} \quad (2.27)$$

then the boundary conditions takes the form:

$$\begin{aligned} v_u &= \frac{dY_u}{dt} = \frac{\partial Y_u}{\partial t} + u \frac{\partial Y_u}{\partial x} + v \frac{\partial Y_u}{\partial y} + w \frac{\partial Y_u}{\partial z} (y_u = Y_u); \\ v_l &= \frac{dY_l}{dt} = \frac{\partial Y_l}{\partial t} + u \frac{\partial Y_l}{\partial x} + v \frac{\partial Y_l}{\partial y} + w \frac{\partial Y_l}{\partial z} (y_l = Y_l). \end{aligned} \quad (2.28)$$

It is easy to notice that equations of the potential flow (2.18), (2.26) and the boundary conditions (2.28) are nonlinear.

§ 2.2. Using small perturbation method for linearization of equations

If the body placed in the flow is well-streamlined, then the perturbations introduced by it will be sufficiently small [70, 71]. Then equations (2.18), (2.26) and (2.28) can be linearized with respect to perturbations of the velocity potential ϕ' . An exception is the case of stall flutter in which the nonlinearity is highly essential.

Let the unperturbed flow velocity U be directed parallel to the axis OX (Figure 2.1).

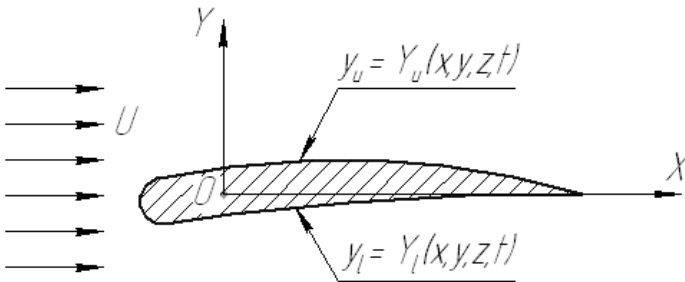


Figure 2.1 – Streamlined aircraft wing profile

Obviously, this velocity slightly changes by a small amount due to the streamlined body. The changed velocity differs from the unperturbed one by an infinitesimal amount with components u' , v' , w' :

$$u = U + u' = U + \frac{\partial \phi'}{\partial x}; v = v' = \frac{\partial \phi'}{\partial y}; w = \frac{\partial \phi'}{\partial z}. \quad (2.29)$$

Similarly, other physical parameters are

$$p = p_0 + p'; \rho = \rho_0 + \rho'; a = a_0 + a', \quad (2.30)$$

where p_0, ρ_0, a_0 – undisturbed parameters.

Moreover, $\varphi = \varphi' + U \cdot x$, where φ' is the disturbed velocity potential. Thus, the velocity vector

$$\vec{V} = \left(U + \frac{\partial \varphi'}{\partial x} \right) \vec{i} + \frac{\partial \varphi'}{\partial y} \vec{j} + \frac{\partial \varphi'}{\partial z} \vec{k} = U \vec{i} + \text{grad} \varphi'. \quad (2.31)$$

Up to the first order terms it can be written:

$$\begin{aligned} \vec{V}^2 &= \left(U \vec{i} + \text{grad} \varphi' \right)^2 \approx U^2 + 2U \frac{\partial \varphi'}{\partial x}; \\ \frac{\partial}{\partial t} (\vec{V}^2) &\approx 2U \frac{\partial^2 \varphi'}{\partial x \partial t}; \\ \vec{V} \text{ grad} \frac{\vec{V}^2}{2} &\approx \left(U \vec{i} + \text{grad} \varphi' \right) \text{grad} \left(U \frac{\partial \varphi'}{\partial x} \right) = U^2 \frac{\partial^2 \varphi'}{\partial x^2}; \\ \int \frac{dp}{\rho} &= \int \frac{dp'}{\rho_0 + \rho'} = \int \left(1 + \frac{\rho'}{\rho_0} \right)^{-1} \frac{dp'}{\rho_0} \approx \frac{p'}{\rho_0}. \end{aligned} \quad (2.32)$$

Due to (2.32) the Bernoulli equation (2.18) can be written:

$$p' = p - p_0 = -\rho_0 \left(\frac{\partial}{\partial t} + U \frac{\partial}{\partial x} \right) \varphi'. \quad (2.33)$$

Similarly, the equation (2.26) can be linearized:

$$\nabla^2 \varphi' - \frac{1}{a^2} \left(\frac{\partial}{\partial t} + U \frac{\partial}{\partial x} \right)^2 \varphi' = 0. \quad (2.34)$$

Introducing into consideration the Mach number

$$M = \frac{U}{a_0} \quad (2.35)$$

allows writing equation (2.34) in the following form:

$$(M^2 - 1) \frac{\partial^2 \varphi'}{\partial x^2} + 2 \frac{M}{a_0} \frac{\partial^2 \varphi'}{\partial x \partial t} + \frac{1}{a_0^2} \frac{\partial^2 \varphi'}{\partial t^2} - \frac{\partial^2 \varphi'}{\partial y^2} - \frac{\partial^2 \varphi'}{\partial z^2} = 0. \quad (2.36)$$

The boundary conditions (2.28) after linearization:

$$\begin{aligned} v_u &= \frac{\partial Y_u}{\partial t} + U \frac{\partial Y_u}{\partial x} (y_u = Y_u); \\ v_l &= \frac{\partial Y_l}{\partial t} + U \frac{\partial Y_l}{\partial x} (y_l = Y_l). \end{aligned} \quad (2.37)$$

Finally, the problem reduces to solving the equation (2.34) or (2.36) with respect to the disturbed velocity potential φ' within



E. Mach
(1838–1916)

Ernst Mach – an Austrian physicist and philosopher, noted for his contributions to physics such as study of shock waves. The ratio of speed to the sound velocity is named by the Mach number in his honour.

the boundary conditions (2.37) with the subsequent determination of pressure p by equation (2.33).

The lift force, which must be used in hydroaeroelasticity problems, is defined as the curvilinear integral over the contour from the pressure difference.

The equation (2.36) particularly can be reduced to the following forms:

1. Transonic nonstationary flow ($M \approx 1$):

$$\frac{2}{a_0} \frac{\partial^2 \varphi'}{\partial x \partial t} + \frac{1}{a_0^2} \frac{\partial^2 \varphi'}{\partial t^2} - \frac{\partial^2 \varphi'}{\partial y^2} - \frac{\partial^2 \varphi'}{\partial z^2} = 0; \quad (2.38)$$

$$p' = -\rho_0 \left(\frac{\partial \varphi'}{\partial t} + U \frac{\partial \varphi'}{\partial x} \right).$$

2. Quasi-stationary transonic flow ($M \approx 1$; $\partial \varphi' / \partial t = 0$):

$$\frac{\partial^2 \varphi'}{\partial y^2} + \frac{\partial^2 \varphi'}{\partial z^2} = 0; \quad (2.39)$$

$$p' = -\rho_0 U \frac{\partial \varphi'}{\partial x}.$$

3. High-frequency oscillations ($U \rightarrow 0$; $\partial \varphi' / \partial x = 0$):

$$\frac{1}{a_0^2} \frac{\partial^2 \varphi'}{\partial t^2} - \frac{\partial^2 \varphi'}{\partial y^2} - \frac{\partial^2 \varphi'}{\partial z^2} = 0; \quad (2.40)$$

$$p' = -\rho_0 \frac{\partial \varphi'}{\partial t}.$$

4. Incompressible fluid flow ($a_0 \rightarrow \infty$; $M \rightarrow 0$):

a. General case:

$$\nabla^2 \varphi' = 0;$$
$$p' = -\rho_0 \left(\frac{\partial \varphi'}{\partial t} + U \frac{\partial \varphi'}{\partial x} \right). \quad (2.41)$$

b. Small width wing:

$$\frac{\partial^2 \varphi'}{\partial y^2} + \frac{\partial^2 \varphi'}{\partial z^2} = 0. \quad (2.42)$$

c. Infinite length wing ($\partial \varphi' / \partial z = 0$):

$$\frac{\partial^2 \varphi'}{\partial x^2} + \frac{\partial^2 \varphi'}{\partial y^2} = 0. \quad (2.43)$$

§ 2.3. Aircraft wing oscillations in two-dimensional incompressible fluid flow

Incompressible fluid flow is described by equations (2.41) for harmonic function φ' with the boundary conditions:

$$v = \frac{\partial Y}{\partial t} + U \frac{\partial Y}{\partial x} \quad (2.44)$$

where $Y = Y(x, t)$ is profile equation.

In a linear formulation, the problem can be divided into two subproblems:

1. Nonstationary flow for the case of zero thickness and zero curvature wing in case of rectilinear forward motion with the velocity U . This motion is superimposed by harmonic oscillations with an infinitesimal amplitude:

a. Flexural oscillations: $y(t) = ye^{i\omega t}$.

b. Torsional oscillations: $y(t) = \alpha xe^{i\omega t}$.

2. Stationary flow for the wing of predetermined small thickness, curvature and an average attack angle α_m within the linear theory.

The first of the abovementioned approaches is the most complicated and can be solved by different techniques:

- conformal mapping [72–74];
- method of hydrodynamic features [75];
- operational calculus (Laplace and Fourier transforms) [76–81].

Unsteady harmonic oscillations of a wing of zero thickness and zero curvature in two-dimensional incompressible fluid flow are considered for the case of an average attack angle $\alpha_m = 0^\circ$. The flow velocity U is parallel to the chord or axis Ox .

The abovementioned problem consists in solving Laplace equation $\nabla^2 \varphi = 0$, in other words, in the determination of the velocity potential satisfying the boundary conditions, that significantly complicate the problem.

A considerable simplification can be achieved by introducing the complex velocity potential

$$W(z) = \varphi(x, y) + i\psi(x, y) \quad (2.45)$$

with using the conformal mapping method [72–74] and Zhoukovsky transform [82]

$$z = \frac{1}{2} \left(\zeta + \frac{1}{\zeta} \right) \quad (2.46)$$

of the unit circle (Figure 2.2 a) $\zeta = e^{i\theta}$; ($0 \leq \theta \leq 2\pi$) to the line segment (Figure 2.2 b) $y = 0$; ($-1 \leq x \leq 1$), where i – imaginary unit ($i^2 = -1$); θ – argument of the complex vector.

If $W(\zeta)$ is well-known complex potential for the cylinder in auxiliary plane [83–85], then a function $W(z)$ can be determined by inverse formulas:

$$\begin{aligned} x &= \cos \mathcal{G}; \\ \mathcal{G} &= \arccos x. \end{aligned} \quad (2.47)$$



P.-S. Laplace
(1749–1827)

Pierre-Simon Laplace – an influential French scholar whose work was important to the development of mathematics, statistics, physics and astronomy. Laplace formulated Laplace’s equation and pioneered the Laplace transform, which appears in many branches of mathematical physics. The Laplacian differential operator is widely used in mathematics and named after him.

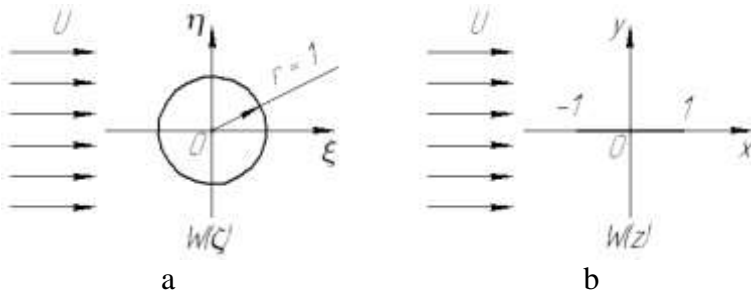


Figure 2.2 – Conformal mapping of the unit circle:
 a – auxiliary plane; b – physical plane

Each fluid motion corresponds to its own complex velocity potential. Consequently, if the function $W(z)$ is known, then potential $\varphi(x, y)$, as well as the velocity components u, v can be determined. Thereafter, the pressure p is determined by the Bernoulli integral.

However, it is more convenient to solve this problem not for the velocity potential, but for the acceleration potential Φ :

$$\begin{aligned}
 a_x &= \frac{du}{dt} = \frac{\partial \Phi}{\partial x}; \\
 a_y &= \frac{dv}{dt} = \frac{\partial \Phi}{\partial y},
 \end{aligned}
 \tag{2.48}$$

where a_x, a_y – components of the acceleration.



J.-B. Fourier
 (1768–1830)

Jean-Baptiste Joseph Fourier – a French mathematician and physicist, best known for initiating the investigation of Fourier series and their applications to the problems of heat transfer and vibrations. The Fourier transform and Fourier’s law are also named in his honour.

Similarly the conjugate function $\Psi(x, y)$ can be introduced:

$$a_x = \frac{\partial \Psi}{\partial y}; \quad a_y = -\frac{\partial \Psi}{\partial x}. \quad (2.49)$$

Thus, the acceleration potential takes the following form:

$$W(z) = \Phi(x, y) + i\Psi(x, y), \quad (2.50)$$

where $z = x + iy$ – complex vector, and functions $\Phi(x, y)$, $\Psi(x, y)$ satisfy the Cauchy–Riemann theorem [86]:

$$\frac{\partial \Phi}{\partial x} = \frac{\partial \Psi}{\partial y}; \quad \frac{\partial \Phi}{\partial y} = -\frac{\partial \Psi}{\partial x}. \quad (2.51)$$

In this case, the complex function $W(z) = \Phi + i\Psi$ is not simply dependent on x and y , but is a function of one complex variable $z = x + iy$, and

$$\frac{dW}{dz} = a_x - ia_y \quad (2.52)$$

as a mirror image of the complex acceleration $a = a_x + ia_y$.



*N. E. Joukowsky
(1847–1921)*

Nikolai Egorovich Zhukowsky – a Russian mechanic, founder of aerodynamics and aeromechanics as sciences. Zhukowsky’s works in the field of aerodynamics were the source of the basic ideas on which the aviation science was built. Zhukovsky discovered a law that determines the lifting power for aircraft wings and determined the main profiles of wings and blades. N. E. Zhukowsky is a founder of the Central Institute of Aerodynamics.

Moreover,

$$\frac{dW}{d\zeta} = \frac{dW}{dz} \cdot \frac{dz}{d\zeta}, \quad (2.53)$$

where due to the equation (2.46)

$$\frac{dz}{d\zeta} = \frac{1}{2} \left(1 - \frac{1}{\zeta^2} \right). \quad (2.54)$$

The introduction of the complex acceleration potential is caused by the fact that the function $\Phi(x, y)$ is absolutely continuous one.

Due to the Bernoulli integral, velocities and pressures at both sides of the edge are equalized while the body is streamlined by steady flow.

In case of unsteady flow pressures are equalized, but velocities are not, what explains the origin of the aerodynamic trail [87]. The function $\varphi(x, y)$ is discontinuous in contrast to $\Phi(x, y)$.

Due to the velocity components $u = U + u'$ and $v = V + v'$, linearization of the acceleration components is carried out according to formulas:



A.-L. Cauchy
(1789–1857)

Augustin-Louis Cauchy – a French mathematician, who made pioneering contributions to analysis. He was one of the first to state and prove theorems of calculus rigorously, rejecting the heuristic principle of the generality of algebra of earlier authors. He almost founded the complex analysis and the study of permutation groups in abstract algebra.

$$\begin{aligned}
 a_x &= \frac{du}{dt} = \frac{\partial u}{\partial t} + u \frac{\partial u}{\partial x} + v \frac{\partial u}{\partial y} \approx \frac{\partial u'}{\partial t} + U \frac{\partial u'}{\partial x}; \\
 a_y &= \frac{dv}{dt} = \frac{\partial v}{\partial t} + u \frac{\partial v}{\partial x} + v \frac{\partial v}{\partial y} \approx \frac{\partial v'}{\partial t} + U \frac{\partial v'}{\partial x},
 \end{aligned}
 \tag{2.55}$$

and $a_x = a'_x$, $a_y = a'_y$, because $U = \text{const}$, as well as the acceleration components are zero at infinity.

It can be shown that a new function also satisfies harmonic Laplace equation. After differentiating continuity equation with respect to time we have:

$$\begin{aligned}
 \frac{d}{dt} \left(\frac{\partial u}{\partial x} + \frac{\partial v}{\partial y} \right) &= \frac{\partial a_x}{\partial x} + \frac{\partial a_y}{\partial y} = \frac{\partial^2 \Phi}{\partial x^2} + \frac{\partial^2 \Phi}{\partial y^2} = 0; \\
 \nabla^2 \Phi' &= 0.
 \end{aligned}
 \tag{2.56}$$

because $\Phi = \Phi_0 + \Phi'$ ($\Phi_0 = \text{const}$) due to $a_x = a'_x$.

The main problem is to identify the harmonic function, which allows determining the pressure. From the Euler's equation

$$\frac{du}{dt} = -\frac{1}{\rho} \frac{\partial p}{\partial x} = -\frac{\partial P}{\partial x} = a_x; \quad \frac{dv}{dt} = -\frac{1}{\rho} \frac{\partial p}{\partial y} = -\frac{\partial P}{\partial y} = a_y, \tag{2.57}$$



B. Riemann
(1826–1866)

Bernhard Riemann – a German mathematician, who made contributions to analysis, number theory and differential geometry. In the field of real analysis, he is mostly known for the first rigorous formulation of the integral, the Riemann integral and his work on Fourier series. His contributions to complex analysis include most notably the introduction of Riemann surfaces.

and due to the equation (2.48):

$$\frac{\partial \Phi}{\partial x} + \frac{\partial P}{\partial x} = 0; \quad \frac{\partial \Phi}{\partial y} + \frac{\partial P}{\partial y} = 0, \quad (2.58)$$

so, $\Phi + P = f(t) = 0$ or

$$\Phi + \int \frac{dp}{\rho} = 0. \quad (2.59)$$

After linearization ($p = p_0 + p'$; $\rho = \rho_0$ in case of incompressible flow) it can be obtained:

$$\begin{aligned} \Phi + \frac{p'}{\rho_0} &= 0; \\ p' &= -\rho_0 \Phi = -\rho_0 \Phi'. \end{aligned} \quad (2.60)$$

Thus, the acceleration potential is proportional to the pressure difference p' that is the physical interpretation of the acceleration potential, which satisfies the Laplace equation (2.55).

The boundary conditions:

1. At the infinity ($u' = v' = 0$): $\Phi' = 0$;
2. On the border:
 - a. For the velocity:

$$v'_w = \frac{\partial Y}{\partial t}; \quad (2.61)$$

- b. For the acceleration: $a'_w = \frac{\partial a'_w}{\partial t} = \frac{\partial^2 Y}{\partial t^2}$ or

$$\frac{\partial \Phi'}{\partial y} = \frac{\partial^2 Y}{\partial t^2}, \quad (2.62)$$

where the subscript “w” means that the velocity or acceleration is on the wing surface.

It is obviously, that the acceleration potential, which satisfies the condition (2.62), does not necessarily satisfy the previous one (2.61). Therefore it is necessary to express the velocity v' through the potential Φ' . From the equations (2.48) and (2.55):

$$a'_y = \frac{\partial v'}{\partial t} + U \frac{\partial v'}{\partial x} = \frac{\partial \Phi'}{\partial y}. \quad (2.63)$$

The last differential equation can be solved for the case of monoharmonic oscillations. A complex presentation of the quantities is used:

$$\begin{aligned} \Phi' &= \Phi(x, y)e^{j\omega t}; \\ v' &= v(x, y)e^{j\omega t}, \end{aligned} \quad (2.64)$$

where j – imaginary unit ($j^2 = -1$).

Substitution of expressions (2.62) into the first order differential equation (2.63) after simple identity transformations gives

$$\frac{\partial v}{\partial x} + \frac{j\omega v}{U} = \frac{1}{U} \frac{\partial \Phi}{\partial y} \quad (2.65)$$

with the condition: $v|_{x \rightarrow -\infty} = 0$.

For solving an equation (2.63) the method of variation of parameters [88, 89] can be used:

$$v = v_1 C(x) + v_2 D(x) + \dots, \quad (2.66)$$

where v_1, v_2, \dots – linearly independent solutions of homogeneous differential equation:

$$\frac{\partial v}{\partial x} + \frac{j\omega v}{U} = 0. \quad (2.67)$$

In case of series expansion (2.64) and taking into account only its first term $v_1 C(x)$ it can be obtained

$$v_1 = e^{-\frac{j\omega x}{U}} \quad (2.68)$$

up to an arbitrary constant. Thus,

$$\frac{dC}{dx} e^{-\frac{j\omega x}{U}} = \frac{1}{U} \frac{\partial \Phi}{\partial y} \quad (2.69)$$

and after integration:

$$C(x) = \frac{1}{U} \int \frac{\partial \Phi}{\partial y} e^{\frac{j\omega x}{U}} dx + D, \quad (2.70)$$

and the velocity function in order to the condition $v|_{x \rightarrow -\infty} = 0$:

$$v(x) = \frac{1}{U} e^{-\frac{j\omega x}{U}} \int_{-\infty}^x \frac{\partial \Phi}{\partial y} e^{\frac{j\omega x}{U}} dx. \quad (2.71)$$

Thus, the boundary condition (2.61) expressed by the acceleration potential, takes the following form:

$$v'_w = v(x, y)e^{j\omega t} = \left(\frac{1}{U} e^{-\frac{j\omega x}{U}} \int_{-\infty}^x \frac{\partial \Phi}{\partial y} e^{\frac{j\omega x}{U}} dx \right) e^{j\omega t} = \frac{\partial Y}{\partial t}. \quad (2.72)$$

In addition to the abovementioned boundary conditions, the flow must satisfy the Kutta–Zhoukovsky–Chaplygin’s postulate [90, 91] about finiteness of the flow velocity in its trailing edge.

Determining the complex acceleration potential in the auxiliary plane is not such a difficult problem as satisfying the boundary conditions on the unit circle, which is due to the fact that these conditions (2.61), (2.62) and (2.72) are given in the physical plane.

For transforming the complex acceleration potential $W(z) = \Phi(x, y) + i\Psi(x, y)$ into the auxiliary plane $W(\zeta) = \Phi(\zeta, \eta) + i\Psi(\zeta, \eta)$ by Zhoukovsky transform (2.46) with using the dependences (2.53), (2.54), the boundary condition at infinity ($|\zeta| \rightarrow \infty$):

$$\left. \frac{dW}{d\zeta} \right|_{\infty} = (a_{\xi} - ia_{\eta})_{\infty} = \frac{1}{2}(a_x - ia_y)_{\infty} = 0, \quad (2.73)$$



M. W. Kutta
(1867–1944)

Martin Wilhelm Kutta – a German mathematician, professor at the RWTH Aachen University, professor at the University of Stuttgart, who co-developed the Runge–Kutta method, used to solve ordinary differential equations numerically. He is also remembered for the Zhoukovsky–Kutta aerofoil, the Kutta–Zhoukovsky–Chaplygin’s postulate and the Kutta condition in aerodynamics.

because of $a_x|_{\infty} = a_y|_{\infty} = 0$ and $a_{\xi}|_{\infty} = a_{\eta}|_{\infty} = 0$.

Thus,

$$W(\xi, \eta)|_{\infty} = \text{const} \quad (2.74)$$

On the border ($\zeta = e^{i\theta}$):

$$\begin{aligned} \frac{dW}{d\zeta} \Big|_{\zeta=e^{i\theta}} &= (a_{\xi} - ia_{\eta}) \Big|_{\zeta=e^{i\theta}} = a_n e^{i\theta} = \\ &= \frac{1}{2} \left(1 - \frac{1}{\zeta^2} \right) (a_x - ia_y) \Big|_{\zeta=e^{i\theta}}, \end{aligned} \quad (2.75)$$

where a_n – normal projection of the acceleration.

Due to $a_x = 0$ on the border, it can be written:

$$\begin{aligned} a_n e^{-i\theta} &= a_y \frac{1}{2i} (e^{i\theta} - e^{-i\theta}) \frac{1}{e^{i\theta}}; \\ a_n \Big|_{r=1; \vartheta=\arccos\theta} &= a_y(x, 0, t) \sin \theta = \frac{\partial^2 Y}{\partial t^2} \sin \theta. \end{aligned} \quad (2.76)$$

Equations (2.74), (2.76), (2.61) and the Kutta–



S. A. Chaplygin
(1869–1942)

Sergey Alexeyevich Chaplygin – a Russian physicist, mathematician and mechanical engineer. He is known for mathematical formulas such as Chaplygin's equation and for a hypothetical substance in cosmology called Chaplygin gas, named after him. He taught mechanical engineering at Moscow Higher Womens' Courses and applied mathematics at Moscow School of Technology.

Zhoukovsky–Chaplygin’s postulate are the general system of the boundary conditions.

According to the first condition (2.74) the function $W(\zeta)$ can be taken in the form of the Laurent series [92, 93]:

$$W(\zeta) = A_0 + \frac{A_1}{\zeta} + \frac{A_2}{\zeta^2} + \dots \quad (2.77)$$

The constant term of this expansion can be set equal to zero, because it does not impact the acceleration gradient. But the Kutta–Zhoukovsky–Chaplygin’s postulate is satisfied due to the series converges at point $\zeta = 1$, which corresponds to the trailing edge. Coefficients A_1, A_2, \dots have been determined from the boundary conditions.

However, Laurent series taken in the form (2.77), can be satisfied for the boundary conditions only for the acceleration. For satisfying the boundary conditions for the velocity it needs to complete the Laurent series by the term, which adds nothing to the normal acceleration on the unit circle, but is the additional component of the normal velocity of the wing. Such term is the complex potential of the dipole $iA_0/(\zeta + 1)$ [94–96] placed in the point $\zeta = -1$ and rotated by 90° using the multiplication by i .

The abovementioned approach takes the possibility for



P. A. Laurent
(1813–1854)

Pierre Alphonse Laurent – a French mathematician, best known as the discoverer of the Laurent series, an expansion of a function into an infinite power series, generalizing the Taylor series expansion.

Laurent was a good engineer, putting his deep theoretical knowledge to good practical use.

satisfying the boundary conditions for the velocity, and the complex acceleration potential can be described in the following form:

$$W(\zeta) = \frac{A_i}{\zeta + 1} + \frac{B_i}{\zeta} + \frac{C_i}{\zeta^2} + \dots \quad (2.78)$$

There are two cases of the wing movements:

1. Vertical oscillations of the wing:

$$y(t) = ye^{j\omega t}; \quad (2.79)$$

2. Rotational wing oscillations about the chord's midpoint:

$$y(t) = -\alpha xe^{j\omega t}. \quad (2.80)$$

In the first case the oscillation frequency can be expressed in terms of the dimensionless reduced frequency

$$k = \frac{\omega b}{U} = \frac{\omega}{U}, \quad (2.81)$$

where b is the half-chord ($b = 1$). Besides, $y_0 = y/b$ is the relative amplitude divided by the half-chord. Thus,

$$y(t) = y_0 e^{jUkt}. \quad (2.82)$$

The boundary conditions for the contour of the physical plane z

$$v'_w = \frac{dy}{dt} = jUky_0 e^{jUkt} = v_w(x, y) e^{jUkt}; \quad (2.83)$$

$$a'_w = \frac{d^2 y}{dt^2} = -U^2 k^2 y_0 e^{jUkt} = a_w(x, y) e^{jUkt}.$$

In the auxiliary plane ζ the normal component of the complex acceleration potential has the following form:

$$a_n|_{|\zeta|=1} = -U^2 k^2 y_0 \sin \theta. \quad (2.84)$$

For this problem, the complex acceleration potential can be taken in the simplified form:

$$W(\zeta) = \frac{Ai}{\zeta + 1} + \frac{Bi}{\zeta}, \quad (2.85)$$

where A, B are unknown constants.

According to the scheme presented on Figure 2, it can be written:

$$\zeta = re^{i\theta}; \quad \zeta + 1 = r_1 e^{i\theta_1}, \quad (2.86)$$

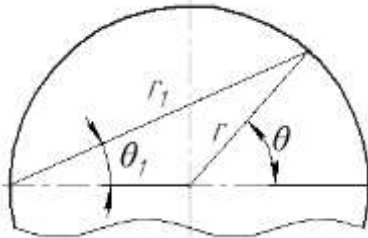


Figure 2.3 – Geometrical dependences on the circle of radius r

as well as the complex acceleration potential $W(\zeta)$ can be expanded on the real Φ and imaginary Ψ parts:

$$\begin{aligned}
 W(\zeta) &= \frac{iA}{r_1} e^{-i\theta_1} + \frac{iB}{r} e^{-i\theta} = \frac{iA}{r_1} (\cos \theta_1 - i \sin \theta_1) + \\
 &+ \frac{iB}{r} (\cos \theta - i \sin \theta) = \Phi_1 + \Phi_2 + i(\Psi_1 + \Psi_2) = \Phi + i\Psi,
 \end{aligned} \tag{2.87}$$

where the following components are introduced:

$$\begin{aligned}
 \Phi_1 &= \frac{A}{r_1} \sin \theta_1; \quad \Phi_2 = \frac{B}{r} \sin \theta; \\
 \Psi_1 &= \frac{A}{r_1} \cos \theta_1; \quad \Psi_2 = \frac{B}{r} \cos \theta; \\
 \Phi &= \Phi_1 + \Phi_2; \quad \Psi = \Psi_1 + \Psi_2.
 \end{aligned} \tag{2.88}$$

By the cosine theorem [97]:

$$r^2 = r_1^2 + r^2 - 2r_1 r \cos \theta_1. \tag{2.89}$$

In case of $r = 1$ the formulas (2.88) and (2.89) can be rewritten:

$$r_1 = 2r \cos \theta_1; \quad \Psi_1 = \frac{A}{2} = \text{const}. \tag{2.90}$$

Thus, the unit circle is the streamline for the acceleration, and at each of its points the acceleration vector is tangent to it. Consequently, the normal component of the acceleration is equal to zero:

$$\left. \frac{\partial \Phi_1}{\partial n} = \frac{\partial \Phi_1}{\partial r} \right|_{r_1=2r \cos \theta_1} = 0. \quad (2.91)$$

Moreover,

$$\begin{aligned} \frac{\partial \Phi}{\partial r} &= \left(\frac{\partial \Phi_1}{\partial r} + \frac{\partial \Phi_2}{\partial r} \right) \Big|_{r_1=2r \cos \theta_1} = -B \frac{\sin \theta}{r^2} \Big|_{r=1} = -B \sin \theta; \\ \frac{\partial \Phi}{\partial r} &= a_n = -U^2 k^2 y_0 \sin \theta = -B \sin \theta; \\ B &= U^2 k^2 y_0. \end{aligned} \quad (2.92)$$

The constant A can be determined from the boundary condition for the velocity v'_w (2.72) with taking into account the reduced frequency k (2.81):

$$v'_w = e^{jUkt} e^{-jkx} \frac{1}{U} \int_{-\infty}^x \frac{\partial \Phi}{\partial y} e^{jkx} dx = jUky_0 e^{jUkt}. \quad (2.93)$$

The variable x on the wing ($-1 \leq x \leq 1$) can be presented in the following form:

$$x = -1 + \varepsilon; \quad (0 \leq \varepsilon \leq 2). \quad (2.94)$$

Then, the boundary condition (2.93) takes the form:

$$jUky_0 = e^{-jk(-1+\varepsilon)} \frac{1}{U} \int_{-\infty}^{-1+\varepsilon} \frac{\partial \Phi}{\partial y} \Big|_{x=-1+\varepsilon} e^{jk(-1+\varepsilon)} d\varepsilon, \quad (2.95)$$

which can be satisfied for all values of ε .

After the differentiation of both parts of equation (2.95) with respect to ε , it can be shown, that equation (2.95) is fulfilled identically:

$$\begin{aligned}
 0 &= -jk(jUky_0) + \frac{e^{-jk(-1+\varepsilon)}}{U} \frac{d}{d\varepsilon} (-1 + \varepsilon) \frac{\partial \Phi}{\partial y} \Big|_{x=-1+\varepsilon} e^{jk(-1+\varepsilon)}; \\
 0 &= Uk^2 y_0 + \frac{e^{-jk(-1+\varepsilon)}}{U} (-U^2 k^2 y_0) e^{jk(-1+\varepsilon)}; \\
 0 &\equiv 0,
 \end{aligned} \tag{2.96}$$

because of the following dependences from (2.83):

$$\begin{aligned}
 a'_w &= -U^2 k^2 y_0 e^{jUkt}; \\
 \frac{\partial \Phi}{\partial y} &= a'_w \frac{1}{e^{jUkt}} = a_y = -U^2 k^2 y_0.
 \end{aligned} \tag{2.97}$$

Consequently, if the equation (2.95) is satisfied at one point of the wing, then it is automatically satisfied on the whole wing contour. Thus, it can be taken $\varepsilon = 0$. After the substitution

$$\frac{\partial \Phi}{\partial y} = -\frac{\partial \Psi}{\partial x} = -\left(\frac{\partial \Psi_1}{\partial x} + \frac{\partial \Psi_2}{\partial x} \right) \tag{2.98}$$

it can be obtained with the use of the integration by parts [98]:

$$\begin{aligned}
 jUky_0 &= \frac{e^{-jk}}{U} \int_{-\infty}^{-1} e^{jkx} \left(\frac{\partial \Psi_1}{\partial x} + \frac{\partial \Psi_2}{\partial x} \right) dx = \\
 &= -\frac{e^{-jk}}{U} \left\{ \left(e^{jkx} \Psi_1 \right) \Big|_{-\infty}^{-1} - \int_{-\infty}^{-1} e^{jkx} \left(jk \Psi_1 - \frac{\partial \Psi_2}{\partial x} \right) dx \right\}.
 \end{aligned} \tag{2.99}$$

Because of

$$\lim_{x \rightarrow -\infty} e^{jkx} = 0; \quad \lim_{x \rightarrow 1} \Psi_1 = \lim_{x \rightarrow 1} A \frac{\cos \theta_1}{r_1} = \frac{A}{2} \quad (2.100)$$

it can be written

$$jUky_0 = -\frac{A}{2} + \frac{e^{jk}}{U} \int_{-\infty}^{-1} e^{jkx} \left(jk\Psi_1 - \frac{\partial\Psi_2}{\partial x} \right) dx, \quad (2.101)$$

where functions Ψ_1 , Ψ_2 are given in the imaginary plane by the equations (2.88), but they have been calculated in the physical plane with the use of the inverse Zhoukovsky transform [99, 100]:

$$\zeta = re^{i\theta} = z + \sqrt{z^2 - 1}, \quad (2.102)$$

where $z = x + iy$.

In case of $-\infty \leq x \leq -1$ due to the integral from the equation (2.101), it is important to consider the negative part of the real axis (Figure 2.4). If $x = -1$, then $\theta = \theta_1 = \pi$, and

$$\begin{aligned} r &= -x + \sqrt{x^2 - 1}; \\ r_1 &= -x - 1 + \sqrt{x^2 - 1} \end{aligned} \quad (2.103)$$

due to $r = r_1 + 1$.

The abovementioned allows rewriting functions Ψ_1 , Ψ_2 in terms of x :

$$\begin{aligned}
 \Psi_1 &= A \frac{\cos \theta_1}{r_1} = \frac{-A}{-x-1+\sqrt{x^2-1}} = \\
 &= \frac{A}{2} \left(1 + \frac{\sqrt{x^2-1}}{x+1} \right) = \frac{A}{2} \left(1 + \frac{x-1}{\sqrt{x^2-1}} \right); \\
 \Psi_2 &= B \frac{\cos \theta}{r} = \frac{-B}{-x+\sqrt{x^2-1}} = B(x+\sqrt{x^2-1}); \\
 \frac{\partial \Psi_2}{\partial x} &= B \left(1 + \frac{x}{\sqrt{x^2-1}} \right).
 \end{aligned} \tag{2.104}$$

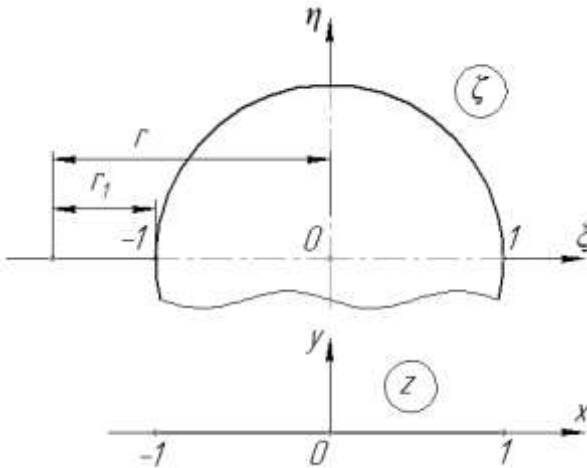


Figure 2.4 – Geometrical dependences of conformal mapping

Substitution Ψ_1 and $\partial \Psi_2 / \partial x$ to the integral of the equation (2.101) allows obtaining the following expression [64]:

$$\int_{-\infty}^{-1} e^{jkx} \left(jk\Psi_1 - \frac{\partial\Psi_2}{\partial x} \right) dx = \frac{A}{2} e^{-jk} - \frac{Ajk}{2} (K_0 + K_2) - \frac{Be^{-jk}}{jk} + BK_1, \quad (2.105)$$

where the modified zero and first order Bessel functions of the second kind [101] are introduced:

$$K_0(jk) = \int_1^{\infty} \frac{e^{-jkx}}{\sqrt{x^2 - 1}} dx; \quad K_1(jk) = \int_1^{\infty} \frac{xe^{-jkx}}{\sqrt{x^2 - 1}} dx \quad (2.106)$$

Thus, the equation (2.101) can be rewritten:

$$jkUy_0 = -\frac{Ajk e^{jk}}{2U} (K_0 + K_2) - \frac{B}{Ujk} + \frac{Be^{-jk}}{U} K_1, \quad (2.107)$$

where $B = U^2 k^2 y_0$. Finally, the constant A can be written in the following form:

$$A = -2jkU^2 y_0 \frac{K_1}{K_0 + K_1} = -2jkU^2 y_0 C(k), \quad (2.108)$$



F. W. Bessel
(1784–1846)

Friedrich Wilhelm Bessel – a German astronomer, mathematician, physicist and geodesist. He was the first astronomer, who determined reliable values for the distance from the sun to another star by the method of parallax. Special mathematical functions, known as Bessel functions, were named after him.

where $C(k)$ – Theodorsen function [48, 102] (Figure 2.5):

$$C(k) = \frac{K_1}{K_0 + K_1} = F(k) + iG(k). \quad (2.109)$$

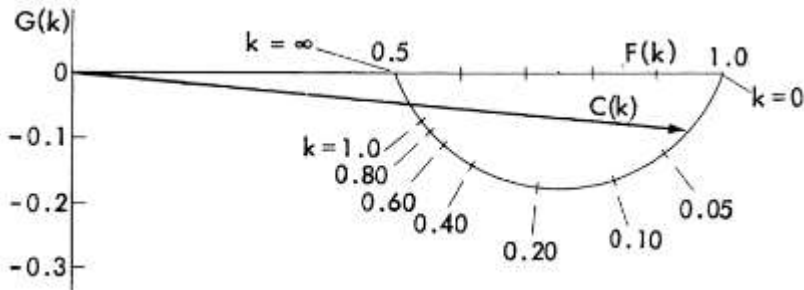


Figure 2.5 – A complex polar plot of Theodorsen function [12]

Theodorsen function can be expressed by Hankel functions H_0, H_1 [103]:

$$C(k) = \frac{H_1}{H_1 + jH_0}; \quad (2.110)$$

$$H_0 = I_0 - jJ_0; \quad H_1 = I_1 - jJ_1,$$

where I_0, I_1 and J_0, J_1 – the first order Bessel functions of



T. Theodorsen
(1897–1978)

Theodore Theodorsen – a Norwegian-American theoretical aerodynamicist noted for his work at National Advisory Committee for Aeronautics (NACA), the forerunner of National Aeronautics and Space Administration (NASA), and for his contributions to the study of turbulence.

zero and the first kind respectively.

According to the abovementioned, all the boundary conditions are satisfied. Moreover, Kutta–Zhoukovsky–Chaplygin’s postulate is satisfied due to the fact, that the function $W(\zeta)$ is continuous near the trailing edge, and the obtained solution (2.85) is closed.

The function Φ (2.88) can be obtained by using the expressions for A (2.108) and B (2.92):

$$\Phi = -2jkU^2 y_0 C(k) \frac{\sin \theta_1}{r_1} + U^2 k^2 y_0 \frac{\sin \theta}{r}, \quad (2.111)$$

which due to the formula (2.90) in case of $r = 1$ takes the form:

$$\Phi = -2jkU^2 y_0 C(k) \operatorname{tg} \theta_1 + U^2 k^2 y_0 \sin \theta, \quad (2.112)$$

where $\theta = 2\theta_1$ for the wing’s contour [64].

Finally, the expression for the pressure p due to the formula (2.64) takes the following form:

$$p = -\rho e^{jUkt} U^2 y_0 \left[-jkC(k) \operatorname{tg} \frac{\theta}{2} + k^2 \sin \theta \right]. \quad (2.113)$$



H. Hankel
(1837–1873)

Hermann Hankel – a German mathematician. His exposition on complex numbers and quaternions is particularly memorable. He solved the problem of products of negative numbers by proving the corresponding theorem.

The aerodynamic force L is the integral of the pressure distribution function p with respect to $x = r \cos\theta$ ($r = 1$):

$$L = -\int_{-1}^1 p dx = -2 \int_0^{\pi} p \sin \theta d\theta. \quad (2.114)$$

It can be obtained by taking into account the previous dependence (2.113):

$$L = \pi\rho U^2 y_0 e^{jUkt} k^2 \left[1 - \frac{2j}{k} C(k) \right]. \quad (2.115)$$

The aerodynamic moment about the chord's midpoint, which is calculated by the following formula

$$M_{1/2} = -\int_{-1}^1 p \cdot x dx = -2 \int_0^{\pi} p \cos \theta \sin \theta d\theta. \quad (2.116)$$

Taking into account the following dependences:

$$\begin{aligned} y &= y_0 e^{jUkt}; \\ \dot{y} &= \frac{dy}{dt} = jUk y_0 e^{jUkt} = jUky; \\ \ddot{y} &= \frac{d^2 y}{dt^2} = -U^2 k^2 y_0 e^{jUkt} = -U^2 k^2 y, \end{aligned} \quad (2.117)$$

the aerodynamic force and moment converts to the following forms:

$$\begin{aligned} L &= -\pi\rho \ddot{y} - 2\pi\rho UC(k)\dot{y}; \\ M_{1/2} &= -\pi\rho UC(k)\dot{y}, \end{aligned} \quad (2.118)$$

where the first component $\pi\rho \ddot{y}$ is caused by the added mass of the fluid, but not due to the flow circulation, and the line of force action passes through the chord's midpoint. Its moment is equal to zero.

The second component $-2\pi\rho UC(k)\dot{y}$ is caused by the added vortices due to the flow circulation, and the line of force action spaces from the chord's midpoint of a quarter chord length $b/4$.

In the second case of small rotational wing oscillations about the chord's midpoint, well-known as pitching movement [104, 105], it is described by the equation (2.80) that due to the formula (2.81) takes the following form:

$$y(t) = -\alpha_0 x e^{jUkt}. \quad (2.119)$$

The boundary conditions for the velocity and acceleration on the wing surface are:

$$\begin{aligned} v'_w - \alpha_0 U e^{jUkt} (1 + jkx) &= v_w(x, y) e^{jUkt}; \\ a'_y &= -j\alpha_0 U^2 k e^{jUkt} (1 + jkx) - j\alpha_0 U^2 k e^{jUkt} = \\ &= -j\alpha_0 U^2 k e^{jUkt} (2 + jkx) = a_y(x, y) e^{jUkt}. \end{aligned} \quad (2.120)$$

In this case the complex acceleration potential can be taken on the following form:

$$W(\zeta) = \frac{iA}{\zeta + 1} + \frac{iB}{\zeta} + \frac{iC}{\zeta^2}, \quad (2.121)$$

and it can be rewritten due to the formula (2.86):

$$\begin{aligned} W(\zeta) &= \frac{iA}{r_1} e^{-i\theta_1} + \frac{iB}{r} e^{-i\theta} + \frac{iC}{r^2} e^{-2i\theta_1} = \\ &= \frac{iA}{r_1} (\cos \theta_1 - i \sin \theta_1) + \frac{iB}{r} (\cos \theta - i \sin \theta) + \\ &+ \frac{iC}{r^2} (\cos 2\theta - i \sin 2\theta) = \Phi_1 + \Phi_2 + \Phi_3 + \\ &+ i(\Psi_1 + \Psi_2 + \Psi_3) = \Phi + i\Psi, \end{aligned} \quad (2.122)$$

where the following components are introduced:

$$\begin{aligned} \Phi_1 &= \frac{A}{r_1} \sin \theta_1; \quad \Phi_2 = \frac{B}{r} \sin \theta; \quad \Phi_3 = \frac{C}{r^2} \sin 2\theta; \\ \Psi_1 &= \frac{A}{r_1} \cos \theta_1; \quad \Psi_2 = \frac{B}{r} \cos \theta; \quad \Psi_3 = \frac{C}{r^2} \cos 2\theta; \quad (2.123) \\ \Phi &= \Phi_1 + \Phi_2 + \Phi_3; \quad \Psi = \Psi_1 + \Psi_2 + \Psi_3. \end{aligned}$$

As it was previously shown, $\Psi_1 = 0$, and the unit circle is the streamline for the acceleration. In addition, due to the dependences (2.91) it can be written:

$$\begin{aligned}
 \frac{\partial \Phi}{\partial r} &= a_n = \left(\frac{\partial \Phi_1}{\partial r} + \frac{\partial \Phi_2}{\partial r} + \frac{\partial \Phi_3}{\partial r} \right) \Bigg|_{r=1} = \\
 &= - \left(B \frac{\sin \theta}{r^2} + 2C \frac{\sin 2\theta}{r^3} \right) \Bigg|_{r=1} = -B \sin \theta - 2C \sin 2\theta = \quad (2.124) \\
 &= a_y(x, y) \sin \theta = -j\alpha_0 U^2 k (2 + jkx) \sin \theta,
 \end{aligned}$$

and taking into account $x = \cos \theta$, it can be obtained:

$$\begin{aligned}
 -B \sin \theta &= -2j\alpha_0 U^2 k \sin \theta; \\
 -2C \sin 2\theta &= \alpha_0 U^2 k^2 \frac{\sin 2\theta}{2}. \quad (2.125)
 \end{aligned}$$

Thus, the coefficients B, C takes the following forms:

$$B = 2j\alpha_0 U^2 k; \quad C = -\frac{1}{4} \alpha_0 U^2 k^2, \quad (2.126)$$

and the constant A is analogously obtained from the boundary condition for the velocity (2.72) [64]:

$$A = 2U^2 \alpha_0 \left[\left(1 + \frac{jk}{2} \right) C(k) - \frac{jk}{2} \right]. \quad (2.127)$$

Finally, the acceleration potential

$$\Phi' = \Phi(x, y) e^{jUkt} = \left(A \frac{\sin \theta_1}{r_1} + B \frac{\sin \theta}{r} + C \frac{\sin 2\theta}{r^2} \right) e^{jUkt}, \quad (2.128)$$

and the aerodynamic force and moment

$$L = \pi\rho U \ddot{\alpha} + \pi\rho UC(k)\dot{\alpha} + 2\pi\rho U^2 C(k)\alpha;$$

$$M_{1/2} = -\frac{1}{8}\pi\rho \ddot{\alpha} - \frac{1}{2}\pi\rho U \dot{\alpha} + \frac{1}{2}\pi\rho UC(k)\dot{\alpha} + \pi\rho U^2 C(k)\alpha. \quad (2.129)$$

In the general case of joint small flexural-torsional harmonic oscillations (Figure 2.6), the aerodynamic force and moment are the results of summarizing formulas (2.118) and (2.129):

$$L = \frac{1}{4}\pi\rho b^2(-\ddot{y} - x_m \ddot{\alpha} + U \dot{\alpha});$$

$$M \cong L\left(\frac{b}{4} + x_m\right), \quad (2.130)$$

where the moment does not contain the component $0,25b\ddot{y}$ because of the line of corresponding force action passes through the centre of gravity.

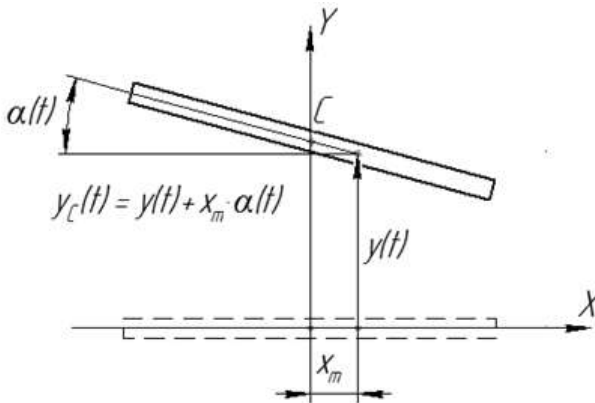


Figure 2.6 – Design scheme for joint flexural-torsional oscillations of the wing

The solution (2.130) was first obtained by T. Theodorsen in 1935, and has several particular cases:

1. Unsteady flow with the low specific frequency ($k \approx 0$) is important for engineering practice. In this case Theodorsen function $C(k) = C(0) = 1$, which corresponds to neglecting the impact of the vortex slipstream [106, 107] on the flow, and the aerodynamic force and moment can be presented in the linear matrix form [108, 109]:

$$\{F\} = [A]\{Y\} + [B]\{\dot{Y}\}, \quad (2.131)$$

where $\{F\} = \{L; M\}^T$ – column vector of the aerodynamic force and moment; $\{Y\} = \{y; \alpha\}^T$, $\{\dot{Y}\} = \{\dot{y}; \dot{\alpha}\}^T$ – column vectors of displacements and velocities; $[A]$, $[B]$ – stiffness and damping matrices:

$$[A] = \begin{bmatrix} A_{11} & 0 \\ 0 & A_{22} \end{bmatrix}; \quad [B] = \begin{bmatrix} B_{11} & B_{12} \\ B_{21} & B_{22} \end{bmatrix}. \quad (2.132)$$

2. The deeper approximation can be obtained for the stationary flow in case of the constant attack angle α directed due to the vector of the total velocity. This case takes place for the slow flatter with frequencies below 20 Hz [64]:

$$\begin{aligned} L &= \pi\rho Ub(-\dot{y} + U\dot{\alpha}); \\ M &\cong L\left(\frac{b}{4} + x_m\right). \end{aligned} \quad (2.133)$$

§ 2.4. Determination of aerodynamic forces in case of high supersonic speed

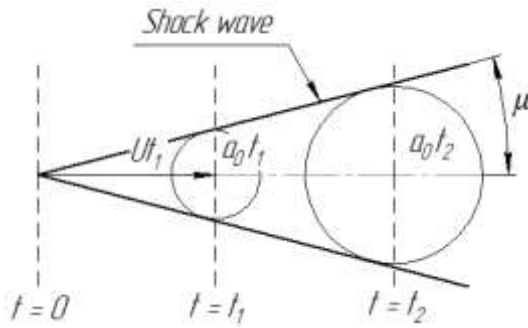
In case of Mach number $M \gg 1$ ($U \gg a_0$) it is possible to significantly simplify the abovementioned theory, if the effects related to density, dissociation and phase transformations on the flow and body borders are not taken into account. Simultaneously, the gas compressibility must be carefully considered. By the way, the small perturbation method underlies the theory of fluid compressibility [110].

The supersonic flow, in contrast to the subsonic one, generates new phenomena [111], which is due to the fact that high wing velocity ($U > a_0$) has a significant impact on the character of perturbations. In case of point source of perturbations streamlined by the flow with supersonic velocity U , all the disturbances of this source is inside the Mach cones [112, 113] schematically shown on Figure 2.7.

There is no perturbations in front of the Mach cone, and the Mach angle μ is determined by the formula:

$$\sin \mu = \frac{a_0 t}{U t} = \frac{1}{M}. \quad (2.134)$$

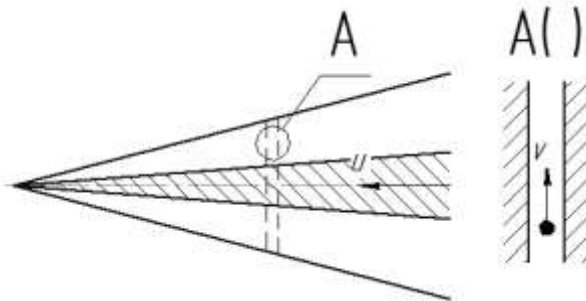
The analogous phenomenon takes place for the streamlined wing (Figure 2.7 b). The wing profile cuts into the gas volume, the particles of which move in narrow regions bounded by vertical planes (Figure 2.7 c). This explanation is called the law of plane sections, which simplifies the theory of supersonic flow [114]. Due to this law, the pressure on the wing surface can be obtained as the pressure on the piston in one-dimensional channel [115]:



a



b



c

Figure 2.7 – Mach cone (a), its manifestation (b)
and the flow of plane sections (c)

$$p = p_0 \left(1 + \frac{\kappa - 1}{2} \frac{v}{a_0} \right)^{\frac{2\kappa}{\kappa - 1}}, \quad (2.135)$$

where κ – polytropic index [116].

This approach caused the appearance of the piston theory [117].

For one-dimensional flow of ideal gas the nonlinear system of the Euler's equation and the continuity equation

$$\begin{cases} \frac{\partial u}{\partial t} + U \frac{\partial u}{\partial x} = -\frac{1}{\rho} \frac{\partial p}{\partial x}; \\ \frac{\partial \rho}{\partial t} + \frac{\partial}{\partial x}(\rho u) = 0 \end{cases} \quad (2.136)$$

has three unknown parameters: velocity u , pressure p and density ρ , which can be expanded for the case of small perturbations:

$$\begin{aligned} u &= u'; \\ p &= p_0 + p'; \\ \rho &= \rho_0 + \rho'. \end{aligned} \quad (2.137)$$

Because of

$$\frac{dp}{dx} = \frac{dp}{d\rho} \frac{d\rho}{dx} = \left(\frac{dp}{d\rho} \right)_0 \frac{d\rho'}{dx} = a_0^2 \frac{d\rho'}{dx}, \quad (2.138)$$

the system of equations (2.137) takes the following form:

$$\begin{cases} \frac{\partial u'}{\partial t} + \frac{a_0^2}{\rho_0} \frac{\partial \rho'}{\partial x} = 0; \\ \frac{\partial \rho'}{\partial t} + \rho_0 \frac{\partial u'}{\partial x} = 0. \end{cases} \quad (2.139)$$

Differentiation of the first equations (2.136) with respect to time t and the second one – with respect to coordinate x allows determining a wave equation [118] after summarizing:

$$\frac{\partial^2 u'}{\partial t^2} + a_0^2 \frac{\partial^2 u'}{\partial x^2} = 0. \quad (2.140)$$

Wave equations for the pressure p' and density ρ' can be obtained analogously.

General solution of the equation (2.140) can be presented as the d'Alembert solution according to the method of standing waves [119]:

$$u' = f_1(x - a_0 t) + f_2(x + a_0 t), \quad (2.141)$$

where functions f_1 and f_2 describe the progression and regression waves respectively, and depend on the initial conditions.

Introduction of moving coordinate systems with coordinates

$$\begin{aligned} \xi_1 &= x - a_0 t; \\ \xi_2 &= x + a_0 t \end{aligned} \quad (2.142)$$

allows describing the solution (2.141) in the following form:

$$u' = f_1(\xi_1) + f_2(\xi_2), \quad (2.143)$$

where $f_1(\xi_1), f_2(\xi_2)$ – simple plane standing waves, which do not depend on time.

Due to the kinematic approach (Figure 2.8), axes ξ_1 and ξ_2 are located along the absolute axis x and move forward towards the positive and negative directions of the axis x with the same module of the velocity a_0 [120].

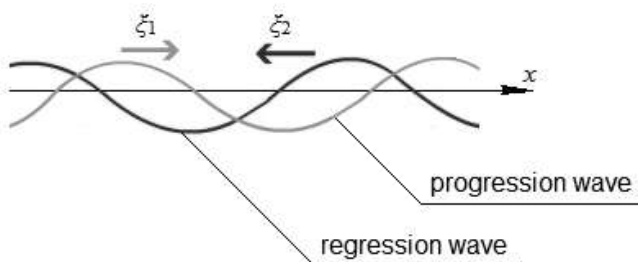


Figure 2.8 – Standing waves

However, propagation of the finite perturbations is more complicated problem. The well-known Riemann's solution [121] shows the presence of a qualitatively different character of waves propagation, that leads to shock waves, which are the discontinuity surfaces for the velocity and gas state parameters (pressure p' and density ρ').



J.-B. d'Alembert
(1717–1783)

Jean-Baptiste le Rond d'Alembert – a French mathematician, mechanician and physicist. d'Alembert's formula for obtaining solutions to wave equation is named after him. Wave equation is referred to d'Alembert's equation.

Due to the piston theory, a cylindrical pipe of infinite length, insulated from the external environment, is considered (Figure 2.9). A piston moves along the pipe with the velocity, which increases instantly from zero value to a certain value at the initial time. The resulting perturbation (compression of the gas) propagates through the tube. The region of the perturbed gas can be divided into an infinite number of infinitesimal volumes that are close to each other. Under the assumption that the distribution of perturbations along the pipe's axis is continuous in time, the theory of small perturbations can be applied in the Galilean (moving) coordinate system, and the velocity of propagation of the perturbations is equal to the sound speed. Thus, the propagation of perturbations, generated by the piston, can be considered as a system of continuously following sound waves, and each subsequent wave moves along the gas disturbed by the previous waves. In this case, the system (2.136) can be supplemented by equation of barotropic motion [122]:

$$p = C\rho^k; \quad \frac{p}{\rho} = RT, \quad (2.144)$$

where C – constant; k – adiabatic index; R – universal gas constant; T – absolute temperature in Kelvin scale.



G. Galilei
(1564–1642)

Galileo Galilei – an Italian astronomer, physicist, engineer and mathematician. He played a major role in the scientific revolution of the 17th century. His contributions to observational astronomy include the telescopic confirmation of the phases of Venus, the discovery of the four largest satellites of Jupiter, and the observation and analysis of sunspots. Galileo also plays a huge role for the development of applied science and technology.

Barotropic gas flow is accompanied by heating:

$$a^2 = \frac{dp}{d\rho} = kC\rho^{k-1} = k \frac{P}{\rho} = kRT; \quad (2.145)$$

$$a = \sqrt{kRT},$$

Due to the last-mentioned formula, compression of the gas increases with temperature, as well as each subsequent wave moves faster than the previous one with respect to the undisturbed flow. As a result, waves catch up to each other, creating one powerful compression wave, called a shock wave [123].

However, when the piston moves backwards, vacuum occurs due to waves cooling and, consequently, decreasing the velocity from wave to wave.

The front of the shock wave is the discontinuity plane for the gas state parameters (pressure p , density ρ and absolute temperature T). It moves in gas with creating an abrupt change of these parameters. Herewith, the unperturbed gas before the shock waves front has higher pressure, density and temperature than after it.

Due to the following dependences for barotropic gas flow

$$\frac{dp}{d\rho} = a^2;$$

$$\frac{1}{\rho} \frac{\partial p}{\partial x} = \frac{\partial P}{\partial x}; \quad (2.146)$$

$$\frac{\partial \rho}{\partial t} = \frac{\partial \rho}{\partial p} \frac{\partial p}{\partial t} = \frac{\rho}{a^2} \frac{\partial P}{\partial t}$$

the system of equations (2.136) can be replaced:

$$\begin{cases} \frac{\partial u}{\partial t} + u \frac{\partial u}{\partial x} + \frac{\partial P}{\partial x} = 0; \\ \frac{1}{a} \frac{\partial P}{\partial t} + a \frac{\partial u}{\partial x} + \frac{u}{a} \frac{\partial P}{\partial x} = 0. \end{cases} \quad (2.147)$$

Introduction of the modified pressure function

$$\begin{aligned} \tilde{P} &= \int_{p_0}^p \frac{dp}{\rho(p)a(p)}; \\ d\tilde{P} &= \frac{dP}{a} = \frac{dp}{\rho a}; \\ \frac{\partial \tilde{P}}{\partial t} &= \frac{1}{a} \frac{\partial P}{\partial t}; \quad \frac{\partial \tilde{P}}{\partial x} = \frac{1}{a} \frac{\partial P}{\partial x} \end{aligned} \quad (2.148)$$

allows rewriting the system of equations (2.147) in the form:

$$\begin{cases} \frac{\partial u}{\partial t} + u \frac{\partial u}{\partial x} + \frac{\partial \tilde{P}}{\partial x} = 0; \\ \frac{\partial \tilde{P}}{\partial t} + a \frac{\partial u}{\partial x} + u \frac{\partial \tilde{P}}{\partial x} = 0, \end{cases} \quad (2.149)$$

and termwise addition and subtraction leads to equations:

$$\begin{cases} \frac{\partial r}{\partial t} + (u + a) \frac{\partial r}{\partial x} = 0; \\ \frac{\partial s}{\partial t} + (u - a) \frac{\partial s}{\partial x} = 0, \end{cases} \quad (2.150)$$

where r, s – Riemann invariants [124]:

$$\begin{aligned} r &= \tilde{P} + u; \\ s &= \tilde{P} - u. \end{aligned} \tag{2.151}$$

The obtained result can be interpreted as the absence of two plane waves propagating along the axis x with the absolute velocities respectively $(u + a)$ and $(u - a)$, where $\pm a$ – relative velocities of waves propagation in gas.

In case of linearized equations for describing the gas movement, the analogous character of waves propagation takes place with the main difference: waves propagate with the constant values of gas parameters and velocity equal to the sound velocity in an undisturbed gas flow.

For one-dimensional wave propagation in ideal gas with disturbances of finite intensity, the second Riemann invariant $s = \text{constant}$, and the pressure $p = p_0$ for $u = 0$, as well as $\tilde{P} = u$ at any point of time. Consequently, the absolute velocity value $(u + a)$ does not vary in coordinate x , thus, the wave is simple. The pressure $p > 0$, as well as $p > p_0$ due to inequality $u > 0$. Thus, disturbances propagated by these waves, lead to compression waves [125]. Analogously, the case of $r = \text{const}$ leads to rarefaction waves [126].

But in case of shock waves it can be considered, that waves propagate in isentropic gas flow, and the modified pressure function \tilde{P} can be expressed in terms of a :

$$\begin{aligned} d\tilde{P} &= \frac{1}{a} dP = \frac{1}{\rho a} dp = \frac{1}{a} \frac{dp}{d\rho} \frac{d\rho}{\rho} = a \frac{dp}{\rho}; \\ a^2 &= k \frac{p}{\rho} = C\rho^{k-1} \end{aligned} \tag{2.152}$$

and

$$2ada = (k-1)C\rho^{k-2}d\rho = (k-1)\frac{a^2}{\rho}d\rho; \quad (2.153)$$

$$\frac{2}{k-1}da = \frac{d\rho}{\rho}a = d\tilde{P}.$$

After integration it can be obtained:

$$\begin{aligned} \tilde{P} = u &= \frac{2}{k-1}(a - a_0); \\ a &= a_0 \left(1 + \frac{k-1}{2} \frac{u}{a_0} \right). \end{aligned} \quad (2.154)$$

Thus, increasing the disturbed gas velocity u leads to increasing absolute $(u + a)$ and relative a velocities of the wave propagation.

As a result, the main difference between the small and finite disturbances can be stated: the initial propagation shape is varying for finite disturbances unlike the case of small ones. Corresponding images are shown on Figure 2.9 for the case of compression waves.

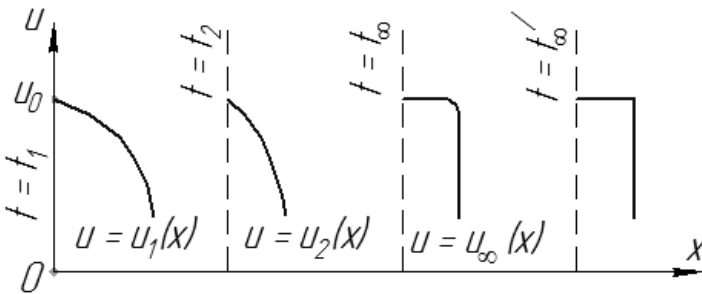


Figure 2.9 – Shapes of compression waves propagation

It can be noted, that the theory of compression waves with finite intensity leads to the inevitable appearance of shock waves.

Gas pressure on the piston can be determined by squaring the formula (2.154) with replacement the variable u to v :

$$\left(\frac{a}{a_0}\right)^2 = \left(1 + \frac{k-1}{2} \frac{v}{a_0}\right)^2. \quad (2.155)$$

Due to the formula (2.144),

$$p = C\rho^k = \rho^k \frac{p_0}{\rho_0^k} = p_0 \left(\frac{\rho}{\rho_0}\right)^k \quad (2.156)$$

and the Clapeyron's formula lead to the following expression [128]:

$$\frac{T}{T_0} = \frac{p}{\rho} \frac{\rho_0}{p} = \frac{p}{p_0} \frac{\rho_0}{\rho} = \frac{p}{p_0} \left(\frac{p_0}{p}\right)^{\frac{1}{k}} = \left(\frac{p}{p_0}\right)^{\frac{k-1}{k}}. \quad (2.157)$$

Due to the formula (2.145):



B. Clapeyron
(1799–1864)

Benoit Paul Emile Clapeyron – a French engineer and physicist, one of the founders of thermodynamics. His research works are aimed at the characterisation of ideal gases and the equilibrium of homogeneous solids.

$$a^2 = kRT; \quad a_0^2 = kRT_0;$$
$$\left(\frac{a}{a_0}\right)^2 = \frac{T}{T_0} = \left(\frac{p}{p_0}\right)^{\frac{k-1}{k}} = \left(1 + \frac{k-1}{2} \frac{v}{a_0}\right)^2, \quad (2.158)$$

and finally

$$p = p_0 \left(1 + \frac{k-1}{2} \frac{v}{a_0}\right)^{\frac{2k}{k-1}}. \quad (2.159)$$

Questions for self-control

1. What questions are used for the determination of the hydroaeroelastic forces?
2. Describe the components of Euler's and continuity equations.
3. Explain the physical meaning of such operators as rotor and gradient.
4. How is the divergence of the vector field determined?
5. Describe and explain the cases of barotropic fluid motion.
6. Describe the pressure function and formula of its calculation. What explains the introduction of this function?
7. Briefly describe the algorithm by which the Bernoulli integral can be obtained. What boundary conditions correspond to the Bernoulli integral?
8. Explain the essence of the small perturbation method. What purposes can it be used for?
9. What is the Mach number? Why, in your opinion, is it introduced into consideration?
10. By which equations is the incompressible fluid flow described? Describe the correspondent boundary conditions.
11. Describe and explain the conformal mapping for the unit circle.
12. What theorem must satisfy the real and imaginary parts of the complex acceleration potential?
13. What are the dependences between Theodorsen, Hankel and Bessel functions?
14. Describe the algorithm for determination of the aerodynamic forces acting on a streamlined surface.
15. Explain the phenomenon of shock waves.

CHAPTER 3.

Static aeroelasticity

§ 3.1. Characteristics of the aircraft wing profiles

The cross-section of a cylindrical surface with an infinite generatrix is denoted under the general name “profile” [64].

The profile of an infinite circular cylinder is a circle, but the circle is a poorly streamlined profile. Special well streamlined hydrodynamic profiles are developed on the basis of the theory of two-dimensional flows. Such profiles are named airfoils [129, 130], their geometric feature is an elongated form along the flow with a gradually thickened edge part (Figure 3.1).

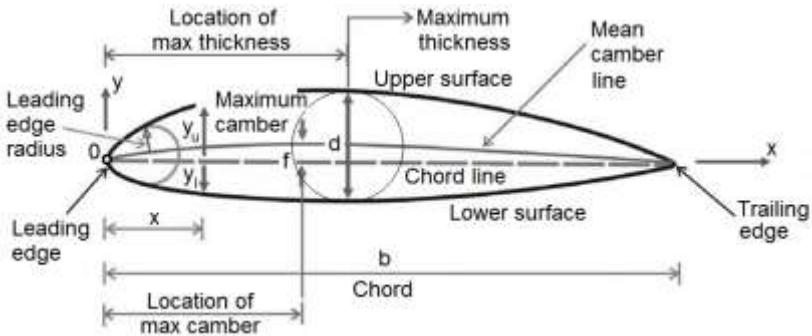


Figure 3.1 – Airfoil geometry

The geometric characteristic of the profile, such as dimensions and shape parameters, are usually expressed in terms of the chord b , which connects the most distant points of the contour, by using dimensionless coordinates:

$$\bar{x} = \frac{x}{b}; \quad \bar{y}_u = \frac{y_u}{b}; \quad \bar{y}_l = \frac{y_l}{b}, \quad (3.1)$$

where y_u, y_l – equations of the lower and upper surfaces.

Airfoils curvature is characterized by the camber line, which is the locus of points located in the middle of the perpendicular to the chord. The airfoil thickness is determined as diameter d of the inscribed circle, as well as dimensionless ordinate of the camber line and maximum camber f are determined by the following formulas:

$$\bar{y}_m = \frac{\bar{y}_u - \bar{y}_l}{2}; \quad \bar{f} = \frac{f}{b}. \quad (3.2)$$

The series of airfoils were developed by the leading aerospace institutes around the world by carrying out theoretical and experimental investigations, and the documents are supplemented by the corresponding aerodynamic characteristics [131, 132].

The airfoil geometrical characteristic is a set of curves reflecting the dependence of the hydrodynamic force and moment on the attack angle, as well as attack angle α is the angle between the chord and direction of the undisturbed flow (Figure 3.2).

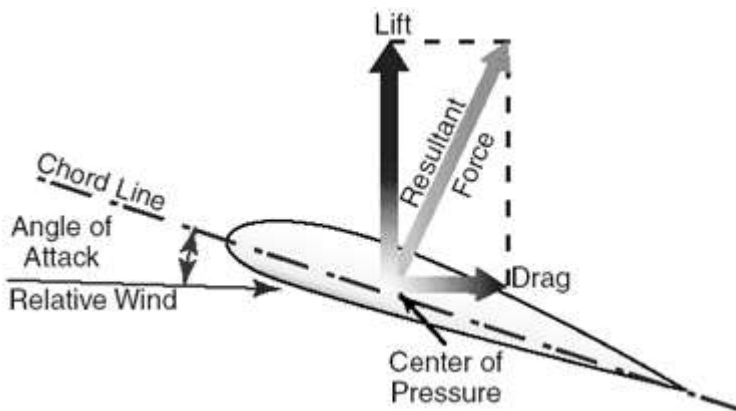


Figure 3.2 – Aerodynamic force acting on the airfoil

If the airfoil model is placed in a plane parallel flow, then the specific hydrodynamic force acts per unit length. The components of this force are the lift force L and the drag force X (Figure 3.2), which can be determined immediately.

The construction of the airfoils characteristics is conveniently carried out by the dimensionless coefficients C_x , C_y for lift and drag forces respectively, whose values describe a series of similar profiles. Lift and drag coefficients are determined by the following equations:

$$C_x = \frac{X}{qb}; \quad C_y = \frac{L}{qb}, \quad (3.3)$$

where q – the dynamic pressure:

$$q = \frac{\rho U^2}{2}. \quad (3.4)$$

Besides the value and direction of the hydrodynamic force, it is necessary to determine the point of its application by the coordinate x_0 :

$$x_0 = \frac{M}{\sqrt{L^2 + X^2}}, \quad (3.5)$$

where M – experimentally identified specific aerodynamic moment.

The dimensionless moment ratio

$$C_m = \frac{M}{qb^2}, \quad (3.6)$$

with coefficients C_x and C_y , which depend on the attack angle α , are the aerodynamic airfoil characteristics (Figure 3.3).

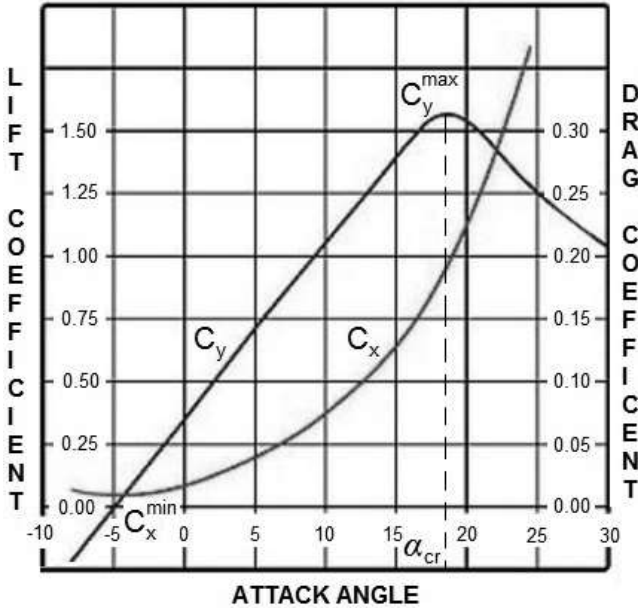


Figure 3.3 – Aerodynamic airfoil characteristics

Experience shows that a small attack angle leads to the linearly increasing lift coefficient C_y :

$$C_y = \frac{\partial C_y}{\partial \alpha} (\alpha - \alpha_0), \quad (3.7)$$

where α_0 – attack angle, at which the lift force is equal to zero. For symmetrical profiles ($y_u = y_l$) this angle $\alpha_0 = 0$, and

$$C_y = \frac{\partial C_y}{\partial \alpha} \alpha. \quad (3.8)$$

However, the linear law occurs only in a certain range of α for a given profile shape, which corresponds to non-separable continuous air flow. A significant increase of the attack angle leads to a nonlinear region. After the critical value $\alpha = \alpha_{cr}$, when C_y reaches its maximum value C_y^{\max} , a flow separation from the upper surface is observed. In the supercritical region ($\alpha > \alpha_{cr}$), the separation region expands, and a lift coefficient decreases sharply.

The drag coefficient C_x reaches its minimum value C_x^{\min} for zero lift force. Increasing the attack angle α leads to slowly increasing the drag coefficient C_x in a subcritical region. But in a supercritical region it increases sharply due to the flow irregularity.

According to the shape of the chord line, the airfoils are divided into symmetrical, slightly and strongly curved, and s-shaped (Figure 3.4) [2, 64, 133].

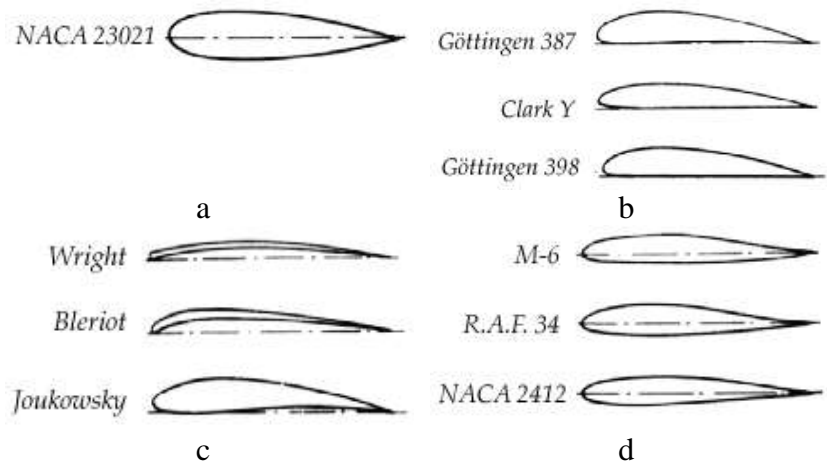


Figure 3.4 – Airfoils classification

Symmetrical airfoils with a straight chord line (Figure 3.4 a) is widely used in cases, when the wing operates

similarly for positive and negative values of the attack angle, for example, as elements of steering wheels.

Slightly curved airfoils (Figure 3.4 b) are used for the wing, which creates irreversible lift force. However, they can operate in case of a small negative attack angle near zero lift force. Such airfoils have a relatively low drag force and high aerodynamic ratio:

$$K = \frac{C_y}{C_x}. \quad (3.9)$$

Strongly curved airfoils (Figure 3.4 c) are used for profiling the impellers of rotor machines.

S-shaped airfoils (Figure 3.4 d) have a relatively good moment ratio C_m , which does not depend on the attack angle α .

At high value of velocity, airfoils need to have low relative thickness. However, the minimum thickness of the profile is limited by the strength conditions [28, 31, 45].

§ 3.2. Divergence of an elastically fixed wing element

Before considering the divergence of a finite-span wing, it is necessary to consider the behaviour of a rigid elastically fixed wing in a two-dimensional flow (Figure 3.5)

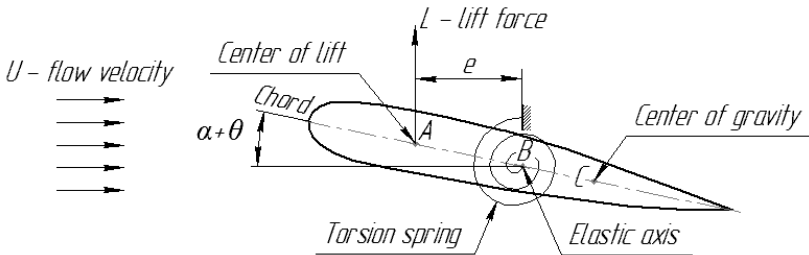


Figure 3.5 – Design model of the rigid elastically fixed wing

This approach is justified, and earlier research works in the field of hydroaeroelasticity were based on the simplified two-dimensional presentation of bearing surfaces. For example, T. Theodorsen used this model for analyzing the flutter problem, calling it as “cross-sectional characteristics” [135]. Herewith, the properties of the model are set so that they correspond to the properties of the real wing at a distance of 70–75 % of the half-span from the root section.

According to the Figure 3.5, the characteristic points of the airfoil are:

- 1) A – a centre of lift (aerodynamic center), to which the resultant of the pressure forces (specific lift force) is applied;
- 2) B – a twist centre, which corresponds to the elastic axis location, around which the wing turns;
- 3) C – a centre of gravity.

Wing stiffness is simulated by the torsion spring with the stiffness k_a . Due to the two-dimensional wing theory [134] for

the case of incompressible fluid flow, the lift centre is located at the distance $b/4$ behind the leading edge. In case of supersonic streamlining, this centre shifts it to the middle of the chord.

The rotation of the wing at a certain angle leads to the appearance of a lift force L applied at the lift centre (Figure 3.5). This force causes the aerodynamic moment, which tends to twist the wing. The elastic moment M_{spr} of the wing (recovery moment) prevents this twisting. Since the elastic characteristics do not depend on the flow velocity U , and the aerodynamic moment is proportional to the squared flow velocity U^2 , the critical velocity can exist, when infinitesimal deformation of the wing leads to a theoretically infinite twist angle. Such velocity is named as critical divergence velocity U_{div} .

In case of linear spring characteristic and zero value of lift force, the system is located at angle α . Due to the wing that is not absolutely rigid, weakening of the elastic connection increases this angle by an amount θ . The problem is in determining the equilibrium position (angle θ) of the wing in the air flow with velocity U . Thus, the aerodynamic force due to formulas (3.3) and (3.4):

$$L = C_y qb = \frac{1}{2} C_y \rho U^2 b, \quad (3.10)$$

where C_y – lift coefficient, which is proportional to the total attack angle ($\alpha + \theta$), which can be obtained due to the formula (3.8):

$$C_y = k(\alpha + \theta). \quad (3.11)$$

A coefficient k is the slope of the curve $C_y(\alpha)$ (Figure 3.3):

$$k = \frac{\partial C_y}{\partial \alpha}. \quad (3.12)$$

The aerodynamic moment about the elastic axes:

$$M = L e = k(\alpha + \theta) q \varepsilon b^2, \quad (3.13)$$

where $e = \varepsilon b$ – distance between the lift centre and elastic axis (Figure 3.5) expressed in terms of dimensionless eccentricity ε . If the elastic centre is behind the lift centre, then $\varepsilon > 0$.

The recovery moment:

$$M_{spr} = k_\alpha \theta. \quad (3.14)$$

The stationary position can be obtained from the static equilibrium equation for moments [136]:

$$M = M_{spr}, \quad (3.15)$$

which can be rewritten by taking into account the equations (3.13) and (3.14):

$$k(\alpha + \theta) q \varepsilon b^2 = k_\alpha \theta, \quad (3.16)$$

and the angle:

$$\theta = \frac{q \varepsilon b^2 k \alpha}{k_\alpha - q \varepsilon b^2 k}. \quad (3.17)$$

It is obvious, that in case

$$k_\alpha = q\epsilon b^2 k \quad (3.18)$$

the angle θ tends to infinity. Thus, the equation (3.18) is the condition for occurrence of divergence. In other words,

$$q_{div} = \frac{k_\alpha}{\epsilon b^2 k}, \quad (3.19)$$

or critical divergence velocity:

$$U_{div} = \sqrt{\frac{2k_\alpha}{\rho\epsilon b^2 k}}. \quad (3.20)$$

Due to the strip theory [137], the coefficient $k = 2\pi$, and dimensionless eccentricity $\epsilon = 1/4$. Thus, finally

$$U_{div} = \sqrt{\frac{4k_\alpha}{\pi\rho b^2}}. \quad (3.21)$$

It should be noted, that today the phenomenon of divergence is unlikely threatening airplanes, because the critical velocity U_{div} is usually higher than the critical flutter velocity. However, the critical divergence velocity U_{div} is a convenient comparative value for investigating the phenomenon of aeroelasticity. Because the calculation of U_{div} is relatively simple, it has been identified in the process of designing an airplane.

§ 3.3. Critical velocity of aileron's reverse

The phenomenon of aeroelasticity, which takes place when attaching to the wing of the steering surface (Figure 3.6 a), is considered under the assumption that aileron is inclined downward by an angle β (Figure 3.6 b).

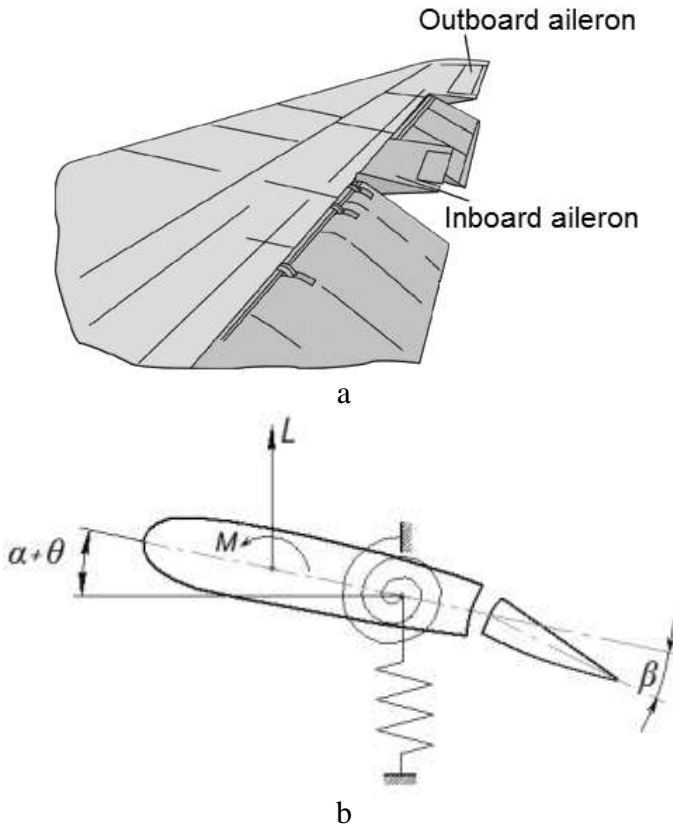


Figure 3.6 – Rigid elastically fixed wing with the aileron

In case of a rigid support, the downward movement of the aileron is accompanied by increasing the lift force L . However, in case of an elastically fixed wing element, the downward movement of the aileron leads to twisting down the leading edge of the wing. Increasing the flow velocity U causes increasing the aerodynamic moment M proportionally to the squared flow velocity, whereas elastic recovery moment M_{spr} is being constant. As a result, efficiency of the aileron in the creation of the lift force decreases with increasing the flow velocity until inefficiency of the aileron is reached. Corresponding flow velocity U_{cr} is the critical velocity of the aileron's reverse [138].

When considering the behaviour of the wing taking into account deflection of the aileron, the lift coefficient C_y is a function of both angles α and β , as well as it can be expanded in a series of these angles. In linear formulation it can be written:

$$C_y = \frac{\partial C_y}{\partial \alpha} \theta + \frac{\partial C_y}{\partial \beta} \beta, \quad (3.22)$$

where $\frac{\partial C_y}{\partial \beta}$ – the change of the lift coefficient C_y per unit angle deviation β of the aileron.

Increasing the angle β also leads to increasing the curvature of the airfoil, which causes the additional aerodynamic moment:

$$M' = C_m q b^2 = \frac{\partial C_m}{\partial \beta} \beta q b^2, \quad (3.23)$$

where C_m – coefficient of the additional aerodynamic moment [139].

The total aerodynamic moment about the elastic centre

$$M = L \cdot e - M' = q \varepsilon b^2 \left(\frac{\partial C_y}{\partial \alpha} \theta + \frac{\partial C_y}{\partial \beta} \beta \right) - \frac{\partial C_m}{\partial \beta} \beta q b^2. \quad (3.24)$$

Taking into account the formula (3.14) for the elastic moment M_{spr} , the ratio of the attack angle θ to the aileron angle β can be determined from the condition of equilibrium (3.15):

$$\frac{\theta}{\beta} = \frac{q b^2 \left(\varepsilon \frac{\partial C_y}{\partial \beta} - \frac{\partial C_m}{\partial \beta} \right)}{k_\alpha - q \varepsilon b^2 \frac{\partial C_y}{\partial \alpha}}. \quad (3.25)$$

The lift force L determined by the formula (3.10), contains the lift coefficient C_y determined by the formula (3.22). Substitution of the formula (3.24) in the formula (3.22), after identical transformations allows obtaining the following dependence of the lift coefficient C_y on the angle β :

$$C_y = \frac{k_\alpha \frac{\partial C_y}{\partial \beta} - q b^2 \frac{\partial C_y}{\partial \alpha} \frac{\partial C_m}{\partial \beta}}{k_\alpha - q \varepsilon b^2 \frac{\partial C_y}{\partial \alpha}} \beta. \quad (3.26)$$

Obviously, the aileron is ineffective in case if the numerator in the formula (3.26) is equal to zero:

$$k_\alpha \frac{\partial C_y}{\partial \beta} = q b^2 \frac{\partial C_y}{\partial \alpha} \frac{\partial C_m}{\partial \beta}, \quad (3.27)$$

and finally, the critical flow velocity:

$$U_{cr} = \sqrt{\frac{2k_{\alpha} \frac{\partial C_y}{\partial \beta}}{\rho b^2 \frac{\partial C_y}{\partial \alpha} \frac{\partial C_m}{\partial \beta}}}. \quad (3.28)$$

Avoiding the reverse of ailerons for the straight wing can be reached by providing a sufficient torsional stiffness of the wing. In case of the sweepback wing [140], the extremely serious problem of the critical velocity of the aileron's reverse is ensured by increasing the flexural stiffness. However, increasing the flexural and torsional stiffness is often accompanied by an unacceptably high weight of the structure. Therefore, other means for increasing the reverse velocity are needed to invent.

In order to clear the above-described quantities, the dependence of aileron's efficiency on the flight velocity is shown on Figure 3.7. Wherein, aileron efficiency is the ratio of the angular roll rate to the aileron deflection angle.

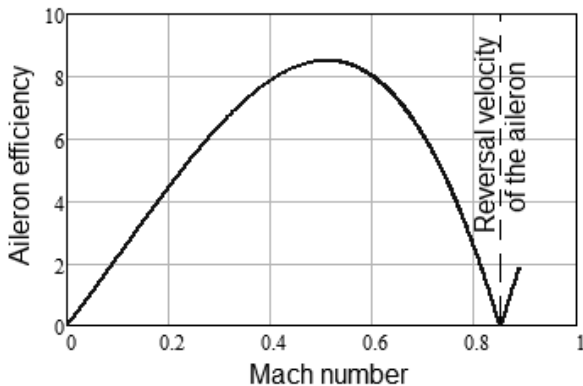


Figure 3.7 – The impact of flight velocity on aileron efficiency

It should be noted, that efficiency and reverse of the lifting rudders and steering wheels are less critical phenomena than efficiency and reverse of ailerons. However, these problems are complicated by a comparative large number of elastic elements, which cause additional components for the total deformation of the tail unit. For example, deformations of the fuselage and joint supports are as important as the deformations of the tail unit. Thus, efficiency of the tail unit as lift force per unit of the angle of the lifting rudder is presented on Figure 3.8.

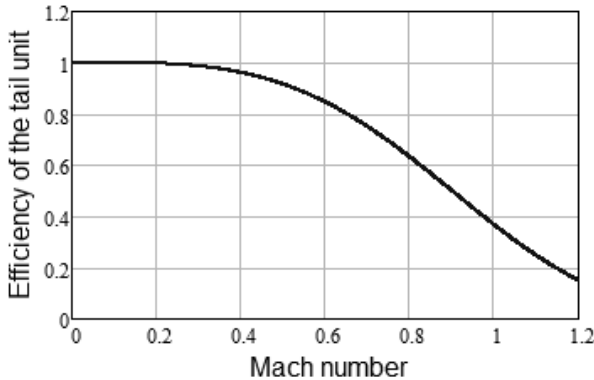


Figure 3.8 – The impact of flight velocity on efficiency of the tail unit

Finally, Figure 3.9 shows three critical velocities, which are the flutter, divergence and reverse velocities.

Comparison of the abovementioned relative values is a necessary process during designing the wing profile:

1. In case of the straight wing of the arbitrary design, twisting divergence takes place for velocities, which are higher than the velocity of aileron's reverse. The last one exceeds the velocity of a flexural-torsional flutter.

2. In case of forward-swept wings, it can be expected that the divergence velocity is less than the flutter velocity, and the last one is less than the velocity of aileron's reverse.

3. In case of the sweepback wing, the velocity of aileron's reverse is less than the flutter velocity, which in turn is less than the divergence velocity.

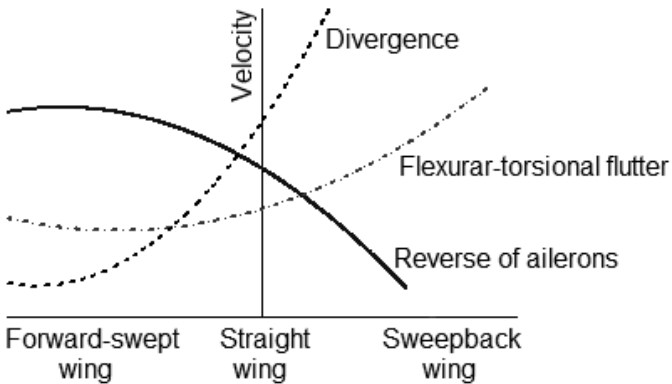


Figure 3.9 – Comparison of critical velocities for the wing

§ 3.4. Divergence of a full-cantilever wing

Torsion of the full-cantilever wing [141], twisted by the aerodynamic moment, is considered for the case of uniform loading along the wing length. From a static equilibrium equation [142] of the infinitesimal wing length (Figure 3.10) it can be obtained:

$$\frac{dM_t}{dz} + M = 0, \quad (3.29)$$

where M – specific aerodynamic moment per unit of the wing length; M_t – torque, which can be calculated by the following expression:

$$M_t = GI_p \frac{d\theta}{dz}; \quad (3.30)$$

GI_p – torsional stiffness of the wing as the product of shear modulus G of wing material and cross-sectional polar moment of inertia I_p [143]; θ – twist angle; z – longitudinal coordinate.

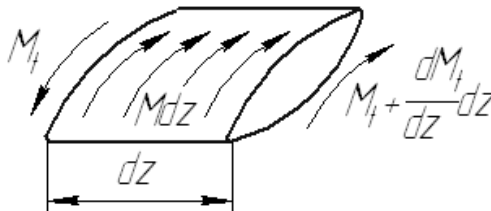


Figure 3.10 – Equilibrium of the infinitesimal wing length

Due to the formula (3.30), an equation (3.29) takes the following form:

$$\frac{d}{dz} \left(GI_p \frac{d\theta}{dz} \right) + M = 0, \quad (3.31)$$

where the aerodynamic moment can be written in the following form:

$$M = q\varepsilon b^2 k\theta, \quad (3.32)$$

where a coefficient k is determined by the formula (3.12). Taking into consideration the following parameter

$$\omega_\alpha = \sqrt{\frac{q\varepsilon b^2 k}{GI_p}} \quad (3.33)$$

for the case of constant torsional stiffness GI_p allows rewrite as a homogeneous second-order differential equation (3.31):

$$\frac{d^2\theta}{dz^2} + \omega_\alpha^2\theta = 0, \quad (3.34)$$

the total integral of which is the harmonic function:

$$\theta(z) = A \sin \omega_\alpha z + B \cos \omega_\alpha z, \quad (3.35)$$

where A, B – constants which can be determined by the boundary conditions:

$$\begin{cases} \theta(0) = 0; \\ M_t|_{z=l} = \left(GI_p \frac{d\theta}{dz} \right) \Big|_{z=l} = 0, \end{cases} \quad (3.36)$$

or due to the formula (3.35):

$$\begin{cases} B = 0; \\ A\omega_\alpha \cos \omega_\alpha l = 0. \end{cases} \quad (3.37)$$

Finally, in case of $A \neq 0$: $B = 0$, and $\omega_\alpha l = \pi n/2$, where n – an arbitrary natural number ($n = 1, 2, \dots$).

Tacking into account the formulas (3.33) and (3.4), the minimum divergence velocity (for the case of $n = 1$) can be obtained in the following form:

$$U_{div} = \frac{\pi}{2bl} \sqrt{\frac{2GI_p}{\rho \varepsilon k}}. \quad (3.38)$$

§ 3.5. Using the influence functions for solving the problems of aeroelasticity

In case of a perfectly elastic body, the dependence between loads and deformations is assumed to be linear, and the reversibility of the loading-unloading process is accepted. Thus, due to the Hooke's law [144], displacement W_i of i -th point under the system of n loading forces Q_j ($j = 1, 2, \dots, n$) can be obtained as the linear form:

$$W_i = \sum_{j=1}^n a_{ij} Q_j, \quad (3.39)$$

where a_{ij} – compliance coefficients. Therewith, a_{ij} is displacement of i -th point under the unit force in j -th point.

The abovementioned approach apparently can be used for two-dimensional and three-dimensional problems of hydroaeroelasticity by introduction the influence function $G(z, \zeta)$, which is the rotation angle of the cross-section with a coordinate z under the unit couple of forces (aerodynamic moment) acting on the cross-section with a coordinate ζ [145].

If the wing is in the static equilibrium state, the total rotation angle $\Theta(z)$ on the arbitrary cross-section is



R. Hooke
(1635–1703)

Robert Hooke – an English architect and polymath, a member of the Royal Council. He is well-known as an important architect of his time, whose influence remains today. Many of Hooke's scientific works were conducted in his capacity as a curator of experiments of the Royal Society.

$$\Theta(z) = \int_0^l G(z, \zeta) M(\zeta) d\zeta, \quad (3.40)$$

where $M(\zeta)$ – distribution function for the aerodynamic moment about the wing length:

$$M(\zeta) = q\varepsilon(\zeta)b^2(\zeta)k\theta(\zeta). \quad (3.41)$$

Finally, the angle $\Theta(z)$ can be obtained by substitution of the formula (3.41) to the formula (3.4):

$$\Theta(z) = qk \int_0^l G(z, \zeta) \varepsilon(\zeta) b^2(\zeta) \theta(\zeta) d\zeta, \quad (3.42)$$

where $b(\zeta)$ – distribution function for the wing width (Figure 3.11).

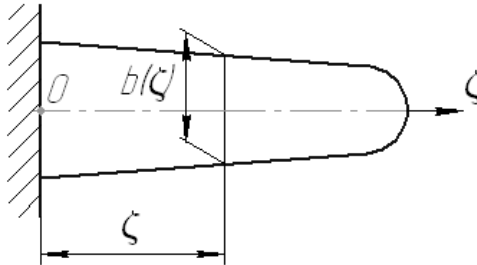


Figure 3.11 – Distribution function for the wing width

Furthermore, the problem of wing twisting under the action of the aileron can be analogously solved by the abovementioned approach.

Questions for self-control

1. Describe the airfoil geometry with the correspondent geometrical parameters.
2. Describe the components of the lift force.
3. What equations allow determining the lift and drag coefficients?
4. Explain the aerodynamic airfoil characteristics.
5. Give the classification of airfoils with their advantages and disadvantages.
6. Describe the design model of the elastically fixed rigid wing and all characteristic points.
7. How can the aerodynamic force be calculated? What parameters does it depend on?
8. Explain the design model of the elastically fixed rigid wing with the aileron.
9. How do the efficiencies of ailerons and tail units depend on the mach number?
10. Describe the algorithm for determination of the critical aileron's velocity.
11. Compare all the critical velocities of the wing.
12. Describe briefly the technique for determination of the divergence velocity of a full-cantilever wing.
13. How can the influence functions be used for solving the problems of aeroelasticity?
14. How can be solved the problem of wing twisting under the action of the aileron?

CHAPTER 4.
Flexural-torsional flutter of
beams and plates

§ 4.1. Equations of small flexural-torsional oscillations of a wing in the gas flow

From the viewpoint of the theory of hydroaeroelasticity, the wing can be considered as an elastic full-cantilever beam with an infinite flexural stiffness in direction x and a finite one, that is equal to EI , in direction y , where I – an axial moment of inertia. The torsional stiffness is equal to GI_p . To simplify the problem, the centre axis is assumed to be straight and directed perpendicular to the flow (Figure 4.1).

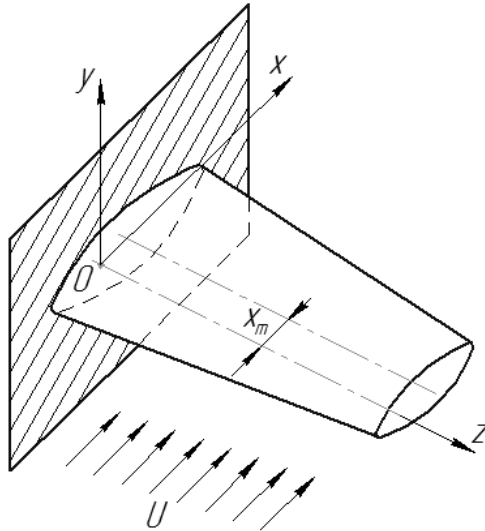


Figure 4.1 – Design scheme of the streamlined wing

Equation of purely flexural oscillations can be obtained by using the basic law of dynamics (the Newton's second law of motion) [146] for an infinitesimal element with specific mass μ :

$$\mu \frac{\partial^2 y}{\partial t^2} = L(t) - \frac{\partial^2 M}{\partial z^2}, \quad (4.1)$$

where $\mu \frac{\partial^2 y}{\partial t^2}$ – specific inertia force.

The component $\frac{\partial^2 M}{\partial z^2}$ of an equation (4.1) is taken into account due to static equilibrium equations for the infinitesimal wing element (Figure 4.2):

$$Q = \frac{\partial M}{\partial z}; \quad L = \frac{\partial Q}{\partial z} = \frac{\partial^2 M}{\partial z^2}, \quad (4.2)$$

where Q – specific share force.

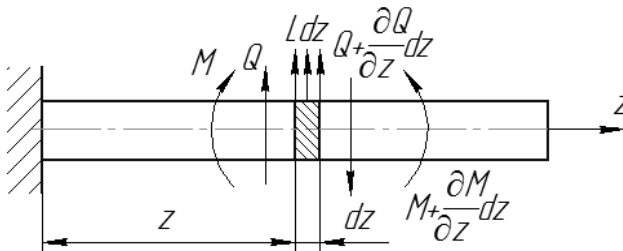


Figure 4.2 – Infinitesimal wing element



I. Newton
(1643–1727)

Isaac Newton – an English mathematician, astronomer and physicist, who is widely recognized as one of the most influential scientists of all the time and a key figure in the scientific revolution. His book “Mathematical principles of natural philosophy” (1687) laid the foundations of classical mechanics.

Due to the formula [147]

$$M = EI \frac{\partial^2 y}{\partial z^2}, \quad (4.3)$$

the equation of purely flexural oscillations (4.1) takes the form:

$$\frac{\partial^2}{\partial z^2} \left(EI \frac{\partial^2 y}{\partial z^2} \right) + \mu \frac{\partial^2 y}{\partial t^2} = L(t). \quad (4.4)$$

The angular momentum theorem [148]

$$\mu r^2 \frac{\partial^2 \alpha}{\partial t^2} = M(t) + \frac{\partial^2 M_t}{\partial z^2} \quad (4.5)$$

due to equations (3.29) and (3.30) for the design scheme presented on Figure 3.10, allows obtaining the equation of torsional oscillations in the following form:

$$-\frac{\partial^2}{\partial z^2} \left(GI_p \frac{\partial^2 \alpha}{\partial z^2} \right) + \mu r^2 \frac{\partial^2 \alpha}{\partial t^2} = M(t), \quad (4.6)$$

where α – rotation angle; $r = I_p/F$ – radius of inertia as the ratio of polar moment of inertia I_p to the cross-sectional area F .

Obviously, in case of the coordinate of the point of lift force application $x_m = BC \neq 0$, there are joint flexural-torsional oscillations (Figure 4.3), which is due to Figure 2.6:

$$y_c = y_B - \alpha x_m. \quad (4.7)$$

Thus, equations (4.4) and (4.6) create the system of differential equations:

$$\begin{cases} \frac{\partial^2}{\partial z^2} \left(EI \frac{\partial^2 y}{\partial z^2} \right) + \mu \frac{\partial^2 y}{\partial t^2} - \mu x_m \frac{\partial^2 \alpha}{\partial t^2} = L(t); \\ -\frac{\partial^2}{\partial z^2} \left(GI_p \frac{\partial^2 \alpha}{\partial z^2} \right) + \mu r^2 \frac{\partial^2 \alpha}{\partial t^2} - \mu x_m \frac{\partial^2 y}{\partial t^2} = M(t), \end{cases} \quad (4.8)$$

which describes small flexural-torsional wing oscillations.

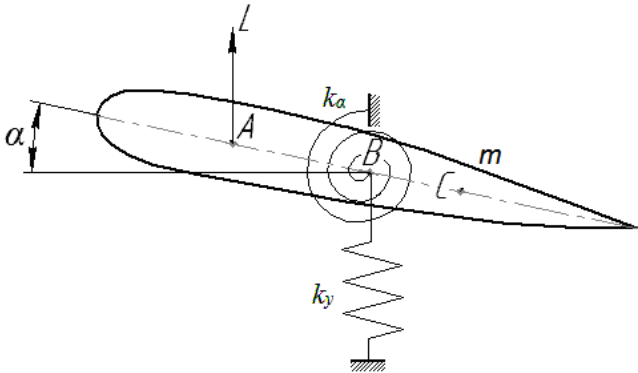


Figure 4.3 – Joint flexural-torsional wing oscillations: C – mass centre; m – specific mass; k_y – linear stiffness coefficient; k_α – angular (torsional) stiffness coefficient

The system of equations (3.8) takes the simplest form in two cases:

1. Using the quasi-stationary theory of subsonic incompressible fluid flow.
2. Taking into consideration high supersonic velocities with using the piston theory.

A simplified solution of equations (4.8) can be obtained under the assumption of a quasisteady character of the

wing motion with the constant linear and angular velocities ($\ddot{y} = \ddot{\alpha} = 0$) in case of a small value of dimensionless reduced frequency. Thus,

$$\begin{cases} L(t) = A_{12}\alpha + B_{11}\dot{y} + B_{12}\dot{\alpha}; \\ M(t) = A_{22}\alpha + B_{21}\dot{y} + B_{22}\dot{\alpha}, \end{cases} \quad (4.9)$$

where A_{i2} , B_{ij} ($i, j = \{1; 2\}$) – stiffness and damping coefficients, which depend on the flow velocity U , and don't depend on time t and coordinate z .

For the abovementioned case, equations of joint flexural-torsional oscillations of the wing are linear with constant coefficients, the solution of which can be written in the following form:

$$\begin{aligned} y &= S(z)e^{\lambda t}; \\ \alpha &= T(z)e^{\lambda t}, \end{aligned} \quad (4.10)$$

where $S(z)$, $T(z)$ – form functions; λ – characteristic index, which can be presented as a complex number:

$$\lambda = p + i\omega. \quad (4.11)$$

In terms of different values of parameters p and ω there are several types of movement. In case of a positive real part ($p > 0$), oscillations amplitude increases, which corresponds to the unstable wing motion. In another case, when $p < 0$, oscillations are damped. The case of $p = 0$ ($\lambda = i\omega$) physically corresponds to a simple harmonic motion. In case of $\omega = 0$ the phenomenon of divergence takes place. The case of $\omega \neq 0$ corresponds to the critical flutter state.

Thus, investigations of the flutter phenomenon can be provided for undamped harmonic oscillations ($p = 0$; $\lambda = i\omega$). This approach allows using the linearized aerodynamic theory [149] and the linear theory of oscillations [16].

The geometrical boundary conditions for the full-cantilever wing at point $z = 0$ are zero displacement y and angle α , as well as zero deviation $\frac{\partial y}{\partial z}$ (the case of fixed cross-section):

$$y|_{z=0} = \frac{\partial y}{\partial z}|_{z=0} = \alpha|_{z=0} = 0. \quad (4.12)$$

The physical boundary conditions at point $z = l$, which corresponds to a free edge, are:

$$Q|_{z=l} = M|_{z=l} = M_t|_{z=l} = 0, \quad (4.13)$$

which can be rewritten due to the formulas (4.2), (4.3) and (3.30) in the following form:

$$\frac{\partial^2 y}{\partial z^2}|_{z=l} = \frac{\partial^3 y}{\partial z^3}|_{z=l} = \frac{\partial \alpha}{\partial z}|_{z=l} = 0. \quad (4.14)$$

§ 4.2. Using Galerkin method for determination of the critical flutter velocity

The consideration of the wing motion for the case of critical flutter ($U = U_{cr}$; $\lambda = i\omega$) allows determining the critical flight velocity U_{cr} . Wherein, harmonic oscillations can be presented in the form (4.10):

$$y = S(z)e^{i\alpha t}; \quad \alpha = T(z)e^{i\alpha t}, \quad (4.15)$$

for the form functions $S(z)$ and $T(z)$, which due to Galerkin method [150] can be taken in the following form:

$$S(z) = \sum_{j=1}^n A_j S_j(z); \quad T(z) = \sum_{j=1}^n B_j T_j(z), \quad (4.16)$$

where A_j, B_j – complex constants in amount of n needed to be found; $S_j(z), T_j(z)$ – linearly independent functions, which satisfy all the geometrical (4.12) and physical (4.14) boundary conditions.

In the first approximation ($n = 1$):

$$S(z) = A_1 S_1(z); \quad T(z) = B_1 T_1(z), \quad (4.17)$$



B. G. Galerkin
(1871–1945)

Boris Grigoryevich Galerkin – a Russian mathematician and engineer. Galerkin method for solving differential equations is known all over the world. Its approach provides a foundation for algorithms in the fields of mechanics, thermodynamics, electromagnetism, hydrodynamics and many others.

where S_1 , T_1 – form functions for purely flexural and torsional oscillations respectively (the case of $x_m = 0$). Then, due to the formula (4.15):

$$y = A_1 S_1 e^{i\alpha z}; \quad \alpha = B_1 T_1 e^{i\omega t}, \quad (4.18)$$

where ω – oscillation frequency.

Due to the formula (4.9), the system of equations (4.4) can be presented in the following form:

$$\begin{cases} \frac{\partial^2}{\partial z^2} \left(EI \frac{\partial^2 y}{\partial z^2} \right) + \mu \frac{\partial^2 y}{\partial t^2} - \mu x_m \frac{\partial^2 \alpha}{\partial t^2} = \\ = A_{12} \alpha + B_{11} \dot{y} + B_{12} \dot{\alpha}; \\ - \frac{\partial^2}{\partial z^2} \left(GI_p \frac{\partial^2 \alpha}{\partial z^2} \right) + \mu r^2 \frac{\partial^2 \alpha}{\partial t^2} - \mu x_m \frac{\partial^2 y}{\partial t^2} = \\ = A_{22} \alpha + B_{21} \dot{y} + B_{22} \dot{\alpha}, \end{cases} \quad (4.19)$$

and with taking into account the formula (4.18):

$$\begin{cases} A_1 \left[\frac{d^2}{dz^2} \left(EI \frac{d^2 S_1}{dz^2} \right) - (\mu \omega^2 + B_{11} i \omega) S_1 \right] + \\ + B_1 (\mu x_m \omega^2 - B_{12} i \omega - A_{12}) T_1 = 0; \\ A_1 (\mu x_m \omega^2 - B_{21} i \omega) S_1 + \\ + B_1 \left[\frac{d^2}{dz^2} \left(GI_p \frac{d^2 T_1}{dz^2} \right) - (\mu r^2 \omega^2 + B_{22} i \omega + A_{22}) T_1 \right] = 0. \end{cases} \quad (4.20)$$

After multiplying the first equation (4.20) by S_1 and the second one by T_1 , after subsequent integration with respect to z

in the range from $z = 0$ to $z = l$ (l – wing length), there can be obtained the homogenous system of linear algebraic equations:

$$\begin{cases} A_1(\omega^2 a_{11} + i\omega b_{11} + c_{11}) + B_1(\omega^2 a_{12} + i\omega b_{12} + c_{12}) = 0; \\ A_1(\omega^2 a_{21} + i\omega b_{21} + c_{21}) + B_1(\omega^2 a_{22} + i\omega b_{22} + c_{22}) = 0, \end{cases} \quad (4.21)$$

where a_{ij} , b_{ij} ($i, j = \{1; 2\}$) – coefficients which depend on the flow (or flight) velocity U , and can be calculated by the following formulas:

$$\begin{aligned} a_{11} &= -\int_0^l \mu S_1^2 dz; & a_{12} &= \int_0^l \mu x_m S_1 T_1 dz; \\ a_{21} &= \int_0^l \mu r^2 S_1 T_1 dz; & a_{22} &= -\int_0^l \mu r^2 T_1^2 dz; \\ b_{11} &= -B_{11} \int_0^l S_1^2 dz; & b_{12} &= -B_{12} \int_0^l S_1 T_1 dz; \\ b_{21} &= -B_{21} \int_0^l S_1 T_1 dz; & b_{22} &= -B_{22} \int_0^l T_1^2 dz; \\ c_{11} &= \int_0^l S_1 \frac{d^2}{dz^2} \left(EI \frac{d^2 S_1}{dz^2} \right) dz; & c_{12} &= -A_{12} \int_0^l S_1 T_1 dz; \\ c_{21} &= 0; & c_{22} &= -\int_0^l T_1 \frac{d}{dz} \left(GI_p \frac{dT_1}{dz} \right) dz - A_{22} \int_0^l T_1^2 dz. \end{aligned} \quad (4.22)$$

The condition of existence of non-trivial solutions of the equation (4.21) is vanishing the determinant [151]:

$$\begin{vmatrix} \omega^2 a_{11} + i\omega b_{11} + c_{11} & \omega^2 a_{12} + i\omega b_{12} + c_{12} \\ \omega^2 a_{21} + i\omega b_{21} + c_{21} & \omega^2 a_{22} + i\omega b_{22} + c_{22} \end{vmatrix} = 0. \quad (4.23)$$

The obtained complex determinant is a frequency equation in the Galerkin form. Its disclosure must be accompanied by the separation of the real part from the imaginary one. As a result, both equations with respect to ω and U create the following system of nonlinear algebraic equations:

$$\begin{cases} a_1 \omega^4 + b_1 \omega^2 + c_1 = 0; \\ b_2 \omega^2 + c_2 = 0, \end{cases} \quad (4.24)$$

where the following coefficients are introduced:

$$\begin{aligned} a_1 &= a_{11}a_{22} - a_{12}a_{21}; \\ b_1 &= a_{11}c_{22} + a_{22}c_{11} + b_{12}b_{21} + a_{21}c_{12}; \\ b_2 &= a_{11}b_{22} + b_{11}a_{22}; \\ c_1 &= c_{11}c_{22}; \quad c_2 = b_{22}c_{11} + b_{11}c_{22}. \end{aligned} \quad (4.25)$$

Oscillation frequency can be determined from the second equation (4.24):

$$\omega = \sqrt{-\frac{c_2}{b_2}}. \quad (4.26)$$

Substitution of this frequency to the equation (4.24) allows obtaining an equation for determining the critical flutter velocity:

$$a_1 c_2^2 - b_1 b_2 c_2 + b_2^2 c_1 = 0. \quad (4.27)$$

It can be shown, that the equation (4.27) can be rewritten in the form of biquadratic equation [64]

$$aU_{cr}^4 + bU_{cr}^2 + c = 0 \quad (4.28)$$

with the constants a, b, c .

The minimum value of real roots

$$U_{cr} = \sqrt{\frac{-b \pm \sqrt{b^2 - 4ac}}{2a}} \quad (4.29)$$

corresponds to the critical flutter velocity U_{cr} .

Due to the practical necessities, the critical flutter velocity U_{cr} is usually determined, rather than the oscillation form. Therefore, the solution of the aeroelasticity problem ends at this stage.

It should be noted, that in general case the aerodynamic force L and the moment M depend on the Theodorsen function, which leads to the nonlinearity of the abovementioned equations for determining the oscillation frequency ω and the critical flutter velocity U_{cr} .

§ 4.3. Flutter of a single-mass system with two degrees of freedom

The flexural-torsional wing oscillations as the single-mass system can be considered by taking into account the design scheme presented on Figure 4.3. Wherein, the total specific mass m of the system is concentrated at point C . The system has two degrees of freedom corresponding to transverse displacement y_C of the mass centre C and rotation around it at the angle α .

Equations of purely flexural and torsional oscillations of the partial systems have the following forms [152]:

$$m\ddot{y} + k_y y = L(t); \quad (4.30)$$

$$I_\alpha \ddot{\alpha} + k_\alpha \alpha = M(t), \quad (4.31)$$

where k_y , k_α – linear and angular (torsional) stiffness coefficient respectively; I_α – polar moment of inertia.

The system of equations, which describes the joint flexural-torsional oscillations, can be obtained by using the formula [4.7]:

$$\begin{cases} \ddot{y} + \omega_k^2 y - x_m \ddot{\alpha} = \frac{L(t)}{m}; \\ \ddot{\alpha} + \omega_\alpha^2 \alpha + q\ddot{y} = \frac{M(t)}{m}, \end{cases} \quad (4.32)$$

where ω_k , ω_α – eigenfrequencies of partial systems:

$$\omega_k = \sqrt{\frac{k_y}{m}}; \quad \omega_\alpha = \sqrt{\frac{k_\alpha}{I_\alpha}}, \quad (4.33)$$

and q – coefficient calculated by the formula:

$$q = \frac{mx_m}{I_\alpha}. \quad (4.34)$$

The list force $L(t)$ and its moment $M(t)$ can be taken into account in the coarsest approximation (2.133). In this case, the equations (4.32) take the following form:

$$\begin{cases} \ddot{y} + \omega_k^2 y - x_m \ddot{\alpha} = cU^2 \left(\alpha - \frac{\dot{y}}{U} \right); \\ \ddot{\alpha} + \omega_\alpha^2 \alpha + q\ddot{y} = dU^2 \left(\alpha - \frac{\dot{y}}{U} \right), \end{cases} \quad (4.35)$$

where coefficients are introduced:

$$c = \frac{\pi\rho b}{m}; \quad d = \frac{\pi\rho b^2}{4I_\alpha} \left(1 + \frac{4x_m}{b} \right). \quad (4.36)$$

The system of equations (4.35) can be reduced to the following form:

$$\begin{cases} \ddot{y} + cU \dot{y} + \omega_k^2 y - x_m \ddot{\alpha} + cU^2 \alpha = 0; \\ q\ddot{y} + dU \dot{y} + \ddot{\alpha} + (\omega_\alpha^2 - dU^2) \alpha = 0, \end{cases} \quad (4.37)$$

the solutions of which can be obtained in the form:

$$\begin{aligned} y &= Ae^{i\omega t}; \\ \alpha &= Be^{i\omega t}. \end{aligned} \quad (4.38)$$

The substitution of expressions (4.38) into the fourth order system of differential equations (4.37) gives the homogeneous system of two linear algebraic equations with respect to unknown amplitudes A and B :

$$\begin{cases} (-\omega^2 + i\omega cU + \omega_y^2)A + (\omega^2 x_m - cU^2)B = 0; \\ (-\omega^2 q + i\omega dU)A + (-\omega^2 + \omega_\alpha^2 - dU^2)B = 0. \end{cases} \quad (4.39)$$

The condition of existence of non-trivial solutions of the equation (4.39) is vanishing of the following determinant:

$$\begin{vmatrix} -\omega^2 + i\omega cU + \omega_y^2 & \omega^2 x_m - cU^2 \\ -\omega^2 q + i\omega dU & -\omega^2 + \omega_\alpha^2 - dU^2 \end{vmatrix} = 0 \quad (4.40)$$

as the complex frequency equation, which after its disclosure can be described by the following system of nonlinear algebraic equations with respect to ω and U :

$$\begin{cases} (c + x_m d)\omega^2 - c\omega_\alpha^2 = 0; \\ (1 + x_m q)\omega^4 - (\omega_\alpha^2 + \omega_y^2)\omega^2 + (cq + d)\omega^2 U^2 + \\ + \omega_y^2(\omega_\alpha^2 - dU^2) = 0. \end{cases} \quad (4.41)$$

The eigenfrequency ω of the joint flexural-torsional oscillations can be obtained from the first equation of the system (4.41):

$$\omega = \frac{\omega_\alpha}{\sqrt{1 + \frac{d}{c} x_m}}, \quad (4.42)$$

and the velocity U – from the second one:

$$\left(\frac{2U}{b\omega_\alpha^2} \right)^2 = \frac{4}{b^2 d} \frac{(1 + x_m q) \frac{\omega_\alpha^4}{\omega_\alpha^4} - \left(1 + \frac{\omega_y^2}{\omega_\alpha^2} \right) \frac{\omega^2}{\omega_\alpha^2} + \frac{\omega_y^2}{\omega_\alpha^2}}{\frac{\omega_y^2}{\omega_\alpha^2} - \frac{\omega^2}{\omega_\alpha^2} \left(1 + \frac{cq}{d} \right)}. \quad (4.43)$$

It should be noted, that in case of zero value of the eigenfrequency ($\omega = 0$), the critical divergence velocity U_{div} can be obtained:

$$\left(\frac{2U_{div}}{b\omega_\alpha^2} \right)^2 = \frac{4}{b^2 d} = \frac{16I_\alpha}{\pi \rho b^2}, \quad (4.44)$$

which corresponds to the equation (3.21).

The critical flutter velocity U_{cr} can be obtained by substitution of the eigenfrequency ω (4.42) to the equation (4.43):

$$\left(\frac{2U_{cr}}{b\omega_\alpha^2} \right)^2 = \frac{4}{\left(1 + \frac{c}{x_m d} \right) b^2 d} \frac{\left(1 + \frac{x_m d}{c} \right) \frac{\omega_y^2}{\omega_\alpha^2} - \left(1 - \frac{cq}{d} \right)}{\left(1 + \frac{x_m d}{c} \right) \frac{\omega_y^2}{\omega_\alpha^2} - \left(1 + \frac{cq}{d} \right)}, \quad (4.45)$$

graphically presented on Figure 4.4 as an example for the different values of x_m/b and ω_y/ω_α .

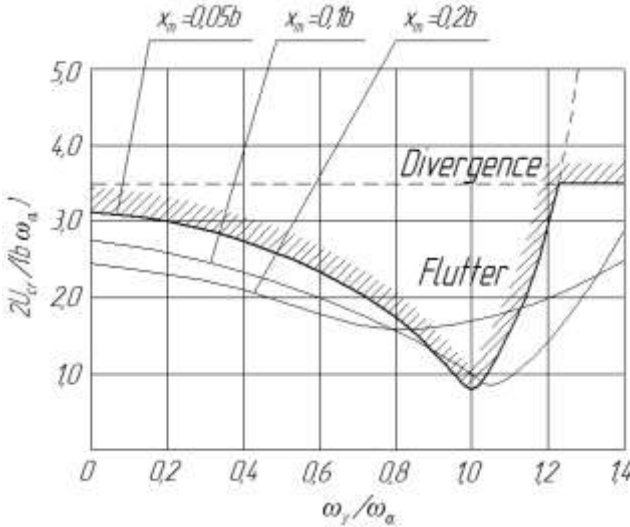


Figure 4.4 – Dependence of the critical flutter velocity on the partial frequencies

Analysis of the abovementioned formula determines the following conclusions:

1. The partial frequency ratio ω_y / ω_α has a significant impact on the critical flutter velocity U_{cr} .
2. The critical flutter velocity U_{cr} can be either higher or lower than the divergence velocity U_{div} .
3. Divergence is dangerous only for small torsional stiffness k_α of the system: $\omega_\alpha \ll \omega_y$.

§ 4.4. Using Routh–Hurwitz criterion for determination of the critical flutter velocity

The general problem related to the stability of the cantilever wing at a certain flight velocity U can be investigated by solving the system of equations (4.19). Wherein, the solution is found in the form:

$$\begin{aligned} y &= AS(z)e^{\lambda t}; \\ \alpha &= BT(z)e^{\lambda t}, \end{aligned} \quad (4.46)$$

where A , B – constants needed to be found; $S(z)$, $T(z)$ – functions that satisfy all the geometrical (4.12) and physical (4.14) boundary conditions; λ – solution of the characteristic equation described below.

Due to the formula (4.46) the system of equations (4.19) can be rewritten in the following form:

$$\left\{ \begin{aligned} &A \left[\frac{d^2}{dz^2} \left(EI \frac{d^2 S}{dz^2} \right) + (\mu \lambda^2 - B_{11} \lambda) S \right] - \\ &- B (\mu x_m \lambda^2 + B_{12} \lambda + A_{12}) T = 0; \\ &- A (\mu x_m \lambda^2 + B_{21} \lambda) S + \\ &+ B \left[\frac{d^2}{dz^2} \left(GI_p \frac{d^2 T}{dz^2} \right) + (\mu r^2 \lambda^2 - B_{22} \lambda - A_{22}) T \right] = 0. \end{aligned} \right. \quad (4.47)$$

For the approximate solution, Galerkin method is applied. In this case, after multiplying the first equation (4.47) by S and the second one by T , after subsequent integration with respect to z in the range from $z = 0$ to wing length $z = l$, there

can be obtained the homogenous system of linear algebraic equations:

$$\begin{cases} (\lambda^2 a_{11} + \lambda b_{11} + c_{11})A + (\lambda^2 a_{12} + \lambda b_{12} + c_{12})B = 0; \\ (\lambda^2 a_{21} + \lambda b_{21} + c_{21})A + (\omega^2 a_{22} - \lambda b_{22} + c_{22})B = 0, \end{cases} \quad (4.48)$$

where a_{ij} , b_{ij} ($i, j = \{1; 2\}$) – coefficients, that can be calculated with the following formulas:

$$\begin{aligned} a_{11} &= -\int_0^l \mu S^2 dz; & a_{12} &= \int_0^l \mu x_m ST dz; \\ a_{21} &= \int_0^l \mu r^2 ST dz; & a_{22} &= -\int_0^l \mu r^2 T^2 dz; \\ b_{11} &= B_{11} \int_0^l S^2 dz; & b_{12} &= B_{12} \int_0^l ST dz; \\ b_{21} &= B_{21} \int_0^l ST dz; & b_{22} &= B_{22} \int_0^l T^2 dz; \\ c_{11} &= -\int_0^l S \frac{d^2}{dz^2} \left(EI \frac{d^2 S}{dz^2} \right) dz; & c_{12} &= A_{12} \int_0^l ST dz; \\ c_{21} &= 0; & c_{22} &= \int_0^l T \frac{d}{dz} \left(GI_p \frac{dT}{dz} \right) dz + A_{22} \int_0^l T^2 dz. \end{aligned} \quad (4.49)$$

The condition of existence of non-trivial solutions of the equation (4.49) is vanishing of the following determinant:

$$\begin{vmatrix} \lambda^2 a_{11} + \lambda b_{11} + c_{11} & \lambda^2 a_{12} + \lambda b_{12} + c_{12} \\ \lambda^2 a_{21} + \lambda b_{21} + c_{21} & \lambda^2 a_{22} + \lambda b_{22} + c_{22} \end{vmatrix} = 0, \quad (4.50)$$

disclosure of which leads to the fourth degree algebraic equation:

$$\lambda^4 + A_3\lambda^3 + A_2\lambda^2 + A_1\lambda + A_0 = 0, \quad (4.51)$$

with the constant coefficients A_i ($i = \{0; 1; 2; 3\}$).

It should be noted that Routh–Hurwitz approach is based on investigation of the roots of equation (4.51).

The equation (4.51) has two pairs of complex conjugate roots [153]:

$$\lambda_{1,2} = -p_1 \pm i\omega_1; \quad \lambda_{3,4} = -p_2 \pm i\omega_2. \quad (4.52)$$

Minus sign “–” before real parts p_1 and p_2 is chosen for ensuring stability of the system.

Moreover, the following expression is valid:

$$(\lambda - \lambda_1)(\lambda - \lambda_2)(\lambda - \lambda_3)(\lambda - \lambda_4) = 0 \quad (4.53)$$

or after expanding:

$$\begin{aligned} &\lambda^4 - (\lambda_1 + \lambda_2 + \lambda_3 + \lambda_4)\lambda^3 + \\ &+ (\lambda_1\lambda_2 + \lambda_1\lambda_3 + \lambda_1\lambda_4 + \lambda_2\lambda_3 + \lambda_2\lambda_4 + \lambda_3\lambda_4)\lambda^2 - \\ &- (\lambda_1\lambda_2\lambda_3 + \lambda_2\lambda_3\lambda_4 + \lambda_3\lambda_4\lambda_1 + \lambda_4\lambda_1\lambda_2)\lambda + \lambda_1\lambda_2\lambda_3\lambda_4 = 0. \end{aligned} \quad (4.54)$$



E. J. Routh
(1831–1907)

Edward John Routh – an English mathematician, well known for his contribution for systematization of the mathematical theory of mechanics, as well as for development of modern control systems theory. He derived the stability criterion for linear systems.

Thus, substitutions of the roots (4.52) in the equation (4.54) with taking into account the formula (4.51) gives the expressions for determining unknown coefficients A_i ($i = \{0; 1; 2; 3\}$):

$$\begin{aligned} A_0 &= (p_1^2 + \omega_1^2)(p_2^2 + \omega_2^2); \\ A_1 &= 2[p_1(p_2^2 + \omega_2^2) + p_2(p_1^2 + \omega_1^2)]; \\ A_2 &= p_1^2 + p_2^2 + 4p_1p_2 + \omega_1^2 + \omega_2^2; \\ A_3 &= 2(p_1 + p_2). \end{aligned} \quad (4.55)$$

As a result, all the coefficients A_i are positive, which is the necessary condition for stability of the wing oscillations. However, the positivity of the coefficients A_i is not sufficient condition for ensuring stability of the system. In addition, the compatibility condition [154] for the coefficients (4.55) are:

$$A_1A_2A_3 = A_1^2 + A_0A_3^2, \quad (4.56)$$

which can be ensured on the stability threshold. But, the unknown fact is from which side of this equality the stability takes place. This can be determined for one of the particular cases for the values of the parameters p_i, ω_i ($i = \{1; 2\}$).

For example, $p_1 = \omega_1 = 1; p_2 = \omega_2 = 2$. In this case $A_0 = 16, A_1 = 24, A_2 = 18$ and $A_3 = 6$. Finally, $A_1A_2A_3 > A_1^2 + A_0A_3^2$ due to $2592 > 1152$, as well as the



A. Hurwitz
(1859–1919)

Adolf Hurwitz – a German mathematician, who worked on algebra, analysis, geometry and number theory, and well-known for his works in the field of control systems and dynamical systems theory. Independently of E. J. Routh, he derived the stability criterion for linear systems by a different method.

Routh–Hurwitz conditions of the stability are:

$$\begin{cases} A_i = 0 \quad (i = \overline{0..3}); \\ A_1 A_2 A_3 > A_1^2 + A_0 A_3^2. \end{cases} \quad (4.57)$$

It can be shown, that the conditions (4.57) lead to the equation (4.28), which was obtained previously, as well as the critical flutter velocity is determined by the formula (4.29).

§ 4.5. Flexural-torsional flutter of a plate

Oscillations of the streamlined elastically fixed rectangular plate are considered (Figure 4.5). Supporting stiffness on the leading edge is k_1 and on the trailing edge is k_2 . The lift force L acting on the plate is applied at point B located at a distance e from the mass centre C . Due to the formulas (3.3), (3.4), (3.8) and taking into account the strip theory [137] ($\partial C_y / \partial \alpha = 2\pi$), the total lift force is approximately determined by a formula:

$$L = C_y q b l = \frac{\partial C_y}{\partial \alpha} \alpha \frac{\rho U^2}{2} b l = \pi \rho U^2 b l \alpha, \quad (4.58)$$

where ρ – fluid density; U – flow velocity; α – attack angle; b – chord; l – plate length.

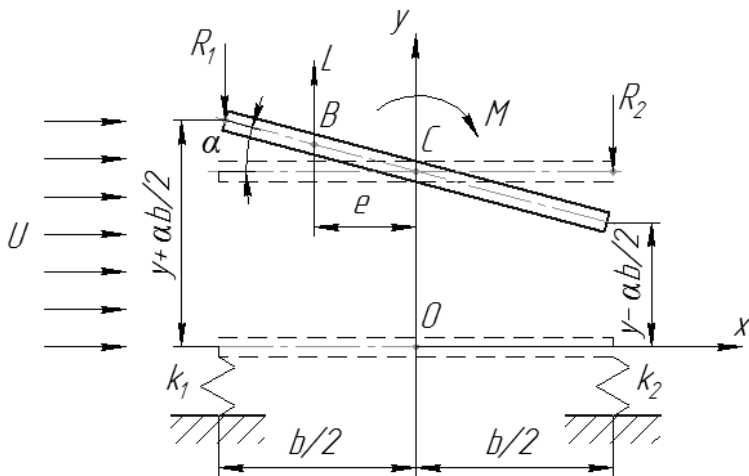


Figure 4.5 – Design scheme of the streamlined elastically fixed rectangular plate

Due to the elastic supports, the elastic forces act on the plate:

$$R_1 = k_1 l \left(y + \frac{\alpha b}{2} \right); \quad R_2 = k_2 l \left(y - \frac{\alpha b}{2} \right). \quad (4.59)$$

The aerodynamic and elastic forces lead to flexural-torsional oscillations of the plate, which can be described by linearized differential equations for plane movement of the mechanical system [155]:

$$\begin{cases} m\ddot{y} = L - R_1 - R_2; \\ I\ddot{\alpha} = Le - R_1 \frac{b}{2} + R_2 \frac{b}{2}, \end{cases} \quad (4.60)$$

where m – mass of the plate; I – axial moment of inertia of the rectangular plate about the mass centre C [155]:

$$\begin{aligned} m &= \mu b l; \\ I &= \frac{1}{12} m b^2 = \frac{1}{12} \mu b^3 l; \end{aligned} \quad (4.61)$$

μ – specific mass per unit area.

Due to the formulas (4.58) and (4.60), the system of equations (4.60) takes the form:

$$\begin{cases} \mu b l \ddot{y} = \pi \rho U^2 b l \alpha - R_1 - R_2; \\ \frac{1}{12} \mu b^3 l \ddot{\alpha} = \pi \rho U^2 b l \alpha e - R_1 \frac{b}{2} + R_2 \frac{b}{2} \end{cases} \quad (4.62)$$

which can be rewritten by taking into account eccentricity $e = \varepsilon b$ (ε – dimensionless eccentricity) and the formula (4.59):

$$\begin{cases} \mu b l \ddot{y} = \pi \rho U^2 b l \alpha - k_1 l \left(y + \frac{\alpha b}{2} \right) - k_2 l \left(y - \frac{\alpha b}{2} \right); \\ \frac{\mu b^3 l \ddot{\alpha}}{12} = \pi \rho U^2 \varepsilon b^2 l \alpha - k_1 l \left(y + \frac{\alpha b}{2} \right) \frac{b}{2} + k_2 l \left(y - \frac{\alpha b}{2} \right) \frac{b}{2}, \end{cases} \quad (4.63)$$

or after identical transformations:

$$\begin{cases} \ddot{y} + \frac{k_1 + k_2}{\mu b} y + \left(\frac{k_1 - k_2}{2\mu} - \frac{\pi \rho U^2}{\mu} \right) \alpha = 0; \\ \ddot{\alpha} + \frac{6(k_1 + k_2)}{\mu b^2} y + \left[\frac{3(k_1 + k_2)}{\mu b} - \frac{12\pi \rho \varepsilon U^2}{\mu b} \right] \alpha = 0. \end{cases} \quad (4.64)$$

Introduction of the coefficients

$$\begin{aligned} a_{11} &= \frac{k_1 + k_2}{\mu b}; & a_{12} &= \frac{k_1 - k_2}{2\mu} - \frac{\pi \rho U^2}{\mu}; \\ a_{21} &= \frac{6(k_1 + k_2)}{\mu b^2}; & a_{22} &= \frac{3(k_1 + k_2)}{\mu b} - \frac{12\pi \rho \varepsilon U^2}{\mu b} \end{aligned} \quad (4.65)$$

allows rewriting the system of the differential equations (4.64):

$$\begin{cases} \ddot{y} + a_{11}y + a_{12}\alpha = 0; \\ \ddot{\alpha} + a_{21}y + a_{22}\alpha = 0. \end{cases} \quad (4.66)$$

The case of $\ddot{y} = \ddot{\alpha} = 0$ describes the plate divergence:

$$\begin{cases} a_{11}y + a_{12}\alpha = 0; \\ a_{21}y + a_{22}\alpha = 0. \end{cases} \quad (4.67)$$

The condition of existence of non-trivial solutions of the equation (4.67) is vanishing of the following determinant:

$$\begin{vmatrix} a_{11} & a_{12} \\ a_{21} & a_{22} \end{vmatrix} = a_{11}a_{22} - a_{12}a_{21} = 0. \quad (4.68)$$

Taking into account the expressions (4.65) gives:

$$\begin{aligned} & \frac{k_1 + k_2}{\mu b} \left[\frac{3(k_1 + k_2)}{\mu b} - \frac{12\pi\rho\varepsilon U^2}{\mu b} \right] - \\ & - \left(\frac{k_1 - k_2}{2\mu} - \frac{\pi\rho U^2}{\mu} \right) \frac{6(k_1 + k_2)}{\mu b^2} = 0, \end{aligned} \quad (4.69)$$

or after simplifying:

$$2k_1k_2 - \pi\rho U^2 [k_2(1 + 2\varepsilon) - k_1(1 - 2\varepsilon)] = 0. \quad (4.70)$$

Thus, the divergence velocity can be obtained:

$$U_{div} = \sqrt{\frac{2k_1k_2}{\pi\rho [k_2(1 + 2\varepsilon) - k_1(1 - 2\varepsilon)]}}. \quad (4.71)$$

Resulting the formula (4.71) let's consider the following partial cases:

1. Due to the strip theory [137], dimensionless eccentricity $\varepsilon = 1/4$:

$$U_{div} = \sqrt{\frac{4k_1k_2}{\pi\rho(3k_2 - k_1)}}. \quad (4.72)$$

In this case divergence is possible for $3k_2 > k_1$.

2. In case of zero eccentricity ($\varepsilon = 0$):

$$U_{div} = \sqrt{\frac{2k_1k_2}{\pi\rho(k_2 - k_1)}}, \quad (4.73)$$

And divergence takes place for $k_2 > k_1$.

3. In case of infinite stiffness $k_2 \rightarrow \infty$ (Figure 4.6 a):

$$U_{div} = \sqrt{\frac{2k_1}{\pi\rho}}. \quad (4.74)$$

However, the case $k_1 \rightarrow \infty$ (Figure 4.6 b) cannot lead to divergence.

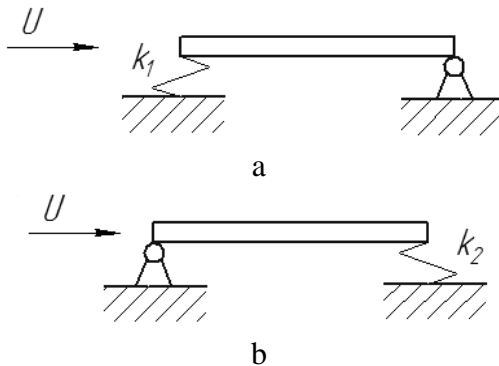


Figure 4.6 – Design scheme for the case of infinite stiffness

In the general case of the flexural-torsional oscillations described by the fourth order system of homogeneous differential equations (4.66), the solution can be presented in the form of mono-harmonic oscillations [156]:

$$\begin{aligned} y &= Ae^{i\omega t}; \\ \alpha &= Be^{i\omega t}, \end{aligned} \quad (4.75)$$

where A , B – unknown amplitudes; ω – oscillation frequency.

Substitution of the formula (4.75) to the equations (4.66) leads to the homogeneous system of linear algebraic equations with respect to amplitudes A and B :

$$\begin{cases} (a_{11} - \omega^2)y + a_{12}\alpha = 0; \\ a_{21}y + (a_{22} - \omega^2)\alpha = 0. \end{cases} \quad (4.76)$$

The condition of existence of non-trivial solutions of the equation (4.76) is vanishing of the following determinant:

$$\begin{aligned} &\begin{vmatrix} a_{11} - \omega^2 & a_{12} \\ a_{21} & a_{22} - \omega^2 \end{vmatrix} = \\ &= \omega^4 - (a_{11} + a_{22})\omega^2 + a_{11}a_{22} - a_{12}a_{21} = 0, \end{aligned} \quad (4.77)$$

which is the frequency equation. Its roots are:

$$\omega^2 = \frac{a_{11} + a_{22}}{2} \pm \sqrt{\frac{(a_{11} + a_{22})^2}{4} - (a_{11}a_{22} - a_{12}a_{21})}. \quad (4.78)$$

It should be noted, that the following conditions must be satisfied:

1. Square eigenfrequency ω^2 is real:

$$a_{11}a_{22} - a_{12}a_{21} \leq \frac{(a_{11} + a_{22})^2}{4}. \quad (4.79)$$

2. Square eigenfrequency ω^2 is positive:

$$a_{11}a_{22} - a_{12}a_{21} > 0. \quad (4.80)$$

On the stability threshold, the first condition (4.79) after equivalent transformation leads to an equation:

$$(a_{11} - a_{22})^2 + 4a_{12}a_{21} = 0, \quad (4.81)$$

which can be rewritten due to formulas (4.65) in the form of biquadratic equation (4.28) with the following coefficients:

$$\begin{aligned} a &= (12\pi\rho\varepsilon)^2; \\ b &= -24\pi\rho[k_1 - k_2 + 2\varepsilon(k_1 + k_2)]; \\ c &= 16(k_1^2 - k_1k_2 + k_2^2). \end{aligned} \quad (4.82)$$

Its roots (4.29) take the form:

$$\begin{aligned} U_{cr}^2 &= \frac{k_1 - k_2 + 2\varepsilon(k_1 + k_2)}{(12\pi\rho\varepsilon)^2} \pm \\ &\pm \frac{k_1 - k_2}{(12\pi\rho\varepsilon)^2} \sqrt{1 + 4\varepsilon \frac{k_1 + k_2}{k_1 - k_2} - 12\varepsilon^2}. \end{aligned} \quad (4.83)$$

In case of small eccentricity ($\varepsilon \ll 1$), the coefficients (4.82) take the form:

$$\begin{aligned} a &= 0; \\ b &= -24\pi\rho(k_1 - k_2); \\ c &= 16(k_1^2 - k_1k_2 + k_2^2), \end{aligned} \quad (4.84)$$

and the biquadratic equation (4.28) reduces to a quadratic equation:

$$bU_{cr}^2 + c = 0, \quad (4.85)$$

the positive root of which

$$U_{cr} = \sqrt{-\frac{c}{b}} = \sqrt{\frac{2(k_1^2 - k_1k_2 + k_2^2)}{3\pi\rho(k_1 - k_2)}}. \quad (4.86)$$

Thus, the flexural-torsional flutter is possible under the condition $k_1 > k_2$.

Questions for self-control

1. Explain the design model of small flexural-torsional oscillations of a wing streamlined by the gas flow. What equations can be used for describing such oscillations?

2. Describe Galerkin method for determination of the critical flutter velocity.

3. Describe briefly the approach for determining the critical flutter velocity of a single-mass system with two degrees of freedom.

4. Explain graphically the dependence between the critical flutter velocity and the partial frequencies of a single-mass system with two degrees of freedom.

5. Specify Routh–Hurwitz criterion for determination of the critical flutter velocity.

6. Explain the approach for investigating oscillations of the streamlined elastically fixed rectangular plate, elastically supported on the leading and tailing edges.

7. Describe the special cases of the design schemes of the elastically fixed rectangular plate.

8. What design scheme of the streamlined elastically fixed rectangular plate cannot lead to divergence?

9. Set the differences and similarities between using Galerkin method and Routh–Hurwitz criterion for investigating small flexural-torsional oscillations of a wing.

CHAPTER 5.
Oscillations of poorly
streamlined beams
in the gas flow

§ 5.1. Oscillations of a cylinder in the gas flow

Oscillations of a circular cylinder, poorly streamlined by the gas flow, are considered. A characteristic feature of this phenomenon is the appearance of Karman vortex street (Figure 5.1) as well-ordered set of vortices moving periodically in space and in time [51–53, 55].

Separation of the single vortex from the cylinder surface is accompanied by the flow circulation, which changes by the amount equal to intensity of the vortex. If Karman vortex street forms behind the cylinder, then vortices emerge alternately on the opposite directions from the cylinder surface in equal time intervals. Therefore, the lift force is changed periodically, which is the cause of the oscillations occurring transversely to the flow direction [64].

The abovementioned phenomenon of emerging the trailing vortices was investigated for the first time by T. Karman. His experimental research allows determining the dependence between the frequency of vortex shedding f , cylinder diameter d and flow velocity U :

$$St = \frac{fd}{U} = 0.2, \quad (5.1)$$

where St – Strouhal number [156], which physically means the specific frequency of vortex shedding.

The more accurate empirical formula [157]

$$St = 0.195 \left(1 - \frac{20.1}{Re} \right) \quad (5.2)$$

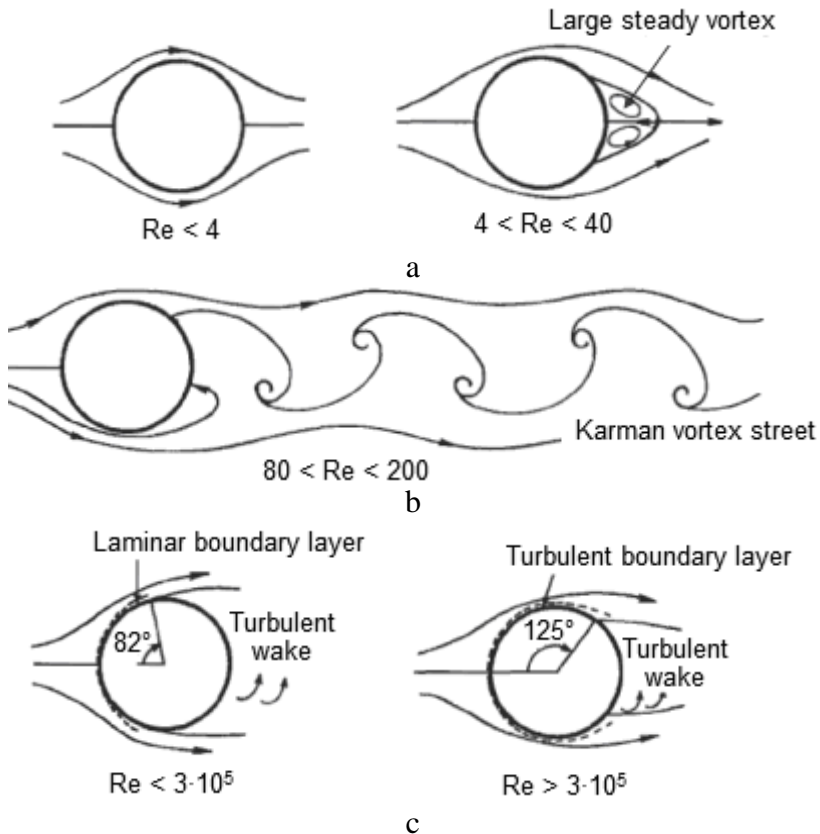


Figure 5.1 – Flow separation over a cylinder at different Reynolds number



V. Strouhal
(1850–1922)

Vincenc Strouhal – a Czech physicist specializing in experimental physics. He was one of the founders of the Physics department at Charles University in Prague.

takes into account Reynolds number Re [158] in the range of $40 \dots 5 \cdot 10^3$:

$$Re = \frac{Ud}{\nu}, \quad (5.3)$$

where d – a hydraulic diameter; ν – kinematic viscosity of environment.

It should be noted, that there are several cases of the flow pattern due to the Reynolds number:

1. In case of small Reynolds numbers ($Re < 40$), smooth flow about a cylinder occurs (Figure 5.1 a).

2. In case of $Re = 40$, vortices become asymmetric, they detach from the cylinder surface and move downstream alternately on its both sides.

3. The case of $40 < Re \leq 150$ corresponds to the regular vortex detaching (Figure 5.1 b).

4. The case of $150 < Re < 300$ corresponds to a transient mode.

5. There is irregular vortex street with random amplitude at Reynolds numbers $Re \geq 300$.

6. The turbulent wake appears at Reynolds numbers $Re > 10^5$ (Figure 5.1 b).

However, the theoretical investigation of the vortex street under assumption of an ideal fluid cannot disclose the impact



O. Reynolds
(1842–1912)

Osborne Reynolds – a prominent innovator in the understanding of fluid dynamics. Separately, his studies of heat transfer between solids and fluids brought improvements in boiler and condenser design. He spent his entire career at University of Manchester. Reynolds most famously studied the conditions in which the flow of fluid in pipes transitioned from a laminar flow to a turbulent one.

of Reynolds number Re on the flow pattern. Simultaneously, allowance of friction involves certain mathematical complexities.

Thus, vortex detaching from the cylinder surface caused the periodically changing force perpendicular to the flow direction. Its amplitude can be presented in the following form:

$$q_0 = C_k \frac{\rho U^2}{2} d, \quad (5.4)$$

where ρ – density of environment; U – flow velocity; d – cylinder diameter (Figure 5.2).

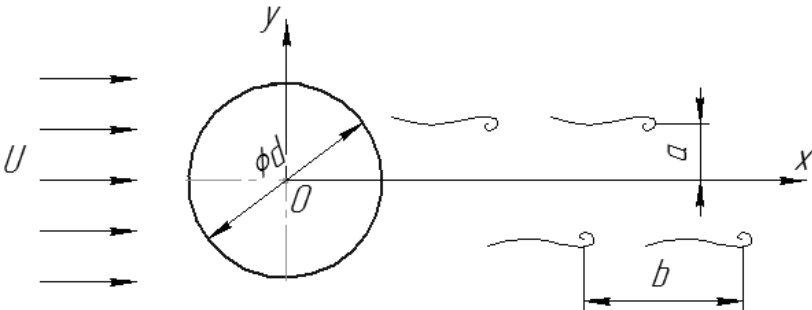


Figure 5.2 – Karman vortex street

Karman's coefficient C_k takes values in the range 0,5...1,7 and can be determined by the following formula [159]:

$$C_k = 2\sqrt{2} \frac{b}{d} \left(1 - \frac{b}{d} St \right), \quad (5.5)$$

where b – vortex step (Figure 5.2).

Due to the huge experimental experience, oscillations of poorly streamlined bodies can be interpreted from two viewpoints:

- 1) forced oscillations in the system with delay [160];
- 2) self-oscillations [39, 40].

The first case corresponds to the fluid flow, whereas the second one is more suitable for the gas flow.

The design scheme describing forced oscillations of the streamlined cylinder in the fluid flow is presented on Figure 5.3.

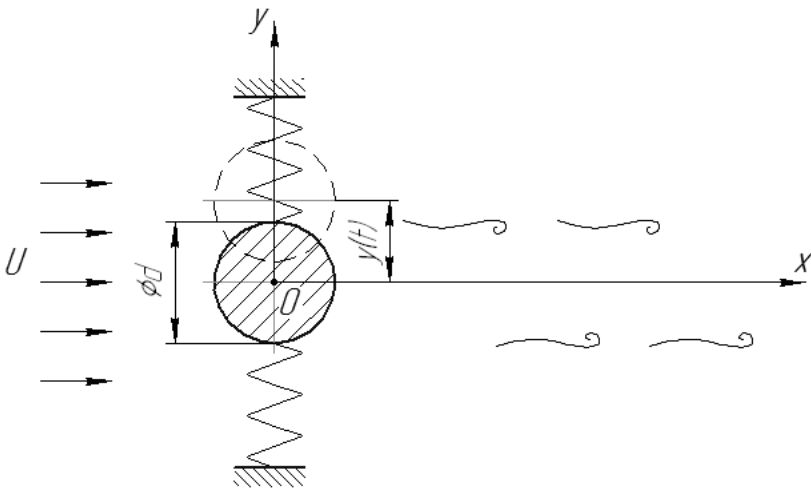


Figure 5.3 – Design scheme of forced oscillations of the streamlined cylinder in the fluid flow

An equation of oscillations of the damped single-mass system has the following form [161]:

$$\ddot{y} + 2n\dot{y} + \omega^2 y = \frac{q[y(t)]}{m}, \quad (5.6)$$

where m – specific mass; y – displacement of the centre mass; n – damping coefficient; ω – eigenfrequency; q – specific square-wave external force (Figure 5.4):

$$q(t) = \begin{cases} q_0, & -\frac{\pi}{2f} + \tau \leq t < \frac{\pi}{2f} + \tau; \\ q_0, & \frac{\pi}{2f} + \tau \leq t < \frac{3\pi}{2f} + \tau, \end{cases} \quad (5.7)$$

where q_0 – amplitude (5.4); f – frequency; τ – time delay.

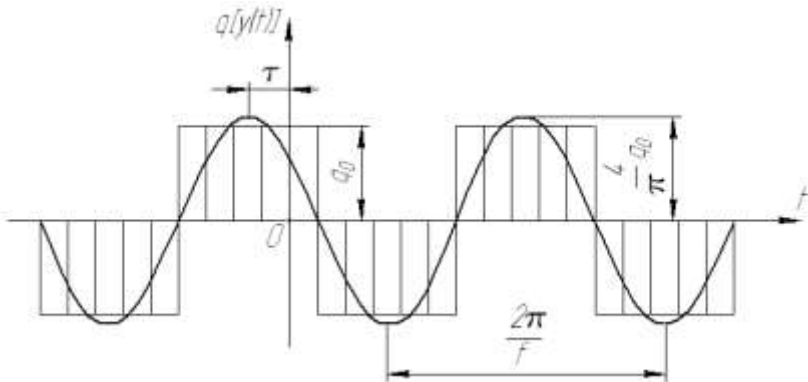


Figure 5.4 – Specific square-wave external force

Displacement is changed by the harmonic law:

$$y(t) = A \cos ft. \quad (5.8)$$

The aerodynamic force $q(t)$ can be expanded as a Fourier series [162]:

$$q(t) = \frac{a_0}{2} + \sum_{i=1}^{\infty} a_i \cos[if(t - \tau)] + \sum_{i=1}^{\infty} b_i \sin[if(t - \tau)], \quad (5.9)$$

the coefficients a_0, a_i, b_i ($i = 1 \dots \infty$) of which are determined by following formulas:

$$\begin{aligned} a_0 &= \frac{1}{T} \int_0^T q(t) dt; \\ a_i &= \frac{1}{T} \int_0^T q(t) \cos[if(t - \tau)] dt; \\ b_i &= \frac{1}{T} \int_0^T q(t) \sin[if(t - \tau)] dt, \end{aligned} \quad (5.10)$$

where $T = 2\pi/f$ – oscillation period.

Restricting the first terms of the expansion

$$\begin{aligned} a_0 &= 0; \quad b_1 = 0; \\ a_1 &= \frac{f}{\pi} \left[q_0 \int_{-\frac{\pi}{2f} + \tau}^{\frac{\pi}{2f} + \tau} \cos f(t - \tau) dt - q_0 \int_{\frac{\pi}{2f} + \tau}^{\frac{3\pi}{2f} + \tau} \cos f(t - \tau) dt \right] = \\ &= \frac{f}{\pi} \left(q_0 \frac{2}{f} + q_0 \frac{2}{f} \right) = \frac{4q_0}{\pi}. \end{aligned} \quad (5.11)$$

allows obtaining the following law of external force:

$$q(t) = \frac{4q_0}{\pi} \cos f(t - \tau). \quad (5.12)$$

Taking into account trigonometric equality

$$\cos f(t - \tau) = \cos ft \cos f\tau + \sin ft \sin f\tau \quad (5.13)$$

with substitution of the formulas (5.8) and (5.12) to the second order, the differential equation (5.6) leads to the following trigonometric equation [163]:

$$\begin{aligned} (\omega^2 - f^2)A \cos ft - 2nfA = \\ = \frac{4q_0}{\pi m} (\cos ft \cos f\tau + \sin ft \sin f\tau), \end{aligned} \quad (5.14)$$

decomposed into two equations of the system:

$$\begin{cases} (\omega^2 - f^2)A = \frac{4q_0}{\pi m} \cos f\tau; \\ -2nfA = \frac{4q_0}{\pi m} \sin f\tau. \end{cases} \quad (5.15)$$

Due to the system (5.15), the oscillation amplitude A and frequency f are the roots of the following transcendental equations [164]:

$$\begin{cases} A = -\frac{2q_0}{\pi f m n} \sin f\tau; \\ f^2 = \omega^2 - \frac{4q_0}{\pi m A} \cos f\tau. \end{cases} \quad (5.16)$$

In the first approximation ($f \approx \omega$) the oscillation amplitude A can be obtained in the following form:

$$A = \omega \sqrt{1 + \frac{\delta}{\pi} \operatorname{ctg} \omega \tau}, \quad (5.17)$$

where δ – logarithmic decrement of damping [165]:

$$\delta = \frac{2\pi n}{\omega}. \quad (5.18)$$

Introduction of the stiffness coefficient

$$c = m\omega^2 \quad (5.19)$$

with taking into account experimental dependence for time delay

$$\tau = \frac{T}{4} = \frac{\pi}{2\omega} \quad (5.20)$$

allows to determine the module of the oscillation amplitude (5.16):

$$A = \frac{4q_0}{c\delta}. \quad (5.21)$$

Obtained formulas remain valid for any cross-sections, differing only by the dimensionless Karman's coefficient C_k and Strouhal number St .

§ 5.2. The Tacoma Narrows Bridge failure

According to the materials [64, 165], the original Tacoma Narrows Bridge located in Washington State was opened to traffic on July 1, 1940. It was the third-longest suspension bridge in the United States at the time, with the average length of 855 m, width 11,7 m and beam height 2,4 m.

Prior to this time, most bridge designs were based on trusses, arches, and cantilevers to support heavy freight trains. Automobiles were obviously much lighter. Suspension bridges were both more elegant and economical than railway bridges. Thus the suspension design became favoured for automobile traffic. Unfortunately, engineers did not fully understand the forces acting upon bridges. Neither did they understand the response of the suspension bridge design to these poorly understood forces [165].

Furthermore, the Tacoma Narrows Bridge was built with shallow plate girders instead of the deep stiffening trusses of railway bridges. Note that the wind can pass through trusses. Plate girders, on the other hand, present an obstacle to the wind. As a result of its design, the Tacoma Narrows Bridge experienced rolling undulations which were driven by the wind. It thus acquired the nickname “Galloping Gertie”.

Strong winds caused the bridge to collapse on November 7, 1940. Initially, 16 m/s winds excited the bridge’s transverse vibration mode, with an amplitude of 0.3 m. This motion lasted 3 hours. The wind then increased to 19 m/s. In addition, a support cable at mid-span snapped, resulting in an unbalanced loading condition. The bridge response thus changed to a 0.2 Hz torsional vibration mode, with an amplitude up to 8.5 m. The torsional mode is shown on Figure 5.5.



Figure 5.5 – The Tacoma Narrows Bridge

The torsional mode shape was such that the bridge was effectively divided into two halves. The two halves vibrated out-of-phase with one another. In other words, one half rotated clockwise, while the other rotated counter-clockwise. The two half spans then alternated polarities [165].

One explanation of this is the law of minimum energy. A suspension bridge may either twist as a whole or divide into half spans with opposite rotations. Nature prefers the two half-span option since this requires less wind energy. The dividing line between the two half spans is called the “nodal line”. Ideally, no rotation occurs along this line.

The bridge collapsed during the excitation of this torsional mode. Specifically, a 183 m length of the centre span broke loose from the suspenders and fell a distance of 58 m into the cold waters below. The failure is shown on Figure 1.4.

The fundamental weakness of the Tacoma Narrows Bridge was its extreme flexibility, both vertically and in torsion. This weakness was due to the shallowness of the

stiffening girders and the narrowness of the roadway, relative to its span length.

There are several failure theories about the Tacoma Narrows Bridge collapse, and engineers still debate the exact cause. Three theories are:

- 1) random turbulence;
- 2) periodic vortex shedding;
- 3) aerodynamic instability (negative damping).

These theories are taken within the work [166] about aerodynamic instability which is the leading candidate.

An early theory was that the wind pressure simply excited the natural frequencies of the bridge. This condition is called “resonance”. The problem with this theory is that resonance is a very precise phenomenon, requiring the driving force frequency to be at, or near, one of the system’s eigenfrequencies in order to produce large oscillations. The turbulent wind pressure, however, would have varied randomly with time. Thus, turbulence would seem unlikely to have driven the observed steady oscillation of the bridge [165].

Theodore von Karman, a famous aeronautical engineer, was convinced that vortex shedding drove the bridge oscillations. T. Karman showed that blunt bodies such as bridge decks could also shed periodic vortices in their wakes.

A problem with this theory is that the natural vortex shedding frequency was calculated to be 1 Hz. The torsional mode frequency, however, was 0.2 Hz, observed by the professor F. B. Farquharson, who witnessed the collapse of the bridge. The calculated vortex shedding frequency was five times higher than the torsional frequency. It was thus too high to have excited the torsional mode frequency.

In addition to Karman vortex shedding, a flutter-like pattern of vortices may have formed at a frequency coincident with the torsional oscillation mode. Whether these flutter

vortices were a cause or an effect of the twisting motion is unclear.

Aerodynamic instability is a self-excited vibration. In this case, the alternating force that sustains the motion is created or controlled by the motion itself. This phenomenon is also modeled as free vibration with negative damping.

Airfoil flutter and transmission line galloping are related examples of this instability. Further explanations of instability are given in the works [167–170]. The following scenario shows how aerodynamic instability may have caused the Tacoma Narrows Bridge to fail. For simplicity, consider the motion of only one span half. Assume that the wind direction was not perfectly horizontal, perhaps striking the bridge span from below, as shown on Figure 5.6 a.

Thus, the bridge is initially at an angle-of-attack with respect to the wind. Aerodynamic lift is generated because the pressure below the span is greater than the pressure above. This lift force effectively places a torque, or moment, on the bridge. The span then begins to twist clockwise as shown on Figure 5.6 b. Specifically, the windward edge rotates upward while the leeward edge rotates downward. The span has rotational stiffness, however. Thus, elastic strain energy builds up as the span rotates. Eventually, the stiffness moment overcomes the moment from the lift force. The span then reverses its course, now rotating counter-clockwise

The span's angular momentum will not allow it to simply return to its initial rest position, however. The reason is that there is little or no energy dissipation mechanism. Thus, the span overshoots its initial rest position. In fact, it overshoots to the extent that the wind now strikes the span from above as shown on Figure 5.6 c. The wind's lift force now effectively places a counter-clockwise moment on the span.

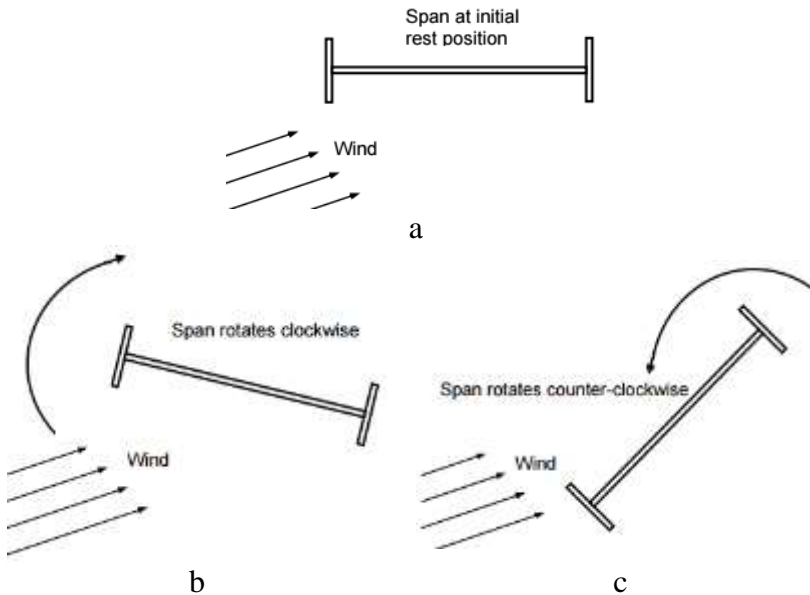


Figure 5.6 – Streamlining of the bridge span

Once again, strain energy builds up in the span material. Eventually, the stiffness moment exceeds the moment from the wind's lift force. The span thus reverses course, now rotating clockwise. Again, it overshoots its rest position. The cycle of oscillation begins anew from the position shown on Figure 5.6 a, except that the span now has rotational velocity as it passes through the original rest position. The cycles of oscillation continue in a repetitive manner.

Note that the wind force varies as a function of the span angle during the cycle. The wind force may also vary with the angular velocity. The wind force is not a function of time, however. Eventually, one of two failure modes occurs. One possibility is that the span experiences fatigue failure due to an excessive number of stress reversals. The other is that the angular displacement increased in an unstable manner until the

material is stressed beyond its yield point, and then beyond its ultimate stress limit. In reality, these two failure modes are interrelated. For example, accumulated fatigue effectively lowers the yield and ultimate stress limits. Regardless, the bridge collapses.

As a final note, the aerodynamic instability oscillation is not a resonant oscillation since the wind does not have a forcing frequency at, or near, the bridge's torsional mode frequency. Some physics and engineering textbooks mistakenly cite the Tacoma Narrows Bridge as an example of resonance. This problem is discussed in the work [171]. Nevertheless, the bridge's collapse remains the most well-know structural failure due to vibration.

A new Tacoma Narrows Bridge was built (Figure 5.7). It has truss girders, which allowed the winds to pass through. It also had increased torsional stiffness because it was thicker and wider. Furthermore, wind tunnel testing was performed to verify the new design prior to its construction.



Figure 5.7 – New design of the Tacoma Narrows Bridge

§ 5.3. Other examples of instability

One of the examples of instability concerns the case of using steel factory pipes systematically falling into the resonance caused by Karman vortices at a wind velocity in the range of 12...14 m/s. However, concrete pipes are not subjected to this phenomenon. The situation with welded pipes is especially bad, but riveted pipes better damp. In this case it is necessary to install a special friction damper built into the wire brace. The energy dissipation in the damper must be the same as in the tube [172].

Another case of instability is so-called galloping of power lines, when oscillations occur with large amplitude and low frequency [173]. A similar phenomenon is observed in countries, where the air temperature fluctuates from 0 °C to either side, and a strong gusty wind in the transverse direction is blowing. In this case self-oscillations occur, caused by the wind acting on the wire, which due to the frost took the shape, that cross-section of the resulting body is no longer circular. Thus, for the case of a wire of non-circular cross-section formed as a result of icing, it is a certain angle between the force and wind directions (Figure 5.8), that is the main cause of self-oscillations.

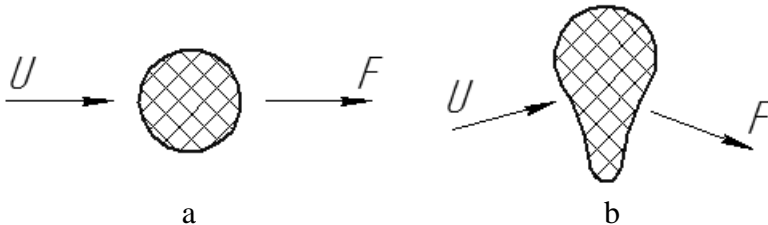


Figure 5.8 – The relative position of the wind force and velocity for cases of circular (a) and non-circular (b) cross-sections of a wire

Unsteady oscillations of wires can also occur for the case of the circular cross-section. Due to the formula (5.1), the critical frequency can be obtained by the following formula:

$$f = St \frac{U}{d} = 0.2 \frac{U}{d}. \quad (5.22)$$

For example, in case of $d = 25$ mm and wind velocity $U = 13$ m/s : $f = 0.2 \cdot 13/0.025 = 104$ (Hz).

Oscillations of power wire lines at such high frequencies with small amplitudes occur quite often and are accompanied by fatigue fractures, i. e. the resonance takes place at higher harmonics, obtained for the span divided into several sinusoidal half-waves in an amount of 20...30. At the same time, it is possible to successfully apply dynamic vibration dampers (Figure 5.9), which should not be installed in the nodes [174]. This device cannot be used when galloping, because the weight should be unacceptably high.

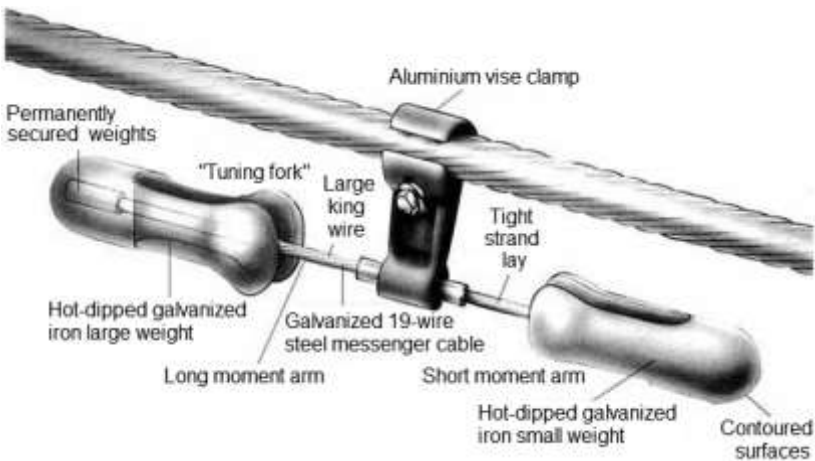


Figure 5.9 – Dynamic vibration damper

Unstable oscillations are experienced by the submarine periscope, which is the six-meter cantilever tube with the diameter 0.2 m. Resonance occurs at the velocity 2.2 m/s, which leads to an unclear image and can lead to fatigue failure. To eliminate this problem, the cross-section of the tube must be non-circular, but well streamlined. However, the periscope must rotate freely. All this leads to constructive complications.

Finally, as meteorological observations show, rain drops in calm air fall vertically except for drops with a diameter of 1 mm. Such drops fall with pulsing in different directions, and their trajectories differ from the vertical ones.

Questions for self-control

1. Explain the physical meaning of Reynolds and Strouhal numbers.
2. Describe the phenomenon of emerging the Karman vortex street. How does the correspondent pattern depend on Reynolds number?
3. What formula allows obtaining Karman's coefficient? In what range does it change?
4. Describe the design scheme of forced oscillations of the streamlined cylinder in the fluid flow.
5. What formula allows expanding the aerodynamic force as a trigonometric series? How are its coefficients determined?
6. Describe the dependences between the logarithmic decrement of damping and oscillation frequency.
7. What formula determines the oscillation amplitude of the poorly streamlined cylinder in case of square-wave external specific force?
8. Specify the main theories for explanation of the Tacoma Narrows Bridge collapse. Which theories are mistaken?
9. Describe and explain the true theory of the Tacoma Narrows Bridge failure.
10. Specify the cause for the instability of the steel factory pipes and electric wires.

CHAPTER 6.

Panel flutter

§ 6.1. Problem shaping

This chapter is devoted to the dynamic problems of hydroaeroelasticity of plates. The fact is that in previous problems on the flutter, deformation of the wing or distortion of its cross-section played an insignificant role, and motion of the wing as a rigid body was taken into consideration for investigating flexural-torsional oscillations.

However, there is another type of the flutter, the main influence on which is deformation along the chord. For example, the case of a rectangular plate with two opposite freely supported edges (Figure 6.1) is taken into consideration.

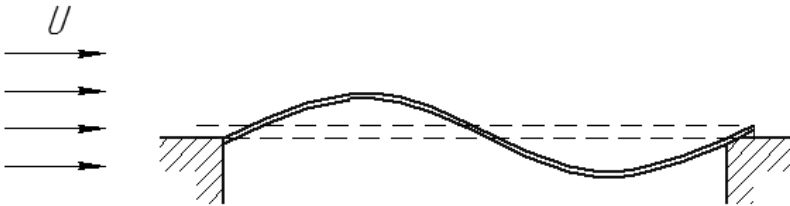


Figure 6.1 – Streamlining of a rectangular plate with two opposite freely supported edges

To simplify the problem, it is assumed that the air flow streamlines a plate only on one side, remaining motionless on the other side. Thus, when streamlining a plate with a supersonic flow, self-oscillations may occur. This phenomenon is known as panel flutter [41–43].

One of the possible causes of the panel flutter of the aircraft wing is thermal stress in wing skin due to aerodynamic heating at high speeds.

Geometrical dimensions, initial curvature, stiffness, ratio of air and body densities, and boundary conditions particularly impact on panel flutter occurrence.

The most practical method of preventing the panel flutter is the creation of tensile forces acting on the wing skin.

In general case, investigation of the abovementioned phenomena of the panel flutter is connected with certain mathematical complexities due to solving non-conservative problem of the theory of elastic stability [175]. However, this problem can be simplified by taking into consideration cylindrical bending [176] or the case presented on Figure 6.1.

§ 6.2. Flutter of a rectangular plate with two opposite freely supported edges

Small oscillations of a rectangular plate streamlined on one edge by supersonic flow (Figure 6.2) are described by the equation [45]:

$$\begin{aligned} \rho_0 h \frac{\partial^2 w}{\partial t^2} + \rho_0 h \delta \frac{\partial w}{\partial t} + D \nabla^2 \nabla^2 w - \\ - \left(N_x \frac{\partial^2 w}{\partial x^2} + N_y \frac{\partial^2 w}{\partial y^2} \right) + p(x, y, t) = 0, \end{aligned} \quad (6.1)$$

where $w(x, y, t)$ – plate displacement function; $p(x, y, t)$ – function of normal pressure due to influence of plate deformations about the undisturbed state; ρ_0, h – plate density and thickness; δ – damping coefficient; N_x, N_y – specific tensile forces (per unit of edge length); ∇^2 – Laplace operator:

$$\nabla^2 = \frac{\partial^2}{\partial x^2} + \frac{\partial^2}{\partial y^2}; \quad (6.2)$$

D – cylindrical stiffness of a plate [177]:

$$D = \frac{Eh^3}{12(1-\mu^2)}; \quad (6.3)$$

E – Young's modulus; μ – Poisson's ratio.

The components $\rho_0 h \frac{\partial^2 w}{\partial t^2}$, $\rho_0 h \delta \frac{\partial w}{\partial t}$ and $D \nabla^2 \nabla^2 w$ of the differential equation (6.1) are specific inertia, damping and elastic forces (per unit of the middle surface area).

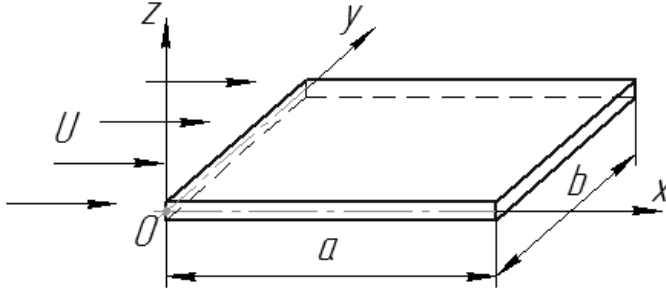


Figure 6.2 – Free supported rectangular plate
streamlined by supersonic flow

Aerodynamic pressure due to linearized formula of the theory of plane flow can be presented in the form [178]:

$$p(x, y, t) = \frac{x}{a_0} p_0 \left(\frac{\partial w}{\partial t} + U \frac{\partial w}{\partial x} \right), \quad (6.4)$$

where p_0 , a_0 – undisturbed pressure and acceleration;
 U – flow velocity.

The system of geometrical and simplified physical boundary conditions [45]

$$\begin{cases} w(x, 0, t) = w(x, b, t) = 0; \\ \left. \frac{\partial^2 w}{\partial x^2} \right|_{x=0} = \left. \frac{\partial^2 w}{\partial x^2} \right|_{x=a} = \left. \frac{\partial^2 w}{\partial y^2} \right|_{y=0} = \left. \frac{\partial^2 w}{\partial y^2} \right|_{y=b} = 0 \end{cases} \quad (6.5)$$

allows to present the solution of the differential equation (6.3) in the following form:

$$w(x, y, t) = w_1(x, t) \sin \frac{n\pi y}{b}, \quad (n = 1, 2, \dots), \quad (6.6)$$

and the equation (6.3) can be rewritten with respect of only two independent parameters x and t :

$$\begin{aligned} & D \left(\frac{\partial^4 w_1}{\partial x^4} - \frac{2\pi^2 n^2}{b^2} \frac{\partial^2 w_1}{\partial x^2} + \frac{\pi^4 n^4}{b^4} w_1 \right) - \\ & - N_x \frac{\partial^2 w_1}{\partial x^2} + N_y \frac{\pi^2 n^2}{b^2} w_1 + \rho_0 h \frac{\partial^2 w_1}{\partial t^2} + \\ & + \rho_0 h \delta \frac{\partial w_1}{\partial t} + \frac{x}{a_0} p_0 \left(\frac{\partial w_1}{\partial t} + U \frac{\partial w_1}{\partial x} \right). \end{aligned} \quad (6.7)$$

An unknown function $w_1(x, t)$ as a solution of the equation (6.7) can be found in the following form:

$$w_1(x, t) = w_n(x) e^{i\omega t}, \quad (6.8)$$

where ω – oscillation frequency; $w_n(x)$ – unknown function obtained by a substitution formula (6.8) to the equation (6.7):

$$\begin{aligned} & \frac{d^4 w_n}{dx^4} - \left(\frac{2\pi^2 n^2}{b^2} + \frac{N_x}{D} \right) \frac{d^2 w_n}{dx^2} + \frac{x p_0}{a_0 D} U \frac{dw_n}{dx} + \\ & + \left[\frac{\pi^4 n^4}{b^4} + \frac{\pi^2 n^2}{b^2} \frac{N_y}{D} - \omega^2 \frac{\rho_0 h}{D} + i\omega \left(\frac{\rho_0 h \delta}{D} + \frac{x p_0}{a_0 D} \right) \right] w_n = 0. \end{aligned} \quad (6.9)$$

An ordinary differential equation (6.9) can be rewritten in the following form

$$\frac{d^4 w_n}{d\xi^4} - 2\pi^2 R \frac{d^2 w_n}{d\xi^2} + \lambda \frac{dw_n}{d\xi} + (\pi^4 R^2 + \sigma) w_n = 0 \quad (6.10)$$

due to introduction of the following parameters:

$$\begin{aligned} \xi &= \frac{x}{a}; R = \frac{1}{2} \bar{N}_x + n^2 \left(\frac{a}{b} \right)^2; \lambda = \frac{a^3 x p_0}{a_0 D} U; \\ \bar{N}_x &= \frac{a^2 N_x}{\pi^2 D}; \bar{N}_y = \frac{a^2 N_y}{\pi^2 D}; \sigma = \Omega^2 + \pi^4 d; \\ \Omega^2 &= \frac{\omega^2}{\omega_0^2} - g \frac{\omega}{\omega_0} i; d = \frac{1}{4} \bar{N}_x^2 + n^2 \left(\frac{a}{b} \right)^2 (\bar{N}_x - \bar{N}_y); \\ \omega_0 &= \frac{1}{a_0^2} \sqrt{\frac{D}{\rho_0 h}}; g = \frac{1}{\omega_0} \left(\delta + \frac{x p_0}{\rho_0 h} \right). \end{aligned} \quad (6.11)$$

Taking into account a form function

$$w_n = C e^{k\xi}, \quad (6.12)$$

the characteristic equation for (6.11)

$$\left(k^2 - \pi^2 R^2 \right)^2 + \lambda k - \sigma = 0 \quad (6.13)$$

has four complex conjugate roots:

$$k_{1,2} = \alpha \pm i\beta; k_{3,4} = -\alpha \pm \sqrt{\beta^2 - 4\alpha^2}, \quad (6.14)$$

and the parameters λ , σ (6.11) take the forms:

$$\begin{aligned}\lambda &= -4\alpha(\beta^2 - \alpha^2 + \pi^2 k); \\ \sigma &= \pi^4 R^4 + (\alpha^2 + \beta^2)(\beta^2 - \alpha^2 + 2\pi^2 R).\end{aligned}\quad (6.15)$$

In general case, the form function (6.12) takes the form:

$$w_n = C_1 e^{k_1 \xi} + C_2 e^{k_2 \xi} + C_3 e^{k_3 \xi} + C_4 e^{k_4 \xi}, \quad (6.16)$$

where C_j – unknown constants; k_j – roots of the characteristic equation ($j = \{1; 2; 3; 4\}$).

The function (6.16) must satisfy all the boundary conditions (6.5), which due to the expressions (6.11) can be rewritten in the following form:

$$\begin{cases} w_n|_{\xi=0} = w_n|_{\xi=1} = 0; \\ \left. \frac{d^2 w_n}{d\xi^2} \right|_{\xi=0} = \left. \frac{d^2 w_n}{d\xi^2} \right|_{\xi=1} = 0, \end{cases} \quad (6.17)$$

that leads to the system of homogeneous algebraic equations

$$\begin{cases} C_1 + C_2 + C_3 + C_4 = 0; \\ k_1^2 C_1 + k_2^2 C_2 + k_3^2 C_3 + k_4^2 C_4 = 0; \\ e^{k_1} C_1 + e^{k_2} C_2 + e^{k_3} C_3 + e^{k_4} C_4 = 0; \\ k_1^2 e^{k_1} C_1 + k_2^2 e^{k_2} C_2 + k_3^2 e^{k_3} C_3 + k_4^2 e^{k_4} C_4 = 0 \end{cases} \quad (6.18)$$

with respect to unknown constants C_1, C_2, C_3, C_4 .

The condition of existence of non-trivial solutions of the system (6.18) is vanishing of the following determinant:

$$\begin{vmatrix} 1 & 1 & 1 & 1 \\ k_1^2 & k_2^2 & k_3^2 & k_4^2 \\ e^{k_1} & e^{k_2} & e^{k_3} & e^{k_4} \\ k_1^2 e^{k_1} & k_2^2 e^{k_2} & k_3^2 e^{k_3} & k_4^2 e^{k_4} \end{vmatrix} = 0, \quad (6.19)$$

which is highly cumbersome for calculations. However, due to the formula (6.14) it can be reduced to a more simplified form:

$$\begin{aligned} & \alpha^2 \left(ch 2\alpha - ch \sqrt{\beta^2 - 2\alpha^2 + 2\pi^2 R} \cos \beta \right) + \\ & + \frac{(\beta^2 - \alpha^2 - \pi^2 R)^2 + 2\alpha^2(\beta^2 - \pi^2 R)}{\sqrt{\beta^2 - 2\alpha^2 + 2\pi^2 R}} \times \\ & \times \frac{\sin \beta}{2\beta} sh \sqrt{\beta^2 - 2\alpha^2 + 2\pi^2 R}. \end{aligned} \quad (6.20)$$

An obtained transcendental equation can be solved numerically with respect to parameters α , β for the certain value of R . Then, parameters λ and σ are calculated by formulas (6.11).

Studying the equation (6.20) allows obtaining qualitative and quantitative characteristics and making conclusions about the impact of various parameters on the stability of the plane shape of the streamlined rectangular plate with two opposite freely supported edges.

§ 6.3. Divergence of a cylindrical panel

The case of a cylindrical panel as a cantilever plate with infinite length $b \rightarrow \infty$ ($\partial/\partial y = 0$) is considered (Figure 6.3) for the case of absence of inertia, damping and tensile forces ($\partial^2 w/\partial t^2 = \partial w/\partial t = 0$; $N_x = N_y = 0$). In this case the function of the plate displacement $w(t)$ depends only on one coordinate x .

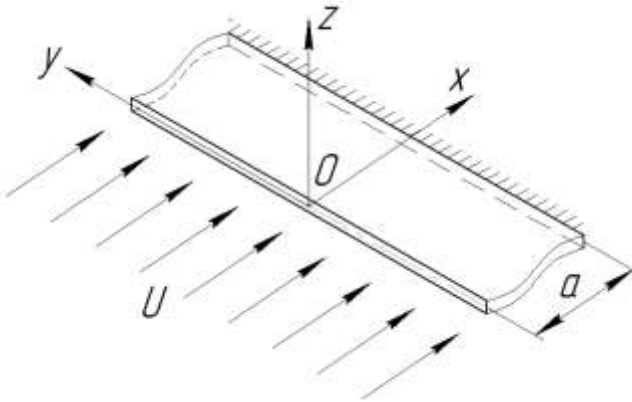


Figure 6.3 – Streamlined cylindrical panel

Due to the abovementioned assumptions, a differential equation (6.7) of plate bending takes the form:

$$D \frac{d^4 w}{dx^4} + \frac{xp_0}{a_0} U \frac{dw}{dx} = 0. \quad (6.21)$$

Introduction of the following parameters

$$\xi = \frac{x}{a}; \quad \lambda = \sqrt{\frac{xp_0}{a_0 D}} \quad (6.22)$$

allows rewriting the equation (6.21):

$$\frac{d^4 w}{d\xi^4} + \lambda^3 \frac{dw}{d\xi} = 0 \quad (6.23)$$

with the boundary conditions [45, 64]:

$$\begin{cases} \left. \frac{d^2 w}{d\xi^2} \right|_{\xi=0} = \left. \frac{d^3 w}{d\xi^3} \right|_{\xi=0} = 0; \\ \left. \frac{dw}{d\xi} \right|_{\xi=1} = w \Big|_{\xi=1} = 0, \end{cases} \quad (6.24)$$

which correspond to the case of free leading edge (zero shearing force and bending moment) and fixed tailing edge (zero deviation and displacement).

A particular solution of the equation (6.3) can be presented in the following form:

$$w(x) = Ce^{k\xi} \quad (6.25)$$

with unknown constant C and characteristic index k as root of characteristic equation

$$k(k^3 + \lambda^3) = 0, \quad (6.26)$$

obtained by substitution of the formula (6.25) to the equation (6.23).

There are four roots of characteristic equation (6.26):

$$k_1 = 0; \quad k_2 = -\lambda; \quad k_{3,4} = \frac{\lambda}{2} (1 \pm i\sqrt{3}), \quad (6.27)$$

and the function of plate displacement $w(x)$ takes the following form:

$$w(x) = C_1 + C_2 e^{-\lambda x} + e^{\frac{\lambda x}{2}} \left(C_3 \sin \frac{\sqrt{3}}{2} \lambda x + C_4 \cos \frac{\sqrt{3}}{2} \lambda x \right). \quad (6.28)$$

In this case, the boundary conditions (6.24) lead to the system of homogeneous algebraic equations

$$\begin{cases} C_2 - \frac{1}{2} C_3 + \frac{\sqrt{3}}{2} C_4 = 0; \\ C_2 + C_3 = 0; \\ -e^{-\lambda} C_2 + \frac{1}{2} e^{\frac{\lambda}{2}} \left(\cos \frac{\sqrt{3}}{2} \lambda - \sqrt{3} \sin \frac{\sqrt{3}}{2} \lambda \right) C_3 + \\ + \frac{1}{2} e^{\frac{\lambda}{2}} \left(\sqrt{3} \cos \frac{\sqrt{3}}{2} \lambda + \sin \frac{\sqrt{3}}{2} \lambda \right) C_4 = 0; \\ C_1 + e^{-\lambda} C_2 + C_3 e^{\frac{\lambda}{2}} \cos \frac{\sqrt{3}}{2} \lambda + C_4 e^{\frac{\lambda}{2}} \sin \frac{\sqrt{3}}{2} \lambda = 0 \end{cases} \quad (6.29)$$

with respect to unknown constants C_1, C_2, C_3, C_4 .

The condition of existence of non-trivial solutions of the system (6.29) is vanishing of the following determinant:

$$\begin{vmatrix} 0 & 1 & -\frac{1}{2} & \frac{\sqrt{3}}{2} \\ 0 & 1 & 1 & 0 \\ 0 & -e^{-\lambda} & \frac{1}{2} e^{\frac{\lambda}{2}} \left(\cos \frac{\sqrt{3}}{2} \lambda - \sqrt{3} \sin \frac{\sqrt{3}}{2} \lambda \right) & \frac{1}{2} e^{\frac{\lambda}{2}} \left(\sqrt{3} \cos \frac{\sqrt{3}}{2} \lambda + \sin \frac{\sqrt{3}}{2} \lambda \right) \\ 1 & e^{-\lambda} & e^{\frac{\lambda}{2}} \cos \frac{\sqrt{3}}{2} \lambda & e^{\frac{\lambda}{2}} \sin \frac{\sqrt{3}}{2} \lambda \end{vmatrix} = 0. \quad (6.30)$$

The equation (6.30) can be simplified and reduced to the equivalent transcendental equation:

$$\cos \frac{\sqrt{3}}{2} \lambda = -\frac{1}{2} e^{-\frac{3}{2} \lambda}, \quad (6.31)$$

which can be solved graphically (Figure 6.4).

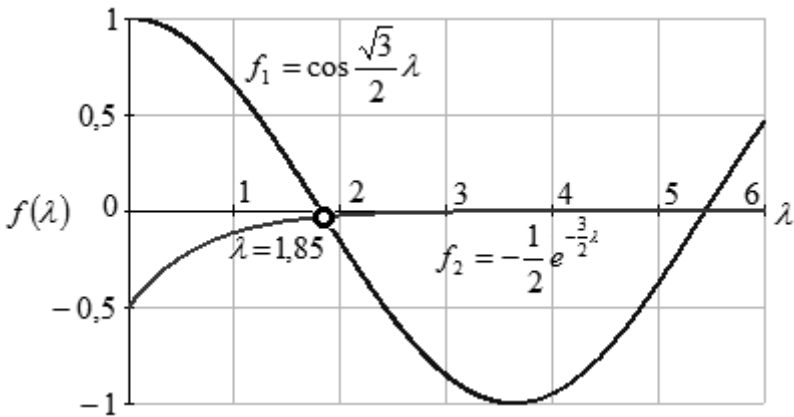


Figure 6.4 – Graphical solving of transcendental equation

Minimum positive root $\lambda = 1.85$ allows obtaining the divergence velocity U_{div} from the formula (6.22):

$$U_{div} = 6,33 \frac{a_0 D}{x p_0 a^3}. \quad (6.32)$$

§ 6.4. Flutter of a cylindrical panel

The case of a cylindrical panel as a cantilever plate with infinite length $b \rightarrow \infty$ ($\partial/\partial y = 0$) is considered (Figure 6.5) for the case of absence of damping and tensile forces ($\partial w/\partial t = 0$; $N_x = N_y = 0$). In this case the function of plate displacement $w(x, t)$ depends only on coordinate x and time t , and the differential equation (6.7) takes the following form:

$$\rho_0 p \frac{\partial^2 w}{\partial t^2} + D \frac{\partial^4 w}{\partial x^4} + \frac{x p_0}{a_0} U \frac{\partial w}{\partial x} = 0. \quad (6.33)$$

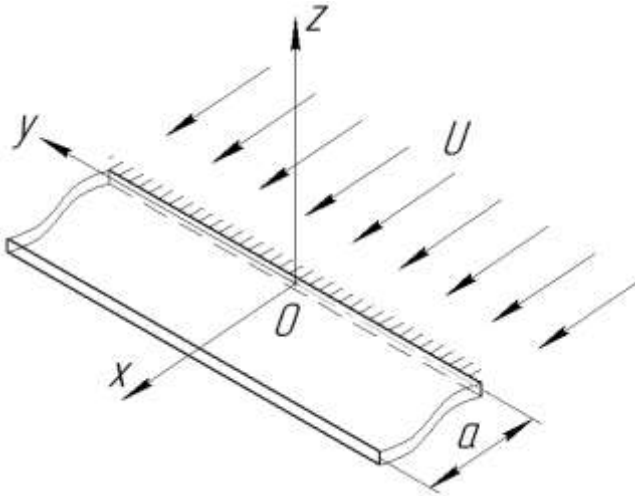


Figure 6.5 – Streamlined cylindrical panel

The solution of an equation (6.33) is found in the form:

$$w(x, t) = w_1(x) e^{i\omega t}, \quad (6.34)$$

where $w_1(x)$ – the form function; ω – vibration frequency.

Substitution of the formula (6.34) to the equation (6.33) allows obtaining the ordinary differential equation with respect to dimensionless coordinate ξ

$$\frac{d^4 w_1}{d\xi^4} + \lambda \frac{dw_1}{d\xi} - \Omega^2 w_1 = 0, \quad (6.35)$$

where the introduced parameters are

$$\begin{aligned} \xi &= \frac{x}{a}; \quad \lambda = \frac{a^3 x p_0}{a_0 D} U; \\ \Omega &= \frac{\omega}{\Omega_0}; \quad \Omega_0 = \frac{1}{a_0^2} \sqrt{\frac{D}{\rho_0 h}}. \end{aligned} \quad (6.36)$$

A particular solution of the equation (6.35) can be presented in the following form:

$$w_1(x) = C e^{k\xi} \quad (6.37)$$

with unknown constant C and characteristic index k as a root of characteristic equation

$$k^4 + \lambda k - \Omega^2 = 0, \quad (6.38)$$

obtained by a substitution formula (6.37) to the equation (6.35).

An algebraic equation (3.38) has four roots k_1, k_2, k_3, k_4 . The first pair can be presented in the complex conjugate form:

$$k_{1,2} = \alpha \pm i\beta, \quad (6.39)$$

and other roots also can be expressed in terms of parameters α and β .

Comparison of the equation (6.38) with its another equal form

$$(k - k_1)(k - k_2)(k - k_3)(k - k_4) = 0 \quad (6.40)$$

or

$$\begin{aligned} & k^4 - k^3(k_1 + k_2 + k_3 + k_4) + \\ & + k^2(k_1k_2 + k_1k_3 + k_1k_4 + k_2k_3 + k_2k_4 + k_3k_4) - \\ & - k(k_1k_2k_3 + k_2k_3k_4 + k_3k_4k_1 + k_4k_1k_2) + \\ & + k_1k_2k_3k_4 = 0 \end{aligned} \quad (6.41)$$

allows concluding that

$$\begin{cases} k_1 + k_2 + k_3 + k_4 = 0; \\ k_1k_2 + k_1k_3 + k_1k_4 + k_2k_3 + k_2k_4 + k_3k_4 = 0, \end{cases} \quad (6.42)$$

which is due to the formula (6.39) leads to the following expressions for the last two roots:

$$k_{1,2} = -\alpha \pm \sqrt{\beta^2 - 2\alpha^2}. \quad (6.43)$$

Furthermore, comparison of the formulas (6.38) and (6.41) allows obtaining parameters λ and Ω :

$$\begin{aligned} \lambda &= -(k_1k_2k_3 + k_2k_3k_4 + k_3k_4k_1 + k_4k_1k_2) = \\ &= 4\alpha(\beta^2 - \alpha^2); \\ \Omega^2 &= -k_1k_2k_3k_4 = (\alpha^2 + \beta^2)(\beta^2 - 3\alpha^2). \end{aligned} \quad (6.44)$$

The general solution of an equation (6.38)

$$w(x) = C_1 e^{k_1 \xi} + C_2 e^{k_2 \xi} + C_3 e^{k_3 \xi} + C_4 e^{k_4 \xi} \quad (6.45)$$

must satisfy the geometrical and physical boundary conditions

$$\begin{cases} w_1 \Big|_{\xi=0} = \frac{dw_1}{d\xi} \Big|_{\xi=0} = 0; \\ \frac{d^2 w_1}{d\xi^2} \Big|_{\xi=1} = \frac{d^3 w_1}{d\xi^3} \Big|_{\xi=1} = 0, \end{cases} \quad (6.46)$$

which lead to the system of homogeneous algebraic equations

$$\begin{cases} C_1 + C_2 + C_3 + C_4 = 0; \\ k_1 C_1 + k_2 C_2 + k_3 C_3 + k_4 C_4 = 0; \\ k_1^2 e^{k_1} C_1 + k_2^2 e^{k_2} C_2 + k_3^2 e^{k_3} C_3 + k_4^2 e^{k_4} C_4 = 0; \\ k_1^3 e^{k_1} C_1 + k_2^3 e^{k_2} C_2 + k_3^3 e^{k_3} C_3 + k_4^3 e^{k_4} C_4 = 0 \end{cases} \quad (6.47)$$

with respect to unknown constants C_1, C_2, C_3, C_4 .

The condition of existence of non-trivial solutions of the system (6.47) is vanishing of the following determinant:

$$\Delta[\lambda(\alpha, \beta); \Omega^2(\alpha, \beta)] = \begin{vmatrix} 1 & 1 & 1 & 1 \\ k_1 & k_2 & k_3 & k_4 \\ k_1^2 e^{k_1} & k_2^2 e^{k_2} & k_3^2 e^{k_3} & k_4^2 e^{k_4} \\ k_1^3 e^{k_1} & k_2^3 e^{k_2} & k_3^3 e^{k_3} & k_4^3 e^{k_4} \end{vmatrix} = 0. \quad (6.48)$$

A transcendental equation (6.48) can be solved graphically (Figure 6.6).

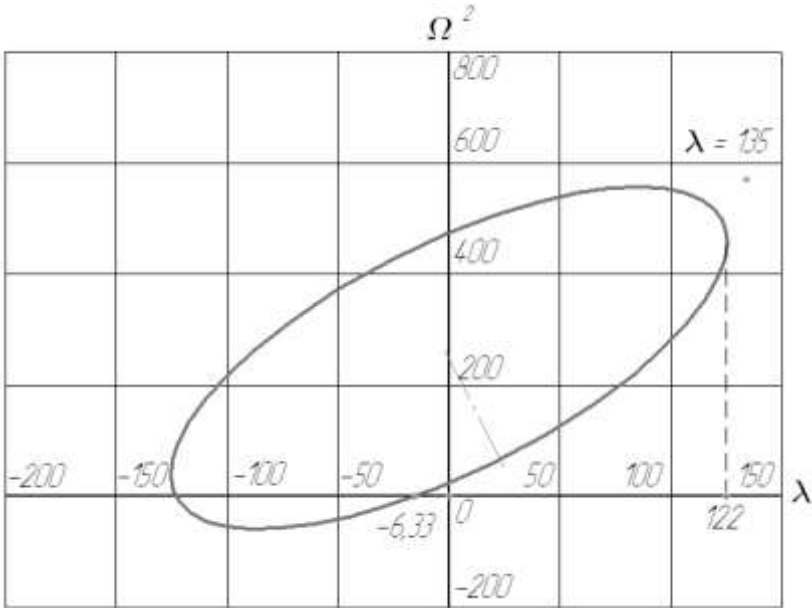


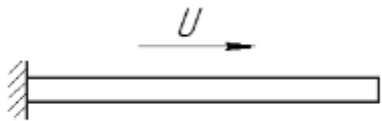
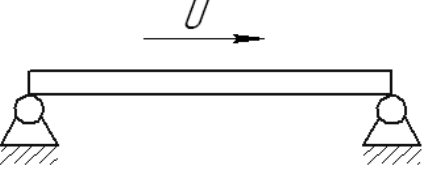
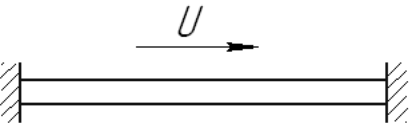
Figure 6.6 – Graphical solving of transcendental equation

In case of $\lambda < 0$, which corresponds to the direction of the flow from the free edge to the fixed one, divergence first occurs with increasing the velocity U . Furthermore, in case of $\lambda > 0$, divergence is not possible, and flutter occurs when $\lambda = \lambda_{cr} = 135$. Thus, taking into account the dependences (6.36), the critical flutter velocity U_{cr} can be obtained by the following formula:

$$U_{cr} = \lambda_{cr} \frac{a_0 D}{a^3 x p_0}. \quad (6.49)$$

It should be noted that for other cases of a boundary condition, the critical flutter velocities U_{cr} can be obtained by the following formulas similar to (6.49) with different values of the coefficient λ_{cr} (Table 6.1).

Table 6.1 – Critical value λ_{cr} of the coefficient λ for determining the critical flutter velocity

	Design scheme	λ_{cr}
Cantilever		135
Simply supported		343
Fixed ended		636

§ 6.5. Euler–Lagrange variational method

The previously considered analytical method for solving the panel flutter problem by using the differential equation of plate oscillations is very limited since it makes possible to take into consideration extremely simple cases. Consequently, the approximate methods of solution can be interesting, particularly Euler–Lagrange variational method [179], the use of which in contrast to Galerkin method [150] allows avoiding the difficulties associated with the choice of the coordinate functions [180].

Variational methods are based on the principle of possible displacements. It consists in the fact that the equilibrium state of the mechanical system is achieved, when the necessary and sufficient condition of stationarity for the total potential energy of the system is satisfied. In other words, the variation of the total strain energy δU must be equal to the sum of the elementary works δA of all the external volume and surface forces applied to this system:

$$\delta(U - A) = 0, \quad (6.50)$$

where U – potential energy of deformation; A – total work of external forces.

The vanishing of the first variation of the total potential energy indicates that it has an extreme value. It can be shown that the second variation $\delta^2(U - A) > 0$ [181], hence the total potential energy of the mechanical system achieves a minimum value: $(U - A) \rightarrow \min$.

It should be noted that the equation (6.50) is valid at a constant temperature. Otherwise, stresses and deformations occur independently of external forces, and potential energy $\Pi = U - A$.

Variational Euler–Lagrange method is applicable to thin plates using the appropriate theory [45], within which the work of external forces

$$A = \iint_{(S)} q w dx dy; \quad \delta A = \iint_{(S)} q \delta w dx dy, \quad (6.51)$$

where (S) indicates that the double integral is determined by the surface area of the plate; q – intensity of total external inertia and aerodynamic forces:

$$q(x, y, t) = -\rho_0 h \frac{\partial^2 w}{\partial t^2} - \frac{x p_0}{a_0} \left(U \frac{\partial w}{\partial x} + \frac{\partial w}{\partial t} \right). \quad (6.52)$$

The potential energy of plate deformation is determined by the following formula [147]:

$$U = \frac{1}{2} \iiint_{(V)} (\sigma_x \varepsilon_x + \sigma_y \varepsilon_y + \tau_{xy} \gamma_{xy}) dx dy dz, \quad (6.53)$$

where σ_x, σ_y – normal stresses; $\varepsilon_x, \varepsilon_y$ – normal deformations; τ_{xy}, γ_{xy} – shear stress and deformation [45]:



J.-L. Lagrange
(1736–1813)

Joseph-Louis Lagrange – an Italian and French Enlightenment Era mathematician and astronomer. He made significant contributions to the fields of analysis, number theory, classical and celestial mechanics.

Lagrange’s treatise on analytical mechanics offered the most comprehensive treatment of classical mechanics since Newton and formed a basis for the development of mathematical physics in the nineteenth century.

$$\begin{aligned}
 \varepsilon_x &= -z \frac{\partial^2 w}{\partial x^2}; \quad \varepsilon_y = -z \frac{\partial^2 w}{\partial y^2}; \quad \gamma_{xy} = -2z \frac{\partial^2 w}{\partial x \partial y}; \\
 \sigma_x &= -\frac{Ez}{1-\mu^2} \left(\frac{\partial^2 w}{\partial x^2} + \mu \frac{\partial^2 w}{\partial y^2} \right); \\
 \sigma_y &= -\frac{Ez}{1-\mu^2} \left(\mu \frac{\partial^2 w}{\partial x^2} + \frac{\partial^2 w}{\partial y^2} \right); \\
 \tau_{xy} &= -\frac{Ez}{1-\mu^2} \frac{\partial^2 w}{\partial x \partial y}.
 \end{aligned} \tag{6.54}$$

The triple integral (6.53) by the plate volume (V) can be reduced to a double integral by the plate surface (S) due to the next equality:

$$\int_{-\frac{h}{2}}^{\frac{h}{2}} \frac{Ez^2}{1-\mu^2} dz = \frac{Eh^3}{12(1-\mu^2)} = D, \tag{6.55}$$

where D – cylindrical stiffness.

Finally, it can be obtained:

$$A = \frac{1}{2} D \iint_{(S)} \left\{ (\nabla^2 w)^2 - 2(1-\mu) \left[\frac{\partial^2 w}{\partial x^2} \frac{\partial^2 w}{\partial y^2} - \left(\frac{\partial^2 w}{\partial x \partial y} \right)^2 \right] \right\} dx dy, \tag{6.56}$$

or due to variational calculation in a simplified form [182]:

$$A' = \frac{1}{2} D \iint_{(S)} \left[\left(\frac{\partial^2 w}{\partial x^2} \right)^2 + 2 \left(\frac{\partial^2 w}{\partial x \partial y} \right)^2 + \left(\frac{\partial^2 w}{\partial y^2} \right)^2 \right] dx dy, \tag{6.57}$$

where A' means a modified expression.

Thus, Euler–Lagrange method allows reducing the boundary value problem of plate oscillations to the condition of stationary value of the following energy functional:

$$R = \iint_{(s)} \left\{ \frac{1}{2} D \left[\left(\frac{\partial^2 w}{\partial x^2} \right)^2 + 2 \left(\frac{\partial^2 w}{\partial x \partial y} \right)^2 + \left(\frac{\partial^2 w}{\partial y^2} \right)^2 \right] - qw \right\} dx dy. \quad (6.58)$$

Due to Rayleigh–Ritz method [180, 183], achieving the stationary value of the functional R (6.58) can be realized by using the series expansion in n linearly independent coordinate functions $\varphi_i(x, y)$:

$$w(x, y, t) = \sum_{i=1}^n \varphi_i(x, y) e^{\lambda t}, \quad (6.59)$$

where a_i – unknown constants; λ – characteristic index.

Substitution of the formula (6.59) to the equation (6.58) leads to the system of n algebraic equations with respect to unknown parameters a_i ($i = \{1; 2; \dots; n\}$):

$$\frac{\partial R(a_1, a_2, \dots, a_n)}{\partial a_i} = 0; \quad (i = \overline{1, n}). \quad (6.60)$$



J. Rayleigh
(1842–1919)

John William Strutt Rayleigh – an English physicist, who discovered argon – an achievement for which he earned the Nobel Prize for Physics in 1904. He also discovered the phenomenon now called Rayleigh scattering, which can be used to explain why the sky is blue, and predicted the existence of the surface waves now known as Rayleigh waves.

The system of equation (6.60) can be solved as the problem of eigenvalues λ .

It should be noted that linearly independent coordinate functions $\varphi_i(x, y)$ for Euler–Lagrange method must satisfy only geometrical boundary conditions, because the physical ones are satisfied automatically.

Another advantage of using the Euler–Lagrange variational method is the possibility of solving the hydroaeroelasticity problems for plates of variable thickness.

In contrast to the Euler–Lagrange method, if replace the energy functional (6.58) by Galerkin’s functional [184]

$$\iint_{(S)} \left\{ D\nabla^2\nabla^2 w + \rho_0 h \frac{\partial^2 w}{\partial t^2} + \frac{xp_0}{a_0} \left(U \frac{\partial w}{\partial x} + \frac{\partial w}{\partial t} \right) \right\} \delta w dx dy = 0, \quad (6.58)$$

the integrand of which corresponds to the differential equation (6.1), all the coordinate functions (6.59) must satisfy both geometrical and physical boundary conditions, which makes Galerkin method practically unsuitable for a number of problems, e. g. for the case of cantilever plates.



W. Ritz
(1878–1909)

Walter Ritz – a Swiss theoretical physicist. He is mostly famous for his work with the Rydberg–Ritz combination principle. Ritz is also known for the variational Ritz method named after him.

§ 6.6. Nonlinear problems of a panel flutter

The problems of hydroaeroelasticity considered below are classified as linear. As it is known, solving problems of the stability of plates and shells in a linear formulation allows determining only the critical velocity of the flutter. Wherein, determination of flutter amplitudes or a limiting cycle of self-oscillations, and buckling amplitudes, as well as behaviour of the panel when the self-oscillations occur, are not completely solved. However, their solution is possible only for a nonlinear formulation of the initial differential equations of dynamics.

It should be noted that the critical flutter velocity as a solution of linear problem of hydroelasticity, in some cases can have the meaning of upper critical velocities, below of which the stable limit cycles arise for sufficiently large initial deviations of the mechanical system.

Furthermore, the solution of hydroaeroelasticity is especially important for a panel flutter, because its appearance due to the predominant geometric nonlinearities has predominantly soft character. This means that getting the system into the flutter region is not catastrophic, because the destruction of the skin due to the fatigue damage occurs after a certain number of loading cycles. Therefore, in contrast to the problem of classical wing flutter, when the excitation is rigid, investigation of the nonlinear problem acquires a special practical meaning related to finding the expected lifetime of the panel. And for this it is necessary to know the amplitude of oscillations in the flutter region.

Methods of the theory of nonlinear oscillations [17] can be applied for evaluation of amplitudes of oscillations, such as a harmonic balance method, a small parameter method, a method of successive approximations, etc. [185]. In the

region near the flutter boundaries, it is rational to apply the small parameter method. For a wider region, more reliable results are obtained by using the harmonic balance method based on trigonometry series.

The most important factor, which limits the amplitudes of flutter and buckling deflections, is nonlinearities of geometric origin associated with the emergence of tensile forces applying to the middle surface, which essentially depend on the boundary conditions. In addition, the effect of constructive nonlinearities also can be considered.

In some problems it is also necessary to take into account physical nonlinearities associated with inelastic or nonlinear elastic effects.

Aerodynamic nonlinearities are important for supersonic flows with high values of Mach number ($M \gg 1$). This problem is especially acute in determination of the possibility of existence of periodic regimes and stable static configurations at velocities, which are lower than the same critical velocity identified by using the linear theory.

Today the nonlinear problems of the flutter are less studied due to difficulties of two kinds:

- 1) difficulties in determining the aerodynamic forces in a nonlinear formulation;
- 2) complexities in solving systems of nonlinear differential equations describing a boundary value problem.

Some investigations in the field of a nonlinear flutter are described below.

In the work [186] a systematic way of applying both perturbations methods and harmonic balance methods to the nonlinear panel flutter problems is developed. The results obtained by both these methods for two-dimensional simply supported and three-dimensional double-clamped plates with six modes agree well with those obtained by the

straightforward direct integration method, yet require less computer time and provide better insight into the solutions. Effects of viscoelastic structural damping on the flutter stability boundary are generally found to be destabilizing and the post-flutter behaviour becomes more explosive.

In the work [187] a nonlinear panel flutter using high-order triangular finite elements is investigated. A 54-degree-of-freedom, high-order triangular plate finite element extended for geometrically nonlinear static and dynamic analysis is used to formulate and analyze the supersonic nonlinear panel flutter problems. The finite element formulation is based on the classical theory of plates. The quasi-steady aerodynamic theory is used, and numerical solution procedures are presented. The limit cycle oscillation analyses are performed for two-dimensional and square panels with all edges simply supported and clamped respectively. The effect of in-plane comprehensive force, mass ratio, and in-plane edges stress free condition are considered. Stress distribution for the limit cycle oscillations of two-dimensional panel is plotted. For the case of panels under the static pressure differential, the results for the steady mean amplitude and flutter dynamic pressure are obtained for the two-dimensional and square panels respectively. The effect of biaxial in-plane comprehensive stress for a simply supported square panel is studied and boundaries among the flat and stable region, dynamically stable buckled region, and the limit cycle oscillation region are found. Alternative analytical and numerical solutions are available for the most examples for comparison and all are in excellent agreement.

In the work [188] the numerically analysis of nonlinear flutter oscillations of elastic plate in a gas flow is studied. In contrast to many other approaches, an inviscid flow model was used instead of a piston theory or other simplified aerodynamic

theories. This study aims to investigate the region of low supersonic Mach numbers ($1 < M < 2$), where several plate eigenmodes can be simultaneously unstable, and resulting oscillations are governed by the nonlinear interaction of growing modes. Three types of unstable plate behaviour have been obtained. First, at $0.76 < M < 1$, the plate diverges. Second, at $1 < M < 1.67$, a single-mode flutter occurs in three distinct forms: limit cycle in the first mode ($1 < M < 1.33$ and $1.5 < M < 1.67$) or higher modes; limit cycle in the first and second modes being in internal 1 : 2 resonance ($1.12 < M < 1.33$ and $1.42 < M < 1.5$); and non-periodic oscillations with several dominating frequencies being in more complex ratio ($1.33 < M < 1.42$). Third, at $M = 1.82$ and increased dynamic pressure, a coupled-mode flutter appears. Amplitudes and spectra of each limit cycle type are analyzed. The role of aerodynamic nonlinearity in the formation of limit cycle oscillations is discussed.

Finally, a new look at nonlinear aerodynamics in analysis of hypersonic panel flutter is stated in the work [189]. A simply supported plate fluttering in hypersonic flow is investigated considering both the airflow and structural nonlinearities. The third-order piston theory is used for nonlinear aerodynamic loading, and the Karman plate theory is used for modeling the nonlinear strain-displacement relation. The Galerkin method is applied to project the partial differential equations into a set of ordinary differential equations in time, which is solved by the numerical integration method. In observation of limit cycle oscillations and evolution of dynamic behaviours, the nonlinear aerodynamic loading produces a smaller positive deflection peak and more complex bifurcation diagrams compared with linear aerodynamics. Moreover, a limit cycle oscillation, obtained with the linear aerodynamics, is mostly a nonsimple harmonic motion; but when the aerodynamic nonlinearity is

considered, more complex motions are obtained, which is important in the evaluation of the fatigue life. The parameters of the Mach number, dynamic pressure, and in-plane thermal stresses all affect the aerodynamic nonlinearity. For a specific Mach number, there is a critical dynamic pressure beyond which the aerodynamic nonlinearity has to be considered. For a higher temperature, a lower critical dynamic pressure is required. Each nonlinear aerodynamic term in the full third-order piston theory is evaluated, based on which the nonlinear aerodynamic formulation has been simplified.

Questions for self-control

1. What factors can cause the emergence of a panel flutter? Describe them briefly.
2. What parameters impact on the panel flutter occurrence?
3. What is the most practical method for preventing a panel flutter?
4. Describe the assumptions that simplify the problem of the panel flutter.
5. Write an equation and boundary conditions describing small oscillations of a rectangular plate streamlined on one edge by a supersonic flow.
6. How do the tensile forces impact on the critical flutter velocity?
7. Write an equation and boundary conditions that allow investigating divergence of a cylindrical panel with the infinite length. Analyze the expression for the divergence velocity.
8. What equation and boundary conditions allow investigating flutter of a cylindrical panel?
9. Analyze the expression for the critical flutter velocity. What does the critical value of the coefficient for determining the critical flutter velocity depend on?
10. Describe Euler–Lagrange variational method and its advantages over Galerkin method.
11. How can Rayleigh–Ritz method be applied to solving the problem of plate oscillations?
12. Identify and characterize the main nonlinear problems of hydroaeroelasticity. How can they be solved?

CHAPTER 7.
Other problems
of hydroaeroelasticity

§ 7.1. Aeroelastic phenomena in turbomachines

In turbomachines, such as steam and gas turbines, air and gas compressors, hydraulic turbines and pumps, the gas or incompressible liquid move through the system of motionless parts, e. g. guide vanes, and the system of rotating blades. And the working process in turbomachines consists in the exchange of energy between the gas or liquid and a rotating impeller [190]. Thus, force interaction between the fluid flow and elastic blades play a significant role, and deformations lead to the possibility of the formation of hydroaeroelastic oscillations, that include the following phenomena:

1. A conventional flexural-torsional flutter, when the energy transfer occurs from the flow to the blades [191].

2. Aerodamping phenomena in oscillations of deformable blades in the aerodynamic grid are streamlined by the flow [192]. In this case the energy transfer occurs from blades to the flow.

3. A latticed flutter [193], which can occur only in grids with purely bending or purely torsional vibrations of all the blades.

4. A stall flutter, for example at large angles of attack [194]. A stall flutter is also possible for one blade, although the interaction between elements of the blade system has a significant effect.

5. A wave flutter, which occurs in case of the supersonic flow and the presence of shock waves interacting with the boundary layer [195].

The complexity of considering the abovementioned problems is that the blades influence the oscillations of adjacent blades. Moreover, individual blades can oscillate with

different amplitudes and phases. The influence is also exerted by the mutual displacement of the profiles.

Recently, a large number of scientific papers have appeared for solving other applied problems of hydroaeroelasticity. For example, the work [196] is devoted to investigating gust loads and aircraft. Hydroelasticity of ships is investigated in the work [197]. Hydroelasticity phenomena in marine hull bottom panels are stated in the work [198]. Hydroelasticity problems with special reference to hydrofoil craft are presented in the work [199].

The following paragraphs are devoted to the presentation of the problems of hydroaeroelasticity, which has recently engaged the departments of the Faculty of Technical Systems and Energy Efficient Technologies at Sumy State University, such as stability of the automatic balancing devices of centrifugal pumps, analysis of the operation of seals with floating rings, and investigations of the aeroelasticity phenomena in the processes of gas separation.

§ 7.2. Stability of the automatic balancing devices of centrifugal pumps

The recent research works of the Department of General Mechanics and Machine Dynamics of Sumy State University were devoted to solve the following problems commissioned by the Ministry of Education and Science of Ukraine and Yuzhnoye State Design Office:

1. Development of methods for numerical simulation and optimization of hydrodynamic characteristics for gap and labyrinth seals, and investigation of their impact on the rotordynamics for centrifugal machines [200].

2. Numerical simulation and optimization of gas-dynamics and vibration characteristics for turbochargers of gas-pumping units and their components [201].

3. Development of the new mathematical models of centrifugal machines rotors and methods of their diagnosis [202].

4. Investigation of oscillations of centrifugal machines rotors associated with nonlinearity reactions in gap bearings and seals, and their vibration diagnosis [203, 221].

5. Rotordynamic research for the turbopumps of the liquid rocket engines [204].

The automatic balancing device and other unloading devices can be used for the equilibration of the axial forces operating on a rotor of multistage centrifugal pumps (Figure 7.1). In case of usage of any unloading device, the presence of persistent bearings and system of consolidation leads to the complication of the system of the axial equilibration of rotor, reduction of its wear-resistance and economy decrease. The reliability of these devices can be decreased in case of intensive wear of a cylindrical throttle

before and after the unloading device of the balancing disk [205].

Therefore, the locking automatic balancing device is offered, operating as the axial hydrostatic bearing with hyper bearing capacity and, simultaneously, as the non-contact consolidation with self-adjustable leaking. The dynamic calculation is based on the equations of pump rotor and regulator rod axial movement and also on equations of the fluid flow balance through the throttles taking into consideration the compression and displacement flow. The methodology of dynamic calculation gives the opportunity to select the main parameters of hydro-mechanical system engineering based on providing stability conditions of the transient processes [206, 207].

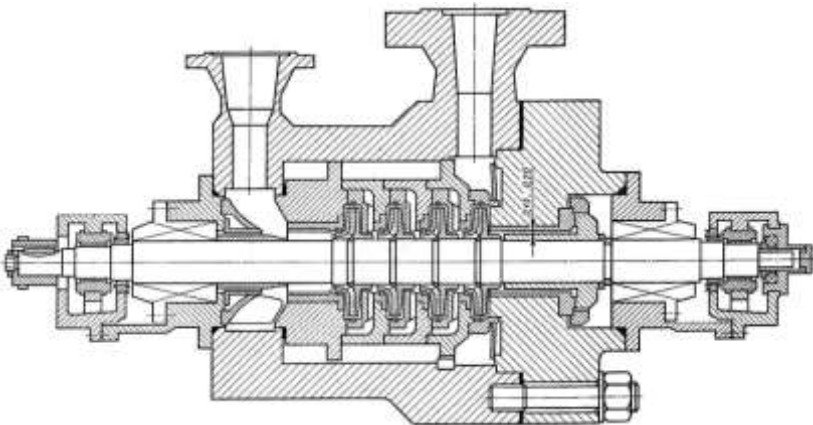


Figure 7.1 – Multistage centrifugal pump

Investigation of the impact of elastic deformations of unloading disk at their static and dynamic stability is the complicated problem of hydroelasticity, the solving of which contributes to the efficiency of the automatic balancing devices [208, 209, 210].

The main elements of the automatic balancing device (Figure 7.2) are the unloading disk 1, rigidly connected to the rotor; radial gap 2 with the constant coefficient of hydraulic resistance; face gap 3, the coefficient of hydraulic resistance of which depends on the gap value varying due to the rotor axial movement.

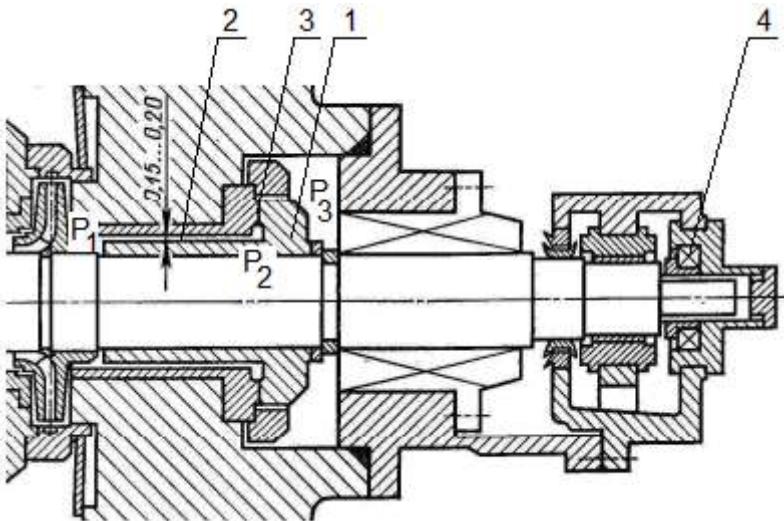


Figure 7.2 – Automatic balancing device

The operation of the abovementioned device is based on the fact that the axial force T acting to the pump rotor depends on the face gap z . Due to the control theory, the rotor is the object of regulation; the face gap z is the regulated parameter; axial force T , as well as the inlet and outlet pressures P_1 and P_3 are external influences.

In the limiting case of zero face gap ($z = 0$) and there is no leakages through the automatic balancing device, the pressure P_2 in the pump chamber of volume V reaches the

maximum value and is equal to the pressure P_1 before the radial gap 2 (inlet pressure), and the pressure difference ratio is

$$\beta = \frac{\Delta P_2}{\Delta P}, \quad (7.1)$$

where $\Delta P_2 = P_2 - P_3$ is the pressure difference through the axial throttle, and $\Delta P = P_1 - P_3$ is the total pressure difference.

In this case, the maximum value of unloading force F acts on the unloading disk.

In another limiting case ($z \rightarrow \infty$), all the pressure difference ΔP is throttled on the radial gap ($\Delta P = \Delta P_1$; $\Delta P_2 = 0$), and the pressure difference ratio $\beta = 0$. Consequently, the axial force decreases to zero.

Under operating conditions, if the axial force T increases, the rotor moves to the left, and z decreases until the pressure P_2 increases to restore the equality $F = T$.

In the steady state, each force value F corresponds to a certain face gap z , at which holds the equation of axial rotor equilibrium is

$$F = T. \quad (7.2)$$

While designing the automatic balancing devices it is necessary to minimize volumetric losses, but at the same time to avoid excessive decreasing of the face gap since this can lead to an unwanted contact of the end pair. Both these conditions are satisfied for a sufficient slope of the static characteristic, when even large changes of the axial force lead to insignificant changes in the face gap value.

The dependence of the unloading force F (or its dimensionless analogue – generalized external impact Φ) on

the face gap value z (or dimensionless face gap u) is the static characteristics of the automatic balancing device (Figure 7.3).

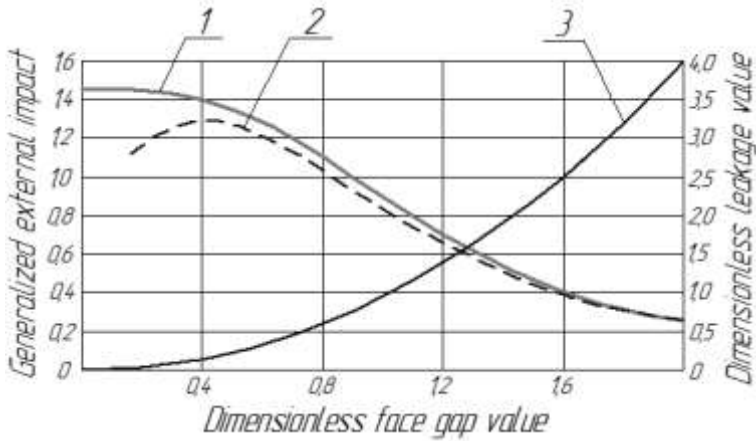


Figure 7.3 – Static and flow characteristics of the automatic balancing device

The curve 1 corresponds to the case without the impact of elastic deformations of the unloading disk, but the curve 2 takes into account such impact. In the region of low face gap values, the system is statically unstable.

Thus, the abovementioned results are achieved due to solving the hydroelasticity problem for the automatic balancing device of the multistage centrifugal machine.

Like any system of automatic control, the system of axial rotor balancing must have certain dynamic properties. Therefore, along with static calculation, it is necessary to investigate the dynamic stability of the hydromechanical system “rotor – automatic balancing device”.

For the abovementioned system, a characteristic equation takes the form of the fourth-order polynomial equation:

$$a_0\lambda^4 + a_1\lambda^3 + a_2\lambda^2 + a_3\lambda + a_4 = 0, \quad (7.3)$$

for which Routh–Hurwitz criterion takes the form of the system of inequalities:

$$\begin{cases} a_i > 0 \quad (i = \overline{1, 4}); \\ a_1 a_2 a_3 > a_0 a_3^2 + a_1^2 a_4. \end{cases} \quad (7.4)$$

The first group of conditions is always satisfied [205], but the second condition has nine independent parameters, the connection between them cannot be obtained in a form convenient for practical use. However, numerical simulations allow asserting that the causes of dynamic instability are the fluid compression in the pump chamber of volume V and deformations of the unloading disk. Thus, in case of incompressible fluid the conditions (7.4) are always satisfied.

Inertia forces of the rotor and fluid in the gaps are destabilizing factors that decrease the reserve of the dynamic stability. The most acceptable means for ensuring the dynamic stability is reduction of the axial dimension of the pump chamber of volume V .

The abovementioned analysis is stated for the case of one-dimensional axial movement of the rigid rotor without taking into consideration connections between axial and flexural oscillations of the flexible rotor. Moreover, a number of limitations was admitted, which allowed only assessing tentatively the impact of individual factors.

§ 7.3. Analysis of the operation of seals with floating rings

Seals with floating rings (Figure 7.4) are used in centrifugal compressors and other types of rotary machines. In some cases, especially for sealing the internal cavities of high-speed machines, seals with floating rings become the most appropriate alternative to conventional gap seals due to their relatively simple design and ability to provide the required reliability and tightness under appropriate debugging [211].

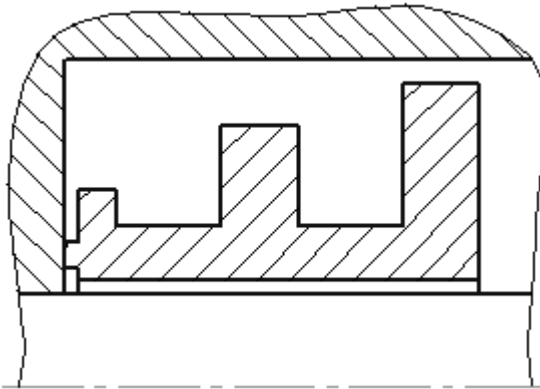


Figure 7.4 – The seal with floating ring

Seals with floating rings are the consecutive set of the radial and face gaps operating under facilitated conditions. The ability of the floating ring to be centred relative to the rotating shaft due to the hydrodynamic forces in the axial gap allows decreasing radial clearance, which leads to sufficiently decreasing leakages without rapid mechanical wear.

Moreover, since the floating ring does not rotate, the loss of frictional power in the end contact pair is significantly

reduced. This fact removes the most complicated problem of the seals designing [212].

From the principle of sealing operation it can be obtained that their advantage is realized especially when the maximum centring force in the radial gap exceeds the frictional force between the surfaces of the axial contact pair. In this connection, the seals with deformable floating rings are of particular interest (Figure 7.5).

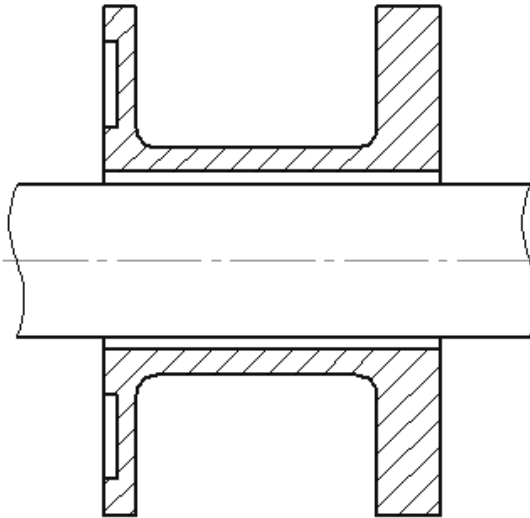


Figure 7.5 – The shaft seal with the deformable floating ring

The appropriate choice of the geometry of the radial cross-section of the ring can provide the certain shape of the throttling gap after deformation due to the pressure difference, which finally increases the hydrostatic stiffness and at the same time reduces leakages [213].

The flow characteristics of seals with deformable and rigid floating rings are presented on Figure 7.6.

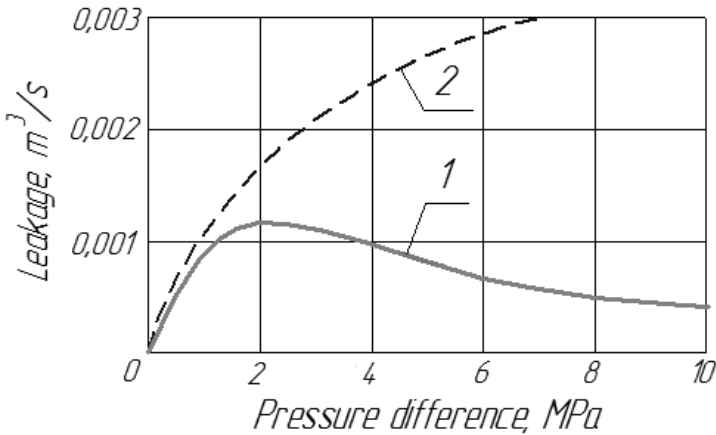


Figure 7.6 – Flow characteristics of seals with floating rings:
1 – deformable ring; 2 – rigid ring.

For the proper designing of the geometric shape of the ring, the problem of hydroelasticity must be solved, because of the equilibrium shape of the throttling gaps is determined by the pressure diagram, which depends on the gap shape.

However, the hydroelasticity problem is complicated by the fact that the hydrodynamic characteristics of the seal, such as stiffness, damping, inertia effects and hydraulic resistance, depend not only on the geometric dimensions and shape of the throttling gap, but also on the nature of the rotor motion. Thus, there is the feedback between the seal and rotor, which creates the unified hydromechanical system “rotor – seal” (Figure 7.7). Radial and angular oscillations of the rotor are due to the hydrodynamic forces and moments, which depend on the nature of the rotor movement.

Another feedback exists between the gap shape, such as average gap and taper parameters, and the pressure difference in the throttle. In other words, deformations of the floating ring

are due to the pressure distribution, which is extremely sensitive to changes of the gap shape.

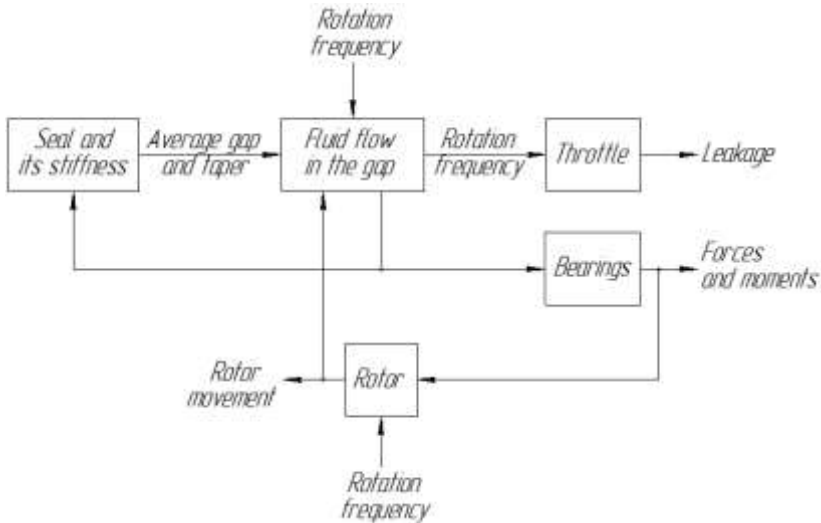


Figure 7.7 – Schematic diagram of the mechanical system “rotor – seal”

Due to the abovementioned, the steady equilibrium deformable state is determined by solving the system of equations for the turbulent flow in the throttle with a complex gap shape taking into account the rotor movement, and equations of the theory of elasticity. Solving this hydroelasticity problem allows creating seals, which are able to self-adjust under operating conditions, and the throttle acquires an optimal geometric shape from the point of view of the hydrodynamic characteristics. Such approach can increase not only the vibrational reliability of the system “rotor – seal”, but also the volumetric efficiency of the centrifugal machine.

§ 7.4. Aeroelasticity phenomena in the processes of gas separation

Close cooperation between the Processes and Equipment of Chemical and Petroleum-Refineries Department and the Department of General Mechanics and Machine Dynamics allows investigating the hydroaeroelasticity phenomena as a result of interdisciplinary research in chemical and petroleum industry within the following problems commissioned by the Oil-Petroleum Companies and Ministry of Education and Science of Ukraine:

1. Development of the “Heater–Treater” equipment for the comprehensive oil treatment. [214].

2. Hydrodynamic parameters of two-phase flows for the heat and mass-transfer granulation and separation equipment [215].

3. Numerical simulation and optimization of the gas-dynamic and vibration characteristics of turbochargers and gas pumping units and their components [216, 217, 218].

4. Development and implementation of energy efficient modular separation devices for oil and gas purification equipment [219].

Natural gas contains a large amount of impurities including water and heavy hydrocarbon fractions of the condensate. Therefore, for its further transportation through the main gas pipeline, it must be processed appropriately in the complex gas processing units, the integral element of which is the separation equipment. The high operational characteristics of this equipment are achieved only under the design values of operational parameters.

The processes of formation and separation of the heterogeneous dispersion system (emulsions, suspensions, aerosols) play an important role in science and technology. In

terms of specific energy consumption and efficiency of separation, the methods of inertial gas-dynamic and inertial-filtering separation, which differ in the ways of forming the geometrical configuration of the separation channels, and the character of movement and the path of flow, are considered to be optimal [220].

The scientific problem of modeling hydrodynamic processes is aimed at ensuring the efficiency by developing the reliable engineering design techniques for the separation equipment.

All the mathematical formulations as a system of the second order nonlinear differential equations have an analytical solution only in very limited cases of the simple geometry. Investigations for the case of flexible walls is directed to the numerical simulation of the gas-dynamic separation, which is associated with the solution of the hydroaeroelasticity problem for interaction of a dispersed gas-liquid flow with baffle elements.

This boundary value problem (Figure 7.8) can be solved by using methods of computational fluid dynamics embedded in the up-to-date software systems [221, 222].

Investigation of the deformable elements oscillations under the separation process for the components of gas-liquid mixture is a highly complicated problem of hydroaeromechanics, which requires carrying out the procedure of parameter identification for the mathematical model describing the interaction between the gas-liquid flow and deformable elements.

The abovementioned approach has certain peculiarities and limitations, such as using dynamic meshing for taking into consideration movement of the deformable plate, as well as the model of contact interaction must be activated by the certain gap value to prevent the appearance of “negative volume” elements.

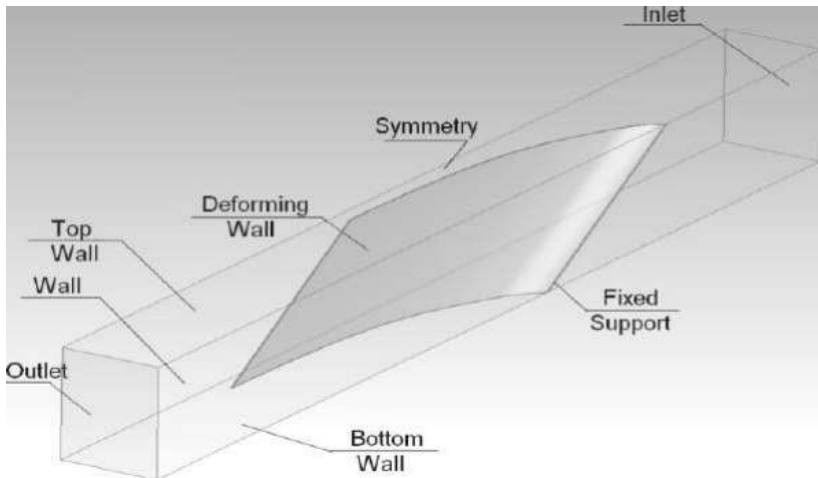


Figure 7.8 – Design scheme for modeling the separation

As a result, displacement of the deformable element can be obtained as a time function for the critical regime corresponding to the critical value of the average flow velocity and self-oscillations of the gas-dynamic separation elements.

Questions for self-control

1. What purposes the automatic balancing devices of multistage centrifugal pumps are used for?
2. What leads to decreasing the reliability of the automatic balancing devices of centrifugal machines?
3. Describe the operation principle of the automatic balancing device of the multistage centrifugal pump.
4. Explain the influence of the unloading disk deformations on static and flow characteristics of the automatic balancing device.
5. Write down and define the characteristic equation describing oscillations of the automatic balancing device.
6. Indicate Routh–Hurwitz criterion of its dynamic stability. What geometrical parameters does a primary impact have on the automatic balancing device stability?
7. What purposes the seals with floating rings are used for?
8. Explain the operation principle of seals with floating rings.
9. Explain the difference between the flow characteristics for seals with deformable and rigid rings.
10. What factors and parameters do the hydrodynamic characteristics of seals with floating rings depend on?
11. Justify the importance of the hydroaeroelasticity problem for the separation of gas-liquid mixtures.
12. Describe the design scheme for the numerical simulation of the gas-liquid dynamic separation process in gas-dynamic separators with deformable elements.

Author Index

B

Bernoulli, D. 32
Bessel, F. W. 59

C

Cauchy, A.-L. 44
Chaplygin, S. A. 50
Clapeyron, B. 78
Collar, A. R. 22

D

d'Alembert, J.-B. 72

E

Euler, L. 28

F

Fokker, A. 17
Fourier, J.-B. 42

G

Galerkin, B. S. 111
Galilei, G. 73
Gromeka, I. S. 29

H

Hankel, H. 61
Hook, R. 101
Hurwitz, A. 124

J

Joukowsky, N. E. 43

K

Karman, T. 24
Kelvin, W. T. 31
Kutta, M. W. 49

L

Lagrange, J.-L. 175
Lamb, H. 30
Langley, S. P. 14
Laplace, P.-S. 41
Laurent, P. A. 51

M

Mach, E. 37

N

Newton, I. 106

R

Rayleigh, J. 177
Reynolds, O. 138
Riemann, B. 45
Ritz, W. 178
Routh, E. J. 123

S

Strouhal, V. 137

T

Theodorsen, T. 60

W

Wright, O. 15
Wright, W. 15

Subject indexes

A

- absolute axis 72
- absolute temperature 73, 74
- absolute velocity 76
- absolutely rigid design 21
- acceleration 42, 50
- acceleration components 44
- acceleration potential 42
- added mass 63
- added vortex 63
- additional aerodynamic force 21
- additional aerodynamic moment 93
- adiabatic flow 31
- adiabatic index 31, 73
- aerodynamic airfoil characteristic 85
- aerodynamic centre 88
- aerodynamic diving moment 23
- aerodynamic force 21
- aerodynamic heating 156
- aerodynamic instability 147
- aerodynamic moment 62
- aerodynamic nonlinearity 182, 183
- aerodynamic ratio 87
- aerodynamic theory 110
- aerodynamic trail 44
- aerodynamics 21, 182
- aeroelastic phenomena 21
- aeroelasticity 91, 187
- aerothermoelasticity 22
- aileron 23, 92
- aileron angle 94
- aileron deflection angle 95
- aileron efficiency 95
- aileron's reverse 23, 92, 95
- aircraft 14, 21
- aircraft industry 14, 26
- aircraft skin 28
- aircraft tail 25
- aircraft wing 20, 82, 156
- airfoil 82, 93, 148
- airfoil curvature 83
- airplane 17, 21, 91
- algebraic equation 113, 162
- angular momentum theorem 107
- angular roll rate 95
- angular velocity 149
- angular stiffness 108, 116
- arbitrary constant 48
- argument 41
- attack angle 16, 40, 83, 126
- automatic balancing device 187
- auxiliary plane 41, 49, 53
- average attack angle 40
- aviation unit 16
- axial moment of inertia 105

B

badly streamlined
 beam 135
barotropic gas flow 74
beam 24, 105, 145
bearing surface 88
Bernoulli equation 36
Bernoulli integral 32, 42
Bessel functions 59, 60
Biplane 14, 16
biquadratic equation 115
blade 24, 28, 186
boundary conditions 32, 51
boundary layer 186
bridge destruction 18
broken wing 17
buckling 23
buckling amplitude 179
buffing 24

C

camber line 83
Cauchy–Riemann
 theorem 43
centre of gravity 66, 88
centre axis 105
centre of lift 88
character of perturbation 68
characteristic equation 121
characteristic index 109
characteristic point 88, 103
chimney 24
chord 40, 82, 126, 156

chord line 86
chord's midpoint 52, 62, 63
circular cylinder 82
Clapeyron's formula 78
classical flutter 19, 24
coefficient of the additional
 aerodynamic moment 93
Collar's triangle
 of forces 21, 22
column vector 67
compatibility condition 124
complex acceleration
 potential 44, 49, 52, 63
complex conjugate
 roots 123, 161
complex determinant 114
complex number 61, 109
complex vector 41, 43
complex velocity
 potential 41, 42
compliance coefficient 101
components of the
 acceleration 42
components of the
 velocity 29
compression wave 74, 76
compressor 20, 186, 194
condition of equilibrium 94
conformal mapping
 method 41
conjugate function 43
continuity equation 30, 33
control process 22

-
- control system 22, 23, 123
 - coordinate function 174
 - cosine theorem 54
 - couple of forces 101
 - coupled-mode flutter 182
 - critical divergence
 - velocity 89, 91, 119
 - critical flutter state 109
 - critical flutter velocity 91
 - critical value 86, 173, 200
 - critical flow velocity 95
 - critical velocity of the
 - aileron's reverse 93, 95
 - cross-sectional area 107
 - cross-sectional
 - characteristic 88
 - cross-sectional polar
 - moment of inertia 98
 - curvature 40, 93, 156
 - curvilinear integral 38
 - cylinder diameter 136, 139
 - cylindrical bending 157
 - cylindrical panel 164, 168
 - cylindrical pipe 73
 - cylindrical stiffness 158
- D**
- d'Alembert solution 71
 - damping coefficient 109
 - damping matrix 67
 - deflection 23, 93, 180
 - deformable body 21
 - deformable shape 28
 - deformation 16, 101, 156
 - degree of freedom 116
 - density 29, 31, 70, 71, 126
 - determinant 113, 131, 162
 - deviation 93, 110, 165, 179
 - differential equation 47, 99
 - dimensionless
 - coefficient 84
 - dimensionless
 - coordinate 82, 169
 - dimensionless
 - eccentricity 11, 90, 130
 - dimensionless reduced
 - frequency 52, 55, 109
 - dipole 51
 - discontinuity surface 72
 - displacement 67, 101, 141
 - displacement function 158
 - distribution function 102
 - divergence 14, 23, 88, 91
 - divergence operator 30
 - divergence velocity 89, 120
 - double-clamped plate 180
 - downward movement 93
 - drag coefficient 84, 86
 - drag force 84
 - dynamic pressure 84, 159
 - dynamic problem 24, 156
 - dynamic vibration
 - damper 152

E

eccentricity 90, 91, 128
eigenfrequency 118, 132
elastic axis 88, 90
elastic body 101
elastic centre 90, 94
elastic connection 89
elastic deformation 22, 189
elastic force 127, 159
elastic moment 89, 94
elastically fixed wing 88
elementary work 174
elevator 15
energy functional 177, 178
equations of motion 31
equilibrium position 89
Euler–Lagrange variational
 method 174, 178
Euler’s equation 28, 45, 70
external environment 73
extreme load 19

F

first variation 174
flexible structure 22
flexural oscillations 40, 105
flexural stiffness 95, 105
flexural-torsional flutter 96
flexural-torsional
 oscillations 18, 66, 105
flight velocity 14, 23, 95
flow characteristic 192, 195
flow circulation 63, 136

flow energy 24
fluid flow 39, 89, 108, 140
flow irregularity 86
flow separation 86, 137
flow velocity 35, 40, 49, 89
fluid compressibility 68
flutter 15, 18, 24, 35, 88, 96
flutter velocity 91, 97, 114
form function 109, 111, 161
forward-swept wing 97
Fourier series 42, 141
Fourier transform 40, 42
freely supported edge 156
frequency equation 114
frequency of vortex
 shedding 136
full-cantilever beam 105
full-cantilever wing 98, 110
fuselage 96

G

Galerkin method 111, 121
Galilean coordinate
 system 73
gas flow 21, 23
gas separation 187, 198
gas state parameters 72, 74
gas volume 68
generatrix 82
geometrical boundary
 conditions 110, 178
geometrical dependence 53
gradient 29, 51

H

half-chord 52
half-span 88, 146
Hankel function 60
harmonic function 40, 99
harmonic oscillations 40
heeling moment 23
high-frequency
 oscillations 38
high-order plate 181
high-speed aircraft 17, 18
high supersonic speed 68
high wing velocity 68
homogenous system 113
hydraulic diameter 138
hydroaerodynamics 21
hydroaeroelasticity 14
hydrodynamics 30, 111
hydrodynamic force 83
hydroaeroelastic force 28
hydroaeroelasticity
 problem 21, 38, 178, 199
hydrodynamic profile 82
hydroelasticity 14, 21, 179

I

ideal gas 70, 76, 78
imaginary unit 41, 47
impeller 87, 186
incompressible fluid 31, 39
incompressible flow 46
independent parameters 160
inertia force 21, 106, 193

inertial-filtering
 separation 198
infinite circular cylinder 82
infinite flexural
 stiffness 105
infinite generatrix 82
infinite length wing 39
infinitesimal amount 35
infinitesimal volume 73
infinitesimal wing
 element 106
influence function 101
initial conditions 71
initial pressure 32
initial time 73
inscribed circle 83
intrinsic elasticity 21
inverse formula 41
irreversible lift force 87
isentropic gas flow 76
isothermal flow 31

J

joint support 96

K

Karman plate theory 182
Karman vortex street 24,
 136, 154
Karman's coefficient 144
Kelvin scale 31, 73
Kutta–Zhoukovsky–
 Chaplygin's postulate 49

L

Laplace equation 41, 45, 46
Laplace operator 158
Laplace transform 41
large attack angle 20
Laurent series 51
leading edge 89, 126, 165
lift coefficient 85, 89, 93
lift force 23, 84, 103, 136
lifting rudder 96
line segment 41
linear algebraic
 equation 113, 118, 122
linear formulation 40, 93
linear matrix form 67
linear theory of
 oscillations 110
linearization 35, 37, 44, 46
linearized theory of
 potential flow 24
linearly independent
 functions 111
loading-unloading
 process 101
logarithmic decrement of
 damping 144, 154
longitudinal coordinate 98
law of plane sections 68
lower surface 34

M

Mach angle 68
Mach cone 68, 69

Mach number 37, 68, 180
mass centre 108, 116, 126
mass force 29, 31
maximum camber 83
mechanical system 127
meteorological
 observation 153
method of hydrodynamic
 features 40
method of variation of
 parameters 48
middle surface 23, 159, 180
midpoint 52, 62, 63
modified pressure
 function 75, 76
module of the velocity 72
moment ratio 84, 87
monoharmonic
 oscillations 47
monoplane 14, 15, 16
moving coordinate
 system 71

N

natural number 100
negative damping 147, 148
Newton's second law 105
non-circular cross-
 section 151
nonlinear algebraic
 equation 114, 118
nonlinear region 86
non-separable air flow 86

nonstationary flow 38, 40
non-trivial solution 113
normal component of the
 complex acceleration
 potential 53
normal deformation 11, 175
normal pressure 158
normal projection 50
normal stress 175
normal velocity 51

O

one-dimensional channel 68
operational calculus 40
oscillation amplitude 143
oscillation form 115
oscillation frequency 52

P

panel flutter 24, 155, 174
partial systems 116
physical boundary
 conditions 110, 159, 171
physical plane 42, 49, 52
pitching movement 63
plate 23, 24, 126, 145, 156
pipe 73, 138, 151, 154, 198
piston 68, 73, 78, 108, 182
piston theory 73, 108, 181
plane parallel flow 84
plate displacement
 function 158
plate divergence 129

plate length 126
point source 68
Poisson's ratio 158
polar moment
 of inertia 98, 107, 116
polynomial equation 193
polytropic index 70
poorly streamlined
 profile 82
potential energy 174
potential flow 24, 28, 34
potential flow equations 28
potential of the dipole 51
powerful vortex flow 25
pressure 29, 31, 38, 42, 44
pressure difference 38, 191
pressure force 88
pressure function 32, 33, 75
progression wave 71
profile equation 40
propeller 20
pump 186, 187, 193, 198

Q

quadratic equation 115, 132
quarter chord length 63
quasi-static load 23
quasi-stationary theory 108
quasi-stationary transonic
 flow 38
quasi-steady aerodynamic
 theory 181
quasisteady character 108

R

radius of inertia 107
random amplitude 138
random turbulence 147
rarefaction waves 76
Rayleigh–Ritz method 177
real axis 57
real part 109, 114, 123
recovery moment 89, 90, 93
rectangular plate 126, 156
rectilinear forward
 motion 40
reduced frequency 52, 55
regression wave 71
relative amplitude 52
resonance 18, 147, 150, 182
reverse effect 21
reverse of ailerons 95, 96
reverse of rudders 23
Reynolds number 137, 154
Riemann invariants 75
Riemann’s solution 72
rigid elastically fixed
 wing 88, 92
rigid torsion connection 15
root section 88
rotation angle 101, 107
rotational wing
 oscillations 52, 63
rotor 188, 189, 193, 196
rotor operator 30
Routh–Hurwitz
 criterion 121, 193

S

screw 24
seal with floating ring 194
second variation 174
self-excited vibration 148
self-oscillations 24, 140
separation channel 199
separation region 86
series expansion 48, 177
shear deformation 175
shear modulus 98
shear stress 175
shell 23, 24, 179
shock wave 37, 72, 186
simplified aerodynamic
 theories 182
single-mass system 116
slightly curved airfoil 87
slow flutter 67
small flexural-torsional
 oscillations 105
small oscillations 158, 184
small perturbation
 method 35, 68
small thickness 40
small width 39
sound velocity 33, 37, 76
specific aerodynamic
 moment 84, 98
specific damping force 159
specific elastic force 159
specific hydrodynamic
 force 84

specific inertia force 106
specific lift force 88
specific mass 29, 105, 141
specific mass force 29
specific square-wave
 external force 141
specific tensile force 158
spring characteristic 89
s-shaped airfoil 87
stable equilibrium 21
static equilibrium
 equation 90, 98, 106
static equilibrium state 101
stall flutter 20, 24, 35, 186
standing wave 71, 72
static buckling 23
static characteristic 191
static equation 23
static instability 23
static phenomena 23
static problem 23
steady flow 44
steering surface 92
steering wheel 23, 87, 96
stiffness 23, 88, 156, 196
stiffness coefficient 108
stiffness matrix 67
straight chord line 86
streamlined body 35
streamlined cylinder 140
streamlined surface 24, 34
streamlined wing 68, 105
strip theory 91, 126, 130

strong gusty wind 151
Strouhal number 136, 144
structural mechanics 21, 23
subcritical region 86
submarine periscope 153
subsonic flow 68, 108
supercritical region 68
supersonic speed 68
supersonic streamlining 89
supporting stiffness 126
supporting surface 25
sweepback wing 95, 97
symmetrical airfoil 86
system with delay 140

T

Tacoma Narrows
 Bridge 18, 19, 145, 150
tail unit 96
Theodorsen function 60, 67
theory of elasticity 21, 23
theory of oscillations 22
theory of plane flow 159
theory of supersonic
 flow 68
theory of two-dimensional
 flow 82
thermal load 22
thickness 40, 83, 158, 178
time delay 141, 144
time function 32, 200
torsion spring 88
torsional divergence 14

torsional mode 145, 150
torsional oscillations 18, 19
torsional stiffness 95, 98
total aerodynamic
 moment 94
total attack angle 89
total deformation 96
total rotation angle 101
total strain energy 174
total velocity 67
trailing edge 49, 51, 61
transcendental equation 143
transient mode 138
transverse direction 151
truss girder 150
trigonometric equation 143
turbine 20, 186
turbomachine 25, 186
twist angle 89, 98
twist centre 88
two-dimensional flow 82
two-dimensional wing
 theory 88

U

undamped oscillations 110
undisturbed
 acceleration 159
undisturbed gas flow 76
undisturbed pressure 159
undisturbed state 158
undisturbed parameter 36
unit circle 41, 49, 54, 64, 80

unit couple of forces 101
unit force 101
unit vector 29
universal gas constant 31
unknown constant 53, 162
unloading force 191, 192
unsteady flow 44, 67
unsteady harmonic
 oscillations 40
upper surface 82, 86

V

velocity 29, 35, 40, 44, 51
velocity components 42, 44
velocity potential 31, 35, 41
velocity vector 36
vertical oscillations 52
vertical plane 68
viscoelastic structural
 damping 181
vortex 29, 63, 138
vortex breakdown 19
vortex flow 25
vortex shedding 136, 147
vortex step 139

W

waves propagation 72, 76
well streamlined profile 82
wind energy 146
wing 16
wing contour 56
wing oscillations 40, 52, 63

wing motion 109, 111
wing profile 35, 68, 82, 96
wing stiffness 88
wing streamlining 20
wing surface 47, 63, 68
wing twisting 102, 103
wing width 102
wire 24, 151

Y

Young's modulus 158

Z

zero thickness 40

zero curvature 40

Zhoukovsky transform 41

References

1. Gordon J. E. Structures: Or why things don't fall down / J. E. Gordon. – London : Penguin Books, 1987.
2. Anderson J. D. A history of aerodynamics: And its impact on flying machines / J. D. Anderson. – Cambridge : Cambridge University Press, 2001.
3. Jarrett P. Biplane to monoplane: Aircraft development 1919–1939 / P. Jarrett. – Sydney : AbeBooks, 1997.
4. Murphy J. D. Military aircraft, 1919–1945: An illustrated history of their impact / J. D. Murphy, M. A. McNiece. – California : ABC-CLIO, 2008.
5. Gray P. German aircraft of the First World War / P. Gray, T. Owen. – London : Putnam & Company Ltd, 1970.
6. Pigott P. Brace for impact: Air crashes and aviation safety / P. Pigott. – Toronto : Dundurn Press, 2016.
7. Fuller R. G. Twin views of the Tacoma Narrows Bridge collapse / R. G. Fuller, C. R. Lang, R. H. Lang. – Riverdale : American Association of Physics Teachers, 2000.
8. Perelmuter A. Handbook of mechanical engineering / A. Perelmuter, V. Slivker. – Singapore : World Scientific Publishing, 2013.
9. Carta F. O. Stall flutter / F. O. Carta, C. F. Niebanck. – United Aircraft Corporation, Sikorsky Aircraft Division, 1969.
10. Betz A. Hydro- and aerodynamics / A. Betz. – Berlin : Military Government of Germany, 1948.
11. Tietjens O. G. Hydro- and aeromechanics / O. G. Tietjens. – New York : Dower Publications, 1957.
12. Bisplinghoff R. Aeroelasticity / R. Bisplinghoff, A. Holt, R. Halfman. – Mideola, New York : Dover publications, Inc., 1996.

-
13. Andronov A. A. Theory of oscillations / A. A. Andronov, C. E. Chaikin. – Michigan : University Microfilms, 1979.
 14. Zubov V. I. Theory of oscillations / V. I. Zubov. – Singapore : World Scientific Publishing, 1998.
 15. Pavlenko I. V. Finite element method for the problems of oscillations of mechanical systems / I. V. Pavlenko. – Sumy : Sumy State University, 2007.
 16. Rabinovich M. I. Oscillations and waves: In linear and nonlinear systems / M. I. Rabinovich, D. I. Trubetskoy. – Dordrecht : Kluwer Academic Publishers, 1984.
 17. Nekorkin V. I. Introduction to nonlinear oscillations / V. I. Nekorkin. – Weinheim : Higher Education Press, 2015.
 18. Landa P. S. Nonlinear oscillations and waves in dynamical systems / P. S. Landa. – Dordrecht : Kluwer Academic Publishers, 1996.
 19. Agarwal R. P. Oscillation theory for second order linear, half-linear superlinear and sublinear dynamic equations / Agarwal R. P., S. R. Grace. – Dordrecht : Kluwer Academic Publishers, 2002.
 20. Bogoliubov N. N. Asymptotic methods in the theory of non-linear oscillations / N. N. Bogoliubov, Y. A. Mitropolsky. – Zurich : Gordon and Breach Science Publishers, 1985.
 21. Dugundji J. Research on aerothermoelasticity / J. Dugundji. – Fort Belvoir : Defense Technical Information Center, 1969.
 22. Hirschel E. H. Basics of aerothermodynamics / E. H. Hirschel. – Berlin, Heidelberg : Springer International Publishing, 2015.
 23. Bryson A. E. Applied optimal control – Optimization, estimation and control / A. E. Bryson, Y. Ho. – New York : Hemisphere, 1975.

24. Landau L. D. Theory of elasticity / L. D. Landau, E. M. Lifshitz. – Amsterdam : Elsevier Ltd, 2007.
25. Lurie A. I. Theory of elasticity / A. I. Lurie. – Berlin, Heidelberg : Springer-Verlag, 2005.
26. Maceri A. Theory of elasticity / A. Maceri. – Berlin, Heidelberg : Springer-Verlag, 2010.
27. Slaughter W. S. The linearized theory of elasticity / W. S. Slaughter. – Boston : Birkhauser, 2002.
28. Pavlenko I. V. Finite element method for the problems of strength of materials and linear theory of elasticity / I. V. Pavlenko. – Sumy : Sumy State University, 2006.
29. Hjelmstad K. D. Fundamentals of structural mechanics / K. D. Hjelmstad. – New York : Springer Science and Business Media, Inc., 2005.
30. Carpinteri A. Structural mechanics – A unified approach / A. Carpinteri. – Oxford : Taylor & Francis Group, 1997.
31. Karintsev I. B. Strength of materials / I. B. Karintsev. – Sumy : Sumy State University, 2003.
32. Nayfeh A. H. Linear and nonlinear structural mechanics / A. H. Nayfeh, P. F. Pai. – Weinheim : Wiley-WCH Verlag, 2004.
33. Bittnar Z. Numerical methods in structural mechanics / Z. Bittnar, J. Sejnoha. – New York : American Society of Civil Engineers Press, 1996.
34. Guarracino F. Energy methods in structural mechanics. A comprehensive introduction to matrix and finite element methods of analysis / F. Guarracino, A. Walker. – London : Thomas Telford Publishing, 1999.
35. Shames I. H. Energy and finite element methods in structural mechanics / I. H. Shames, C. L. Dym. – New Delhi : New Age International Ltd Publishers, 2006.

-
36. Rozvany G. Topology optimization in structural mechanics / G. Rozvany. – Berlin, Heidelberg : Springer-Verlag, 1997.
 37. Hodges D. H. Introduction to structural dynamics and aeroelasticity / D. H. Hodges, G. A. Pierce. – Cambridge : Cambridge University Press, 2011.
 38. Noor A. K. Structural dynamics and aeroelasticity / A. K. Noor. – New York : American Society of Mechanical Engineers, 1993.
 39. Aguilar L. T. Self-oscillations in dynamic systems / L. T. Aguilar, I. Boiko et al. – Berlin, Heidelberg : Springer International Publishing, 2010.
 40. Groszkowski J. Frequency of self-oscillations / J. Groszkowski. – Warsaw : Polish Scientific Publishers, 1964.
 41. Fung Y. A summary of the theories and experiments on panel flutter / Y. A. Fung. – California : California Institute of Technology, 1960.
 42. Presnell J. G. Experimental panel flutter results for some flat and curved titanium skin panels at supersonic speeds / J. G. Presnell. – Washington : National Aeronautics and Space Administration, 1963.
 43. Anderson W. J. Panel flutter of cylindrical shells / W. J. Anderson. – Michigan : University of Michigan, 2005.
 44. Amabili M. Nonlinear vibrations and stability of shells and plates / M. Amabili. – Cambridge : Cambridge University Press, 2008.
 45. Pavlenko I. V. Theory of plates and shells / I. V. Pavlenko. – Sumy : Sumy State University, 2010.
 46. Brown G. linearized potential flow theory for airfoils with spoilers / G. P. Brown, G. V. Parkinson. – Cambridge : Cambridge University Press, 2006.
 47. Ward G. N. Linearized theory of steady high-speed flow / G. N. Wang. – Cambridge : Cambridge University Press, 2015.

48. Fung Y. C. An introduction to the theory of aeroelasticity / Y. C. Fung. – Mideola, New York : Dover publications, Inc., 2002.

49. Dowell E. H. A modern course of aeroelasticity / E. H. Dowell, R. Clark et al. – Dordrecht : Kluwer Academic Publishers, 2005.

50. Gazzola F. Mathematical models for suspension bridges. Nonlinear structural instability / F. Gazzola. – Berlin, Heidelberg : Springer International Publishing, 2015.

51. Lim C. C. Dynamics of the von Karman vortex street / C. C. Lim. – Providence : Brown University, 1987.

52. Clark G. F. Effects of multiple cylinders on the formation of von Karman vortex streets / G. F. Clark. – Fort Belvoir : Defense Technical Information Center, 1983.

53. Gursul I. Interaction of Karman vortex street with an elliptical leading-edge / I. Gursul. – Bethlehem : Lehigh University, 1988.

54. Chen S. Breakdown of the Karman vortex street due to forced convection and flow compressibility / S. Chen. – Washington : National Aeronautics and Space Administration, 1992.

55. Namer I. An experimental investigation of the interaction between a Karman vortex street and a premixed laminar flame / I. Namer. – Berkeley : Berkeley University of California, 1980.

56. Saffman P. G. Vortex dynamics / P. G. Saffman. – Cambridge : Cambridge University Press, 1995.

57. Hopalkrishnan R. Vortex-induced forces on oscillating bluff cylinder / R. Hopalkrishnan. – Woods Hole : Woods Hole Oceanographic Institution, 1993.

58. Sumer B. M. Hydrodynamics around cylindrical structures / B. M. Sumer, J. Fredsoe. – Singapore : World Scientific Publishing, 2006.

-
59. Blevins R. D. Flow-induced vibration / R. D. Blevins. – New York : Van Nostrand Reinhold, 1977.
60. Naudascher E. Practical experiences with flow-induced vibrations / E. Naudascher, D. Rockwell. – Berlin, Heidelberg : Springer-Verlag, 1980.
61. Anagnostopoulos P. Flow-induced vibrations in engineering practice / P. Anagnostopoulos. – Ashurst : WIT Press, 2002.
62. Merkulov V. I. Amazing hydromechanics / V. I. Merkulov. – Bloomington : Author House, 2012.
63. Balakrishnan A. V. Aeroelasticity. The continuum theory. / A. V. Balakrishnan. – Berlin, Heidelberg : Springer-Verlag, 2012.
64. Karintsev I. B. Hydroaeroelasticity / I. B. Karintsev. – Sumy : Sumy State University, 2000.
65. Bielawa R. L. Rotary wing structural dynamics and aeroelasticity / R. L. Bielawa. – Reston : American Institute of Aeronautics and Astronautics, 2006.
66. Dowell E. H. Aeroelasticity of plates and shells / E. H. Dowell. – Leyden : Noordhoff International Publishing, 1975.
67. Atassi H. M. Unsteady Aerodynamics, Aeroacoustics, and Aeroelasticity of Turbomachines and Propellers / H. M. Atassi. – Berlin, Heidelberg : Springer-Verlag, 1993.
68. Naudascher E. Hydrodynamic forces / E. Naudascher. – Oxford : Taylor & Francis Group, 1991.
69. Prasuhn A. L. Fundamentals of fluid mechanics / A. L. Prasuhn. – New Jersey : Prentice-Hall, 1980.
70. Sears W. R. Small perturbation theory / W. R. Sears. – Princeton : Princeton University Press, 1960.
71. Hinch E. J. Perturbation methods / E. J. Hinch. – Cambridge : Cambridge University Press, 1995.

72. Schinzinger R. Conformal mapping. Methods and applications / R. Schinzinger R., P. Laura. – New York : Dover Publications, 2003.

73. Papamichael N. Numerical conformal mapping. Domain decomposition and the mapping of quadrilaterals / N. Papamichael, N. Stylianopoulos. – Singapore : World Scientific Publishing, 2010.

74. Kythe P. K. Computational conformal mapping / P. K. Kythe. – New York : Springer Science and Business Media, 1998.

75. Haszpra O. Modelling hydroelastic vibrations / O. Haszpra. – Budapest : Kiado Academy, 1979.

76. Mikusinski J. Operational calculus / J. Mikusinski. – Warsaw : Polish Scientific Publishers, 2011.

77. Kuhfittig P. Introduction to the Laplace transform / P. Kuhfittig. – New York : Springer Science and Business Media, 1980.

78. Dyke P. An introduction to Laplace transform and Fourier series / P. Dyke. – New York : Springer Science and Business Media, 2014.

79. Bellman R. E. The Laplace transform / R. S. Roth. – Singapore : World Scientific Publishing, 1984.

80. Schiff J. L. The Laplace transform. Theory and applications / J. L. Schiff. – New York : Springer Science and Business Media, 1999.

81. Lighthill M. J. An introduction to Fourier analysis and generalized functions / M. J. Lighthill. – Cambridge : Cambridge University Press, 1958.

82. Surhone L. S. Joukowski transform / L. S. Surhone, M. T. Timpledon, S. F. Marseken. – Saarbrücken : VDM Publishing, 2010.

-
83. Bisplinghoff R. Principles of aeroelasticity / R. Bisplinghoff, A. Holt. – Mideola, New York : Dover publications, Inc., 2013.
84. Rama B. B. Principles of aeroelasticity / B. B. Rama. – Boca Raton : CRC Press, 2016.
85. Gryboś R. Drgania konstrukcji wzbudzone przepływem / R. Gryboś. – Gliwice, Wydawnictwo Politechniki Śląskiej, 2005.
86. Miller F. P. Cauchy-Riemann Equations / F. P. Miller, A. F. Vandome, J. McBrewster. – Saarbrücken : Alphascript Publishing, 2010.
87. Holt A. Aerodynamics of wings and bodies / A. Holt. – New York : Dover Publications, Inc., 1985.
88. Lakshmikantham V. Method of variation of parameters / V. Lakshmikantham, S. G. Deo. – Copenhagen : Overseas Publishers Association, 1998.
89. Ang W. T. Ordinary differential equations: Methods and Applications / W. T. Ang, Y. S. Park. – Irvine : Universal Publishers, 2008.
90. Meyer R. E. Introduction to mathematical fluid dynamics / R. E. Meyer. – New York : Dover Publications, Inc., 2007.
91. Maugin G. A. Continuum mechanics through the 20th century / G. A. Maugin. – Dordrecht : Springer Science and Business Media, 2013.
92. Bultheel A. Laurent series and their Pade approximations / A. Bultheel. – Basel : Birkhauser Verlag, 1987.
93. Krantz S. G. A guide to complex variables / S. G. Krantz. – Washington : The Mathematical Association of America, Inc., 2008.

94. Spurk J. S. Fluid mechanics. Problems and solutions / J. S. Spurk. – Berlin, Heidelberg : Springer-Verlag, 1997.
95. Campos L. Complex analysis with applications to flows and fields / L. Campos. – Boca Raton : CRC Press, 2011.
96. Sato K. Complex analysis for practical engineering / K. Sato. – Zurich : Springer International Publishing, 2015.
97. Larson R. Trigonometry / R. Larson, R. Hostetler. – Boston : Cengage Learning, Inc., 2007.
98. Robertson A. Higher mathematics / A. Robertson, D. Brown et al. – Edinburgh : Thomas Nelson & Sons Ltd, 1998.
99. Henne P. A. Applied computational aerodynamics / P. A. Henne. – Reston : American Institute of Aeronautics and Astronautics, 1990.
100. Northington M. C. Asymptotics of Carlman polynomials for level curves of the inverse of a shifted Joukowski transformation / M. C. Northington. – Oxford : University of Mississippi, 2011.
101. Korenev B. G. Bessel functions and their applications / B. G. Korenev. – Boca Raton : CRC Press, 2002.
102. Ito K. Encyclopedic dictionary of mathematics / K. Ito. – Cambridge : The MIT Press, 2000.
103. Kreider K. L. Computer program for Bessel and Hankel functions / K. L. Kreider. – Akron : University of Akron, 1991.
104. Caughey D. A. Frontiers of computational fluid dynamics / D. A. Caughey, M. M. Hafez. – Singapore : World Scientific Publishing, 2002.
105. Gulchat U. Fundamentals of modern unsteady aerodynamics / U. Gulchat. – Singapore : Springer Science and Business Media, 2016.

-
106. Young L. A. Rotor vortex filaments: Living on the slipstream's edge / L. A. Young. – Mountain View : NASA Ames Research Center, 1997.
 107. Ginevsky A. S. Vortex wakes of aircrafts / A. S. Ginevsky, A. I. Zhelannikov. – Berlin, Heidelberg : Springer-Verlag, 2009.
 108. Cullen C. G. Matrices and linear transformation / C. G. Cullen. – New York : Dover Publications, Inc., 1990.
 109. Gilbert G. Linear algebra and matrix theory / G. Gilbert, L. Gilbert. – Cambridge : Academic Press, 1995.
 110. Feireisl E. Mathematical theory of compressible viscous fluids. Analysis and numericals / E. Feireisl, T. G. Karper, M. Pokorný. – Zurich : Springer International Publishing, 2016.
 111. Courant R. Supersonic flow and shock waves / R. Courant, K. O. Friedrichs. – Berlin, Heidelberg : Springer-Verlag, 1991.
 112. Krehl P. History of shock waves, explosions and impact. A chronological and biographical reference / P. Krehl. – Berlin, Heidelberg : Springer-Verlag, 2009.
 113. Nastase A. Computation of supersonic flow over flying configurations / A. Nastase. – Amsterdam : Elsevier Ltd, 2008.
 114. Neiland V. Ya. Asymptotic theory of supersonic viscous gas flow / V. Ya. Neiland, V. V. Bogolepov et al. – Amsterdam : Elsevier Ltd, 2008.
 115. Bertuccio A. High pressure process technology: Fundamentals and applications / A. Bertuccio, G. Vetter. – Amsterdam : Elsevier Science B. V., 2001.
 116. Beater P. Pneumatic drives. System design, modelling and control / P. Beater. – Berlin, Heidelberg : Springer-Verlag, 2007.

117. Zel'dovich Ya. B. Physics of shock waves and high-temperature hydrodynamic phenomena / Ya. B. Zel'dovich, Yu. B. Raizer. – New York : Dover Publications, 2002.
118. David J. Fundamentals and applications of ultrasonic waves / J. David, N. Cheeke. – Boca Raton : CRC Press, 2012.
119. Davis J. L. Mathematics of wave propagation / J. L. Davis. – Princeton : Princeton University Press, 2000.
120. Beggs J. S. Kinematics / J. S. Beggs. – Berlin, Heidelberg : Springer-Verlag, 1983.
121. Drumheller D. S. Introduction to wave propagation in nonlinear fluids and solids / D. S. Drumheller. – Cambridge : Cambridge University Press, 1988.
122. Lunev V. V. Real gas flows with high velocities / V. V. Lunev. – Boca Raton : CRC Press, 2009.
123. Ben-Dor G. Handbook of shock waves / G. Ben-Dor, O. Igra, T. Elperin. – Cambridge : Academic Press, 2001.
124. Toro E. F. Riemann solvers and numerical methods for fluid dynamics: A practical introduction / E. F. Toro. – Berlin, Heidelberg : Springer-Verlag, 2009.
125. Livermore L. Compression waves and phase plots / L. Livermore. – Washington : US Department of Energy, 2011.
126. Berkeley L. Rarefaction waves in Van der Waals fluids with an arbitrary number of degrees of freedom / L. Berkeley. – Washington : US Department of Energy, 2015.
127. Wu C. Thermodynamics and heat powered cycles: A cognitive engineering approach / C. Wu. – Hauppauge : Nova Science Publishers, Inc., 2007.
128. Fai L. C. Statistical thermodynamics: Understanding the properties of macroscopic systems / L. C. Fai, G. M. Wysin. – Boca Raton : CRC Press, 2013.

-
129. Ayton L. Asymptotic approximations for the sound generated by aerofoils in unsteady subsonic flows: Doctoral thesis accepted by the University of Cambridge, UK / L. Ayton. – Zurich : Springer International Publishing, 2015.
130. Corda S. Introduction to aerospace engineering with flight test perspective / S. Corda. – Hoboken : John Wiley & Sons, Inc., 2017.
131. Harris C. D. NASA supercritical airfoils: A matrix of family-related airfoils / C. D. Harris. – Washington : National Aeronautic and Space Administration, Scientific and Technical Information Division, 1990.
132. Eppler R. Airfoil design an data / R. Eppler. – Berlin, Heidelberg : Springer-Verlag, 1990.
133. Kumar B. Illustrated dictionary of aviation / B. Kumar, D. Remer, D. Marshall. – New York : McGraw Hill Professional, 2005.
134. Hitchens F. E. The encyclopedia of aerodynamics / F. E. Hitchens. – Luton : Andrews UK Ltd, 2015.
135. Strommen E. Theory of bridge aerodynamics/ E. Strommen. – Berlin, Heidelberg : Springer-Verlag, 2010.
136. Rao L. R. Engineering mechanics: Static and dynamics / L. R. Rao, J. Lakshminarasimhan et al. – New Dehli : Prentice-Hall of India Private Ltd, 2003.
137. Wright J. R. Introduction to aircraft aeroelasticity and loads / J. R. Wright, J. E. Cooper – Hoboken : John Wiley & Sons, Inc., 2015.
138. Bismarck-Nasr M. N. Structural dynamics in aeronautical engineering / M. N. Bismarck-Nasr. – Reston : American Institute of Aeronutics, Inc., 1999
139. Phillips W. F. Mechanics of flight / W. F. Phillips. – Hoboken : John Wiley & Sons, Inc., 2004.

140. Nancy A. Pilot's handbook of aeronautical knowledge / A. Nancy, S. Keynon, R. Magner et al. – Washington : US Department of Transportation, Federal Aviation Administration, Flight Standards Service, 2016.
141. Peery D. J. Aircraft structures / D. J. Peery. – New York : Dover Publications, Inc., 2013.
142. Niu M. Airframe structural design. Practical design information and data on aircraft structures / M. Niu. – Hong Kong : Conmilit Press Ltd, 1995.
143. Buchholdt H. Structural dynamics for engineers / H. Buchholdt. – London : Thomas Telford Publications, 1999.
144. Gere J. M. Mechanics of materials / J. M. Gere, B. J. Goondo. – Boston : Cengage Learning, Inc., 2009.
145. Hartmann F. Statics and influence functions – From a modern perspective / F. Hartmann, P. Jahn. – Zurich : Springer International Publishing, 2017.
146. Angeles J. Kinematics and dynamics of multy-body systems / J. Angeles, A. Kecskemethy. – Wien : Springer-Verlag, 1995.
147. Timoshenko S. P. Theory of elasticity / S. P. Timoshenko, J. N. Goodier. – York : The Maple Press Company, 1951.
148. Knudsen J. M. Elements of Newtonian mechanics. Including nonlinear dynamics / J. M. Knudsen, P. G. Hjorth. – Berlin, Heidelberg : Springer-Verlag, 2000.
149. Lighthill M. J. Higher approximations in aerodynamic theory / M. J. Lighthill. – Princeton : Princeton University Press, 1960.
150. Dolejsi V. Discontinuous Galerkin method. Analysis and applications to compressible flow / V. Dolejsi, M. Feistauer. – Zurich : Springer International Publishing, 2015.

-
151. Abadir K. M. Matrix algebra / K. M. Abadir, J. R. Magnus. – Cambridge : Cambridge University Press, 2005.
152. Babakov I. M. Theory of oscillations / I. M. Babakov. – Moscow : Science Publishing House, 1968.
153. Polyanin A. D. Handbook of mathematics for engineers and scientists / A. D. Polyanin, A. V. Manzhirov. – Oxford : Taylor & Francis Group, 2007.
154. Vinogradov I. M. Encyclopedia of mathematics / I. M. Vinogradov. – Dordrecht : Kluwer Academic Publishers, 1995.
155. Pavlovskiy M. A. Theoretical mechanics / M. A. Pavlovskiy. – Kyiv, Machinery, 2002.
156. Vulfson I. Dynamics of cyclic machines / I. Vulfson. – Zurich : Springer International Publishing, 2015.
157. Surchone L. M. Strouhal Number / L. M. Surchone, M. T. Timpledon, S. F. Marseken. – Saarbrücken : Betascript Publishing, 2010.
158. Martsynkovskyy V. A. Gap seals: Theory and practice / V. A. Martsynkovskyy. – Sumy : Sumy State University, 2005.
159. Chen S.-H. Hydraulic structures / S.-H. Chen. – Berlin, Heidelberg : Springer-Verlag, 2015.
160. Case J. Strength of materials and structures: An introduction to the mechanics of solids and structures / J. Case, A. H. – London : Chilver Edward Arnold Publishers Ltd, 1986.
161. Bajaj N. K. The physics of waves and oscillations / N. K. Bajaj. – New York : McGraw Hill Publishing, 2006.
162. Bhatia R. Fourier Series / R. Bhatia. – Washington. – The Mathematical Association of America, Inc., 2005.

163. Lawson W. Trigonometry: Solving trigonometric equations and inequalities / W. Lawson, N. H. Nguyen. – Bloomington : Trafford Publishing, 2005.
164. Boyd J. P. Solving transcendental equations / J. P. Boyd. – Philadelphia : Society of Industrial and Applied Mathematics, 2014.
165. Silva C. W. Vibration and shock handbook / C. W. Silva. – Oxford : Taylor & Francis Group, 2005.
166. Irvin T. The Tacoma Narrows Bridge failure / T. Irvin. – Madison : Vibrationdata, 2009.
167. Koughan J. The collapse of the Tacoma Narrows Bridge: Evaluation of competing theories of its demise, and the effects of the disaster of succeeding bridge designs / J. Koughan. – Austin : The University of Texas at Austin, 1996.
168. Hartog D. Mechanical vibrations / D. Hartog. – New York : McGraw-Hill Publishing, 1940.
169. Bachmann H. Vibration problems in structures / H. Bachmann. – Berlin : Birkhauser Verlag, 1995.
170. Levy M. Why buildings fall down / M. Salvadori, M. Salvadori. – New York : Norton, 1992.
171. Billah K. Yu. Resonance, Tacoma Narrows Bridge failure, and undergraduate physics / K. Yu. Billah, R. H. Scanlan // American Journal of Physics. – 1991. – Vol. 59 (118), Issue 2. – P. 118–124.
172. Watkins R. K. Structural mechanics of buried pipes / R. K. Watkins, L. R. Anderson. – Boca Raton : CRC Press, 2000.
173. Kiessling F. Overhead power lines. Planning, design, construction / F. Kiessling, P. Nefzger, J. F. Nolasco, U. Kaintzyk. – Berlin, Heidelberg : Springer-Verlag, 2003.

-
174. Davim J. P. Dynamic methods and process advancements in mechanical, manufacturing, and materials engineering / J. P. Davim. – Berlin : Springer, 2015.
175. Timoshenko S. P. Theory of elastic stability / S. P. Timoshenko, J. M. Gere. – New York : McGraw-Hill Book, 2009.
176. Reddy J. N. Theory and analysis of elastic plates and shells / J. N. Reddy. – Boca Raton : CRC Press, 2007.
177. Leckie F. Strength and stiffness of engineering systems / F. Leckie, D. Bello. – New York : Springer Science and Business Media, 2009.
178. Woods L. C. The theory of subsonic plane flow / L. S. Woods. – Cambridge : Cambridge University Press, 2011.
179. Tabarrok B. Variational methods and complementary formulations in dynamics / B. Tabarrok, F. Rimrott. – New York : Springer Science and Business Media, 1994.
180. Gould S. H. Variational methods for eigenvalue problems. An introduction to the methods of Rayleigh, Ritz, Weinstein, and Aronszajn / S. H. Gould. – New York : Dover Publications, Inc., 1995
181. Smith R. Variational methods in optimization / R. Smith. – New York : Dover Publications, Inc., 1998.
182. Cherkhev A. Variational methods for structural optimization / A. Cherkhev. – Berlin, Heidelberg : Springer-Verlag, 2000.
183. Ilanko S. The Rayleigh–Ritz method for structural analysis / S. Ilanko, L. E. Monterrubio, Y. Mochida. – Hoboken : John Wiley & Sons, Inc., 2014.
184. Mason J. Methods of functional analysis for application in solid mechanics / J. Masdon. – Amsterdam : Elsevier Science Publishing Company, Inc., 1985.

185. Mickens R. E. Truly nonlinear oscillations. Harmonic balance, parameter expansion, iteration, and averaging methods / R. E. Mickens. – Singapore : World Scientific Publishing, 2010.

186. Kuo C.-C. Perturbation and harmonic balance methods for nonlinear panel flutter / C.-C. Kuo, L. Morino, J. Dugundji // The Journal of the Americal Institute of Aeronautics and Astronautics. – 1982. – Vol. 10, No. 11. – P. 1479–1484.

187. Yang T. Y. Nonlinear panel flutter using high-order triangular finite elements / T. Y. Yang, A. D. Han // The Journal of the Americal Institute of Aeronautics and Astronautics. – 1983. – Vol. 21, No. 10. – P. 1453–1461.

188. Shishaeva A. Nonlinear single-mode and multi-mode panel flutter oscillations at low supersonic speeds / A. Shishaeva, V. Vedeneev, A. Aksenov // Journal of Fluid and Structures. – 2015. – Vol. 56. – P. 205–223.

189. Xie D. New look at nonlinear aerodynamics in analysis of hypersonic panel flutter / D. Xie, M. Xu, H. Dai, T. Chen // Mathematical Problems in Engineering. – 2017. – Vol. 2017. – P. 1–13.

190. Miyakozawa T. Flutter and forced response of turbomachinery with frequency mistuning and aerodynamic asymmetry : Ph. D. thesis / T. Miyakozawa. – USA : Duke University, 2008.

191. Thomas C. E. Process technology and equipment / C. E. Thomas. – Boston : Cengage learning, Inc., 2015.

192. Hall K. C. Unsteady aerodynamics, aeroacoustics and aeroelasticity of turbomachines / K. C. Hall, R. E. Kielb, J. P. Thomas. – Berlin, Heidelberg : Springer-Verlag, 2006.

-
193. Castravete S. C. Nonlinear flutter of a cantilever wing including the influence of structure uncertainties : Ph. D. thesis / S. C. Castravete. – USA : Wayne State University, 2007.
194. Jing Li. Experimental investigation of the low speed stall flutter of an airfoil : Ph. D. thesis / Li Jing. – UK : University of Manchester, 2007.
195. Raman A. Post-flutter dynamics of a rotating disk / A. Raman, M. Hansen, C. Mote // *Computational Fluid and Solid Mechanics*. – 2003. – Vol. 1. – P. 598–601.
196. Hoblit M. Gust loads and aircraft: Concept and applications / M. Hoblit. – Reston : AIAA Education Series, 1988.
197. Bishop R. Hydroelasticity of ships / R. Bishop, W. Price. – Cambridge : Cambridge University Press, 1979.
198. Stenius I. Hydroelasticity in marine hull bottom panels: Modelling and characterization / I. Stenius. – Stockholm : KTH School of Engineering Sciences, 2009
199. Abramson H. N. Hydroelasticity with special reference to hydrofoil craft / H. N. Abramson, W. Chu, J. T. Irick. – San-Antonio : Southwest Research Institute, 1966.
200. Martsynkovskyy V. A. Development of methods for numerical simulation and optimization of hydrodynamic characteristics for gap and labyrinth seals, and investigation of their impact on the rotordynamics for centrifugal machines / V. A. Martsynkovskyy, A. V. Zahorulko, I. V. Pavlenko et al. – Sumy : Sumy State University, No. 0106U001385, 2009.
201. Martsynkovskyy V. A. Numerical simulation and optimization of gas-dynamics and vibration characteristics for turbochargers of gas-pumping units and their components / V. A. Martsynkovskyy, A. V. Zahorulko, I. V. Pavlenko et al. – Sumy : Sumy State University, No. 0109U001937, 2012.

202. Simonovskiy V. I. Development of the new mathematical models of centrifugal machines rotors and methods of their diagnosis / V. I. Simonovskiy, I. V. Pavlenko et al. – Sumy : Sumy State University, No. 0113U001522, 2014.

203. Simonovskiy V. I. Investigation of oscillations of centrifugal machines rotors associated with nonlinearity reactions in gap bearings and seals, and their vibration diagnosis / V. I. Simonovskiy, I. V. Pavlenko et al. – Sumy : Sumy State University, No. 0115U000549, 2016.

204. Zahorulko A. V. Rotordynamic research for the turbopumps of the liquid rocket engines / A. V. Zahorulko, V. A. Martsynkovskyy, V. I. Simonovskiy, I. V. Pavlenko et al. – Sumy : Sumy State University, No. 51.24-01.15.SP, 2017.

205. Martsynkovskyy V. A. Non-contact seals of rotary machines / V. A. Martsynkovskyy. – Sumy : Sumy State University, 1980.

206. Pavlenko I. Dynamic analysis of the locking automatic balancing device of the centrifugal pump / I. Pavlenko // Journal of mechanical engineering “Strojnícky časopis”. – Bratislava : Institute of Materials and Machine Mechanics, Slovak Academy of Science. – 2009. – No. 2 (60). – P. 75–86.

207. Pavlenko I. V. Increasing the reliability of the automatic balancing devices of the centrifugal machines : Ph. D. thesis. – Sumy : Sumy State University, 2009.

208. Pavlenko I. Nonstationary fluid flow in a face gap with the oscillating wall / I. Pavlenko // Bulletin of Sumy State University, Series “Mechanization and Automation of Production Processes”. – Sumy : Sumy State University, 2008. – No. 2 (18). – P. 20–25.

209. Pavlenko I. V. Solving the problem of hydroelasticity for the unloading disk of the automatic balancing device / I. V. Pavlenko, A. Korczak, A. // Bulletin of Sumy National Agrarian University. – Sumy : Sumy National Agrarian University, 2005. – Vol. 11, No. 14. – P. 141–145.

210. Pavlenko I. V. Solving the stationary problem of hydroelasticity for the unloading disk of the automatic balancing device in the first approximation / I. V. Pavlenko // 1st Interuniversity Scientific Conference of Sumy State University. – Sumy : Sumy State University, 2006. – P. 111–112.

211. Martsynkovskyy V. A. Rotor vibrations of centrifugal machines / V. A. Martsynkovskyy. – Sumy : Sumy State University, 2002.

212. Martsynkovskyy V. A. Rotor dynamics of centrifugal machines / V. A. Martsynkovskyy. – Sumy : Sumy State University, 2012.

213. Certificate of authorship. The shaft seal / V. A. Martsynkovskyy, V. A. Melnyk et al. – No. 37, 1984.

214. Liaposhchenko O. O. Development of the “Heater-Treater” equipment for the comprehensive oil treatment / O. O. Liaposhchenko, O. V. Nastenko et al. – Sumy : Sumy State University, No. 51.18-04.15.SP, 2015.

215. Sklabinskyi V. I. Hydrodynamic parameters of two-phase flows for the heat and mass-transfer granulation and separation equipment / V. I. Sklabinskyi, O. O. Liaposhchenko et al. – Sumy : Sumy State University, No. 0115U002551, 2015.

216. Martsynkovskyy V. A. Numerical simulation and optimization of the gas-dynamic and vibration characteristics of turbochargers and gas pumping units and their components / V. A. Martsynkovskyy, A. V. Zahorulko et al. – Sumy : Sumy State University, No. 0111U002151.

217. Simonovskiy V. I. Investigation of rotor dynamics for turbopump units and reciprocating compressor plants / V. I. Simonovskiy, I. V. Pavlenko et al. – Sumy : Sumy State University, No. 0117U004922, 2017.

218. Pavlenko I. V. Dynamic analysis of centrifugal machine rotors supported on ball bearings by combined using 3D and beam finite element models / I. V. Pavlenko, V. I. Simonovskiy, M. M. Demianenko // IOP Conference Series: Materials Science and Engineering. – 2017. – Vol. 233 (2017). – P. 1–8.

219. Liaposhchenko O. O. Development and implementation of energy efficient modular separation devices for oil and gas purification equipment / O. O. Liaposhchenko, V. O. Ivanov, I. V. Pavlenko, M. M. Demianenko et al. – Sumy : Sumy State University, No. 15.01.06-01.17/20.ZP, 2017.

220. Demianenko M. M. Solving the Navier-Stokes equations and the problem of hydroaeroelasticity for the separation processes in curvilinear channels / M. M. Demianenko, O. O. Liaposhchenko, I. V. Pavlenko, V. I. Sklabinskyi // Bulletin of V. Karazin Kharkiv National University. – Kharkiv : V. Karazin Kharkiv National University, 2015. – No. 27. – P. 53–64.

221. Demianenko M. M. Solving the problem of hydroaeroelasticity for the process of interaction of the gas-dispersed flow with the dynamic reflecting elements / M. M. Demianenko, I. V. Pavlenko, O. O. Liaposhchenko // Modern Technologies in Industrial Production. – Sumy : Sumy State University, 2015. – No. 1. – P. 127–128.

222. Liaposhchenko O. O. Appliance of inertial gas-dynamic separation of gas-dispersion flows in the curvilinear convergent-divergent channels for compressor equipment reliability improvement / O. O. Liaposhchenko, V. I. Sklabinskyi, V. L. Zavialov, I. V. Pavlenko, O. V. Nastenko, M. M. Demianenko // IOP Conference Series: Materials Science and Engineering. – 2017. – Vol. 233 (2017). – P. 1–8.

Навчальне видання

**Карінцев Іван Борисович,
Павленко Іван Володимирович**

ГІДРОАЕРОПРУЖНІСТЬ

Підручник
(Англійською мовою)

Художнє оформлення обкладинки І. В. Павленка
Редактор Л. В. Штихно
Комп'ютерне верстання І. В. Павленка

Формат 60×84/16. Ум. друк. арк. 13,72. Обл.-вид. арк. 11,84. Тираж 500 пр. Зам. № .

Видавець і виготовлювач
Сумський державний університет,
вул. Римського-Корсакова, 2, м. Суми, 40007
Свідоцтво суб'єкта видавничої справи ДК № 3062 від 17.12.2007.